The Mediterranean Journal of Measurement and Control

Volume 4 / Number 3 / 2008

ISSN: 1743-9310

Published by SoftMotor Ltd.

The Mediterranean Journal of Measurement and Control

Aims and Scope

The journal publishes papers from worldwide in the field of instrumentation, measurement, and control. Its scope encompasses cutting-edge research and development, education and industrial applications. The journal publishes peer-reviewed papers designed to appeal to both researchers and practitioners. It presents up-to-date coverage of the latest developments, offering a unique interdisciplinary perspective. It also includes invited papers, book reviews, conference notices, calls for papers, and announcements of new publications and special issues. The journal covers - but not limited to: All Aspects of Control Theory and its Applications (Linear, Nonlinear, Robust, State Space and Multivariable, Self-Tuning, Adaptive, Optimal, and others), System Identification and Parameter Estimation, and Mathematical Modeling and Simulation, Intelligent Systems and Applications (fuzzy logic, neural networks, genetic algorithms, and others), Machine Vision and Pattern Recognition, Mechatronics and Robotics, and Advanced Manufacturing Systems, Sensors, Measuring Instruments, and Signal Processing, Computing for Measurement, Control and Automation, and Industrial Networks and Communication protocols (FieldBuses, OPC, and others). Papers may be from the following categories: Design: Present a complete “how-to” guide. Connect design procedures to first principles. Explicitly state necessary heuristics and limits of applicability. Provide evidence that the procedures are practicable. Analysis: Clearly develop a fundamental, theoretical analysis of a practice-relevant issue. Explicitly state implications and recommendations for its application. Provide credible examples. Application: Present the results of new (or under-utilized) techniques or novel applications. Provide a complete description of results, including pilot- or plant-scale experimental data, and a revelation of heuristics and shortcomings.

 ISSN: 1743-9310

WELCOME TO THE MEDITERRANEAN JOURNAL OF MEASUREMENT AND CONTROL

We would like to welcome you all to the fourth volume - third issue - of The Mediterranean Journal of Measurement and Control. This issue of the journal, comprising of five papers, is dedicated to the latest research work being done in the analyses of modeling and control of dynamic systems, robotics, and soft computing.

The first paper by Chen deals with control of multi-qubit systems which is an important task for quantum computation and quantum control. An incoherent control approach for multi-qubit systems using quantum measurement and quantum learning is studied in this paper. The projective measurement of quantum systems is adopted as a control method instead of a negative effect for incoherent control. Then a quantum reinforcement learning algorithm is presented to optimize the sequential decision process of the control sequence for multi-qubit systems. An example of five-qubit system is demonstrated to show the feasibility and effectiveness of the presented approach.

The second paper by Merabet designs a robust feedback linearization controller based on state estimation for rigid link robot. The trajectories' tracking for angular positions of the links is the objective to be achieved by this controller. The control law is carried out via a system linearization. The unknown external disturbances, unmodeled quantities and parametric uncertainties are taken into account by designing a disturbance observer. This observer is simplified from the feedback linearization control law and integrated in the control loop as a disturbance compensator. It contains an integral action, which eliminates the steady errors and enhances the robustness of the control scheme. A high gain observer is implemented to deal with robot state estimation. The global stability of the closed loop system (robot, controller, and state observer) and the robustness issue are proved analytically based on the Lyapunov stability theorem. Simulations are carried out for two link rigid robot to verify the performance of the proposed control scheme.

The third paper by Zerar presents a global stabilization and robust Dynamic Output Feedback Controller (DOFC) design methodology for Takagi-Sugeno (T-S) fuzzy systems. Based on a standard robust control structure, one rewrites an original nonlinear model as an extended nonlinear model with exogenous inputs. The latter contains control objectives that are classically introduced in terms of linear weighting functions in robust control theory. In order to point out the interconnection between the extended nonlinear model and the designated DOFC, unsolvable stability conditions are derived using Linear Fractional Transformation (LFT) and H_∞ tools. Based on the universal approximator properties of T-S modeling, the obtained nonlinear stability conditions are then transformed into Linear Matrix Inequalities (LMI) to allow the design of a dedicated Full Parallel Distributed Compensation (FPDC) DOFC. In that case, when a solution is tractable from the proposed LMI conditions, the synthesized controller guarantees the prescribed stability performances. Finally, a numerical example is used to illustrate the validity of the designed approach.

The fourth paper by Tahoun deals with the data-packet dropout that might be potential source to instability and poor performance of networked control systems, the main objective of this paper is to design an adaptive stabilizing controller for networked systems with data-packet dropout. With the continuous-time approach, the case of state feedback is studied in which a new adaptive control model in the presence of data-packet dropout is proposed. The problem is to find upper bounds on the sampling period and the transmission packet dropout, to guarantee stability of the overall adaptive networked control systems. The resulting upper bounds are time varying and can be estimated online. Rigorous mathematical proofs are established, that relies heavily on Lyapunov's stability criterion and its extensions. Illustrative example is given to illustrate the effectiveness of our design approach.

WELCOME TO THE MEDITERRANEAN JOURNAL OF MEASUREMENT AND CONTROL

Finally, the fifth paper by Lakdja deals with the control of power transportation networks without multiplying or creating new lines. The series capacitors controlled by SCRs (Silicon Controlled Rectifiers) represent a good alternative to optimize the existing or the new electric links, because they permit the increase of the dynamic stability, the damping of the power oscillations, while balancing the loads between the parallel circuits. This paper presents an effective method for power distribution by inserting the TCSC (Thyristor controlled Series Capacitors) transit controller in the network. The insertion of the TCSC devices has given satisfying results that are, an increase of the transmitted active power, reduction of active losses, and improvement of the angular stability and the voltage stability without decreasing the transportation capacity.

July 2008

Dr. Mohamed H. Mahmoud
Editor-in-Chief

MEASUREMENT BASED QUANTUM LEARNING CONTROL OF MULTI-QUBIT SYSTEMS

C. Chen [1, 2, *], Z. Zhu [1], X. Zhou [1, 2], Q. Chen [1]

[1] Department of Control and System Engineering, School of Manag. and Eng., Nanjing University, P. R. China

[2] State Key Laboratory for Novel Software Technology, Nanjing University, P. R. China

ABSTRACT

Effective control of multi-qubit systems is an important task for quantum computation and quantum control. An incoherent control approach for multi-qubit systems using quantum measurement and quantum learning is studied in this paper. The projective measurement of quantum systems is adopted as a control method instead of a negative effect for incoherent control. Then a quantum reinforcement learning algorithm is presented to optimize the sequential decision process of the control sequence for multi-qubit systems. An example of five-qubit system is demonstrated to show the feasibility and effectiveness of the presented approach.

Keywords

Multi-qubit System, Quantum Learning Control, Quantum Measurement, Quantum Reinforcement Learning.

1. INTRODUCTION

Analogous to the concept of bit for classical computation and information, quantum bit (qubit) and multi-qubit are the most fundamental concepts of quantum information technologies [1]. Recently, quantum information theory is rapidly developing and it has interested many scientists for the perfect security of quantum communication and the powerful ability of quantum computation [1]. Hence the problem of controlling the multi-qubit systems has drawn the attention of many scientists; especially when the number of qubits increases, controlling qubits to desired states has become an important and key task [2].

Current research of quantum control mainly involves controllability of quantum system [3-5], coherent control [6, 7], quantum optimal control [8] and quantum feedback control [9, 10]. Although coherent control that preserves quantum coherence is the main paradigm to control quantum systems, recent results also show that quantum measurements can be combined with unitary operators to make the nonunitarily controllable systems become controllable [11]. These control schemes based on measurement that destroy the coherent characteristics of quantum systems are also called "incoherent control". In this paper, a measurement based incoherent control approach is investigated to control the multi-qubit systems. This approach consists of two steps: projective measurement on the initial system and an optimal sequential control by quantum learning algorithms.

Quantum algorithms are the key to find an optimal control sequence. All kinds of quantum algorithms are also the most important objectives pursued by many scientists in quantum computation. In 1994, Shor first proposed an effective quantum algorithm (Shor algorithm), which provides a striking exponential speedup for factoring large integers into prime numbers over the best known classical algorithms [12]. After two years, Grover presented another useful quantum algorithm (Grover algorithm), which can achieve a quadratic speedup in unsorted database searching [13]. Recently we have also proposed a novel quantum reinforcement learning algorithm based on quantum state superposition principle [14] and it can deal with some complicated tasks [11]. Here the quantum reinforcement learning algorithm is used to the learning control of multi-qubit systems [2].

This paper is organized as follows. Section 2 gives the formulation of the problem studied in this paper. Section 3 introduces the projective measurement and the quantum incoherent control method using measurement. In Section 4, the quantum reinforcement learning algorithm is presented to find the optimal control sequence to drive the multi-qubit system to a desired state. Section 5 shows the effectiveness of the presented approach to the control problems of multi-qubit systems through a five-qubit example. Conclusions are given in Section 6.

2. PROBLEM FOMULATION

In quantum computation, qubit is represented with quantum state and a qubit is an arbitrary superposition state of two-state quantum system [1]:

$$|\psi\rangle = \alpha|0\rangle + \beta|1\rangle \tag{1}$$

where α and β are complex coefficients and satisfy $|\alpha|^2 + |\beta|^2 = 1$. $|0\rangle$ and $|1\rangle$ are two orthogonal states (also called basis vectors of quantum state $|\psi\rangle$), and they correspond to logic states 0 and 1. $|\alpha|^2$ represents the occurrence probability of $|0\rangle$ when the qubit is measured, and $|\beta|^2$ is the probability of obtaining result $|1\rangle$. The physical carrier of a qubit is any two-state quantum system such as two-level atom, spin-1/2 particle and polarized photon. The value of classical bit is either Boolean value 0 or value 1, but a qubit can be prepared in the coherent superposition state of 0 and 1, i.e. a qubit can simultaneously store 0 and 1, which is the main

*Corresponding author: *E-mail:* andyclchen@gmail.com

 ISSN: 1743-9310

difference between classical computation and quantum computation.

According to quantum computation theory, the quantum computing process can be looked upon as a unitary transformation U from input qubits to output qubits. If one applies a transformation U to a superposition state, the transformation will act on all basis vectors of this superposition state and the output will be a new superposition state by superposing the results of all basis vectors. So when one processes function $f(x)$ by the method, the transformation can simultaneously work out many different results for a certain input X. This is analogous with parallel process of classical computer and is called quantum parallelism. The powerful ability of quantum algorithm is just derived from the parallelism of quantum computation.

Suppose the input qubit $|z\rangle$ lies in the superposition state:

$$|\mathrm{z}\rangle = \frac{1}{\sqrt{2}}(|0\rangle + |1\rangle) \tag{2}$$

The transformation U_z describing computing process is defined as follows:

$$\mathrm{U_z} : |\mathrm{z,y}\rangle \rightarrow |\mathrm{z, y} \oplus \mathrm{f(z)}\rangle \tag{3}$$

where $|z, y\rangle$ represents the input joint state and $|z, y \oplus f(z)\rangle$ is the output joint state. Let $y = 0$ and we can easily obtain [1]:

$$\mathrm{U_z}\,|\mathrm{z}\rangle = \frac{1}{\sqrt{2}}(|0, \mathrm{f(0)}\rangle + |1, \mathrm{f(1)}\rangle) \tag{4}$$

The result contains information about both $f(0)$ and $f(1)$, and we seem to evaluate $f(z)$ for two values of z simultaneously.

Figure 1. A multi-qubit system

A multi-qubit system is shown in Fig. 1. Now consider an n-qubit cluster and it lies in the following superposition state:

$$\begin{aligned} |\psi\rangle &= \sum_{\mathrm{x}=00\cdots0}^{\overbrace{11\cdots1}^{\mathrm{n}}} \mathrm{C_x}\,|\mathrm{x}\rangle \\ \sum_{\mathrm{x}=00\cdots0}^{\overbrace{11\cdots1}^{\mathrm{n}}} &|\mathrm{C_x}|^2 = 1 \end{aligned} \tag{5}$$

where C_x is complex coefficients and $|C_x|^2$ represents occurrence probability of $|x\rangle$ when state $|\psi\rangle$ is measured. $|x\rangle$ can take on 2^n values, so the superposition state can be looked upon as the superposition state of all integers from 0 to $2^n - 1$. Since U is a unitary transformation, computing function $f(x)$ can give:

$$\begin{aligned} \mathrm{U} \sum_{\mathrm{x}=00\cdots0}^{\overbrace{11\cdots1}^{\mathrm{n}}} \mathrm{C_x}\,|\mathrm{x},0\rangle &= \sum_{\mathrm{x}=00\cdots0}^{\overbrace{11\cdots1}^{\mathrm{n}}} \mathrm{C_x U}\,|\mathrm{x},0\rangle \\ &= \sum_{\mathrm{x}=00\cdots0}^{\overbrace{11\cdots1}^{\mathrm{n}}} \mathrm{C_x}\,|\mathrm{x}, f(\mathrm{x})\rangle \end{aligned} \tag{6}$$

With the development of quantum information technology, quantum control theory has drawn the attention of many scientists. The objective of quantum control is to determine how to drive quantum systems from an initial given quantum state to a pre-determined target quantum state using some external fields. According to quantum mechanics, the state $|\psi(t)\rangle$ of arbitrary time t can be reached through an evolution on the initial state $|\psi(0)\rangle$. It can be expressed as

$$|\psi(\mathrm{t})\rangle = \hat{\mathrm{U}}|\psi(0)\rangle \tag{7}$$

where $\hat{U}$ is a unitary operator and satisfies:

$$\hat{\mathrm{U}}\hat{\mathrm{U}}^{+} = \hat{\mathrm{U}}^{+}\hat{\mathrm{U}} = \mathrm{I} \tag{8}$$

where $\hat{U}^{+}$ is the Hermitian conjugate operator of $\hat{U}$. So the control problem of quantum state can be converted into finding an appropriate unitary operator $\hat{U}$ or a sequence of operators $\hat{U}$.

3. MEASUREMENT BASED CONTROL OF MULTI-QUBIT

This section first introduces the projective measurement of a quantum system. Then an incoherent control scheme is presented for the control of a multi-qubit system based on quantum measurements.

3.1 Quantum Projective Measurement

The concept of inertia matching can be extended to humanoid jumping robot as follows. Jumping robot can be considered as a redundant manipulator with a load held at the end-effector [18]. Fig. 2 shows jumping robot and inertia matching ellipsoid (IME).

Projective measurement is an important special case of the general measurement postulate [1]. It can be described as **Definition 1** [15].

Definition 1: (**Projective Measurement**) *A projective measurement is described by an observable, M, a Hermitian operator on the state space of the system being observed. The observable has a spectral decomposition,*

$$M = \sum_{m} m P_m \tag{9}$$

where P_m is the projector onto the eigenspace of M with eigenvalue m. The possible outcomes of the measurement correspond to the eigenvalue m of the observable. Upon measuring the state $|\psi\rangle$, the probability of getting m is given by

$$p(m) = \langle \psi \mid P_m \mid \psi \rangle \tag{10}$$

Given that outcome occurred, the state of the quantum system immediately after the measurement is

$$P_m \mid \psi \rangle \Big/ \sqrt{p(m)} \tag{11}$$

In fact, a quantum state $|\psi\rangle$ can be expressed with its eigenstates according to superposition principle. Assume the eigenstates are $\{\varphi_1, \varphi_2, \ldots, \varphi_n, \ldots, \varphi_i\}$ and they form an orthogonal basis. For convenience, here $|\psi\rangle$ is simply expressed with ψ. Then ψ can lie in their superposition state:

$$\psi = \sum_{n=1}^{i} C_n \phi_n \tag{12}$$

where C_n is complex number, $|C_n|^2$ is the occurrence probability of φ_n when ψ is measured, and satisfies $\Sigma_{n-1}^{i} |C_n|^2 = 1$, i.e., the result must be an eigenstate when we make a projective measurement on a quantum system. The process can be described as Fig. 2 [15].

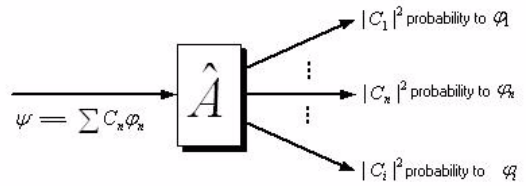

Figure 2. The effect of projective measurement on quantum state

3.2 Quantum Incoherent Control Based on Measurement

Coherent control is a particularly powerful control strategy in quantum control, which has no corresponding strategy in classical control theory. In the coherent strategy, we can manipulate the state of a quantum system by applying semiclassical potentials [7]. Although coherent control has achieved much success in quantum control, a difficult problem in the coherent strategy is the problem of information acquisition since quantum measurements generally destroy the coherent characteristics of quantum systems. Usually the state of a quantum system will collapse into one of its eigenstates under a projective measurement. Hence the projective measurement is sometimes considered as a negative effect to complete some quantum control tasks due to its intrinsic randomness. However, recent results show quantum measurements can improve the controllability of quantum systems in some situations and even sometimes a nonunitarily controllable system can be controlled by the joint action of projective measurement plus unitary evolution [11]. Since quantum measurements destroy the coherent characteristics of quantum systems, this class of control schemes is called "incoherent control".

In this paper, the incoherent control scheme based on projective measurement is used to control the multi-qubit systems. The whole incoherent control scheme can be described as follows:

(1) Analyze the target state $|\psi_{target}\rangle$ and assume it is reachable from an eigenstate $|\psi_e\rangle$;

(2) Make a projective measurement on the initial state $|\psi_0\rangle$;

(3) Read the result $|\psi_j\rangle$;

(4) Find an local optimal path from $|\psi_j\rangle$ to $|\psi_e\rangle$ through quantum learning algorithms;

(5) Drive $|\psi_e\rangle$ to the target state $|\psi_{target}\rangle$ by suitable controls.

4. QRL FOR SEQUENCIAL DECISION OF QUANTUM OPERATIONS

Quantum reinforcement learning (QRL) [14, 16, 17] is a new learning paradigm that fuses quantum computation with reinforcement learning [16, 18, 19]. In this paper, QRL is used to find a suitable sequence of controls to drive $|\psi_j\rangle$ to $|\psi_e\rangle$ for the incoherent control of multi-qubit systems.

One of the most fundamental principles of quantum mechanics is the state superposition principle. Hence in this section, the representation of a QRL system with quantum concepts is first briefly introduced and more details may refer to [14]. Then we have the following definitions and propositions.

Definition 2: (**Eigenvalue of states or actions**) *States S or actions a in a RL system are denoted as corresponding orthogonal quantum states $|s_n\rangle$ (or $|a_n\rangle$) and are called the eigenvalue of states or actions in QRL.*

Then we get the set of eigenvalues of states: $S = |s_n\rangle$ and that of actions for state i: $A_{(i)} = \{|a_n\rangle\}$.

Corollary 1: *Every possible state $|s\rangle$ or action $|a\rangle$ can be expanded in terms of an orthogonal complete set of functions, respectively. We have*

$$|s\rangle = \sum_n \beta_n |s_n\rangle, \quad |a\rangle = \sum_n \beta_n |a_n\rangle$$

where β_n is probability amplitude, which can be a complex number, $|s_n\rangle$ and $|a_n\rangle$ are eigenvalues of states and actions, respectively. The β_n for $|s\rangle$ and $|a\rangle$ is not necessarily the same one, which just mean this corollary holds for both of $|s\rangle$ and $|a\rangle$. $|\beta_n|^2$ means the probability of corresponding eigenvalues and satisfies $\Sigma_n |\beta_n|^2 = 1$.

To implement the QRL system with multi-qubits on a quantum computer, *m* qubits and *n* qubits are used to represent the states and actions, respectively. Thus the states and actions of a QRL system may lie in superposition states:

$$|s^{(m)}\rangle = \sum_{s=00\cdots0}^{\overbrace{11\ldots1}^{m}} C_s |s\rangle, \quad |a^{(n)}\rangle = \sum_{a=00\cdots0}^{\overbrace{11\ldots1}^{n}} C_a |a\rangle$$

where C_s and C_a are both probability amplitudes.

In QRL, the agent is also to learn a policy $\pi : S \times \cup_{i \in S} A_{(i)} \to [0,1]$, which will maximize the expected

sum of discounted reward of each state i.e., the mapping from states to actions is $f(s) = \pi : S \to A$, and we have

$$f(s) = |a_s^{(n)}\rangle = \sum_{a=00\cdots0}^{\overbrace{11\ldots1}^{n}} C_a |a\rangle \tag{13}$$

where C_a is probability amplitude of action $|a\rangle$.

Definition 3: (**Collapse**) *When a quantum state* $|\psi\rangle = \sum_n \beta_n |\psi_n$ *is measured, it will be changed and collapse randomly into one* $|\psi\rangle$ *of its eigenstates with corresponding probability* $|\langle\psi_n|\psi\rangle|^2$*:*

$$|\langle\psi_n|\psi\rangle|^2 = |(|\psi_n\rangle)^* |\psi\rangle|^2 = |\beta_n|^2 \tag{14}$$

Then when an action $|a_s^{(n)}\rangle$ is measured, we will get $|a\rangle$ with the occurrence probability of $|C_a|^2$.

Then according to quantum parallel computation theory, a certain unitary transformation U from input qubit to output qubit can be implemented. Suppose we have such a "quantum black box" which can simultaneously process these 2^m states with the value updating rule

$$V(s) \leftarrow V(s) + \alpha(r + V(s') - V(s)) \tag{15}$$

where α is learning rate, and r is the immediate reward.

The reinforcement strategy is accomplished by changing the probability amplitudes of the actions according to the updated value function. As we know that action selection is executed by measuring action $|a_s^{(n)}\rangle$ related to certain state $|S^{(m)}\rangle$, which will collapse to $|a\rangle$ with the occurrence probability of $|C_a|^2$. So it is no doubt that probability amplitude updating is the key of recording the "trial-and-error" experience and learning to be more intelligent. When an action $|a\rangle$ is executed, it should be able to memorize whether it is "good" or "bad" by changing its probability amplitude C_a.

As action $|a_s^{(n)}\rangle$ is the superposition of n possible eigenactions, to find out $|a\rangle$ and change its probability amplitudes are usually interactional for a quantum system. So we just update the probability amplitude of $|a_s^{(n)}\rangle$ without searching $|a\rangle$, which is inspired by Grover algorithm [13].

The updating of probability amplitude is based on Grover iteration. First, prepare the equally weighted superposition of all eigenactions

$$|a_0^{(n)}\rangle = \frac{1}{\sqrt{2^n}} \left(\sum_{a=00\cdots0}^{\overbrace{11\ldots1}^{n}} |a\rangle \right) \tag{16}$$

We know that $|a\rangle$ is an eigenaction and can get

$$\langle a | a_0^{(n)}\rangle = \frac{1}{\sqrt{2^n}} \tag{17}$$

Now assume the eigenaction to be reinforced is $|a_j\rangle$, and we can construct Grover iteration through combining two reflections U_a and $U_{a_0^{(n)}}$ [1]

$$U_{a_j} = I - 2|a_j\rangle\langle a_j| \tag{18}$$

$$U_{a_0^{(n)}} = 2|a_0^{(n)}\rangle\langle a_0^{(n)}| - I \tag{19}$$

where I is unitary matrix. U_{a_j} flips the sign of the action $|a_j\rangle$, but acts trivially on any action orthogonal to $|a_j\rangle$. Acting on any vector in the 2^n-dimensional Hilbert space, U_{a_j} reflects the vector about the hyperplane orthogonal to $|a_j\rangle$. On the other hand, $U_{a_0^{(n)}}$ preserves $|a_0^{(n)}\rangle$, but flips the sign of any vector orthogonal to $|a_0^{(n)}\rangle$. Grover iteration is the unitary transformation

$$U_{Grov} = U_{a_0^{(n)}} U_{a_j} \tag{20}$$

By repeatedly applying the transformation U_{Grov} on $|a_0^{(n)}\rangle$, we can enhance the probability amplitude of the basis action $|a_j\rangle$ while suppressing the amplitude of all other actions. This can also be looked upon as a kind of rotation in two-dimensional space. Applying Grover iteration U_{Grov} for K times on $|a_0^{(n)}\rangle$ can be represented as [14]

$$\begin{aligned} U_{Grov}^K |a_0^{(n)}\rangle &= \sin((2K+1)\theta)|a_j\rangle \\ &\quad + \cos((2K+1)\theta)|\varphi\rangle \end{aligned} \tag{21}$$

where

$$|\varphi\rangle = \sqrt{\frac{1}{2^n - 1}} \sum_{a \neq a_j} |a\rangle$$

θ satisfying $\sin\theta = 1/\sqrt{2^n}$.

The procedural form of a standard QRL algorithm [14] is described as Fig. 3. For more detailed introduction and analysis of QRL, please refer to [14, 16].

Procedural QRL:

Initialize $|s^{(m)}\rangle = \sum_{s=00\cdots0}^{11\ldots1} C_s |s\rangle$, $f(s) = |a_s^{(n)}\rangle = \sum_{a=00\cdots0}^{11\ldots1} C_a |a\rangle$ and $V(s)$ arbitrarily

Repeat (for each episode)

For all states $|s\rangle$ in $|s^{(m)}\rangle = \sum_{s=00\cdots0}^{11\ldots1} C_s |s\rangle$:

1. Observe $f(s) = |a_s^{(n)}\rangle$ and get $|a\rangle$;
2. Take action $|a\rangle$, observe next state $|s'\rangle$, reward r, then
   (a) Update state value: $V(s) \leftarrow V(s) + \alpha(r + \gamma V(s') - V(s))$
   (b) Update probability amplitudes:
   repeat for $[k(r + V(s'))]$ times
   $U_{Grov}|a_s^{(n)}\rangle = U_{a_0^{(n)}} U_a |a_s^{(n)}\rangle$

Until for all states $|\Delta V(s)| \leq \varepsilon$.

Figure 3. The procedure of QRL

5. EXAMPLE DEMENSTRATION

A five-qubit example is demonstrated to test the presented approach for the control of a five-qubit system [2]. A five-qubit has 32 eigenstates, but in practical quantum information technology, some state transitions can easily be completed

through appropriate unitary transformations while the others are not easy to be accomplished [2].

As shown in Fig. 4, assume we know the state transitions of the five-qubit system satisfy the following equations through some experiments:

$$|00001\rangle = \hat{U}_{00}|00000\rangle;\ |00010\rangle = \hat{U}_{01}|00001\rangle$$

$$|00011\rangle = \hat{U}_{02}|00010\rangle;\ |00100\rangle = \hat{U}_{03}|00011\rangle$$

$$|00101\rangle = \hat{U}_{04}|00100\rangle;\ |00111\rangle = \hat{U}_{11}|00001\rangle$$

$$|01000\rangle = \hat{U}_{12}|00010\rangle;\ |01010\rangle = \hat{U}_{14}|00100\rangle$$

$$|01011\rangle = \hat{U}_{15}|00101\rangle;\ |01000\rangle = \hat{U}_{21}|00111\rangle$$

$$|01011\rangle = \hat{U}_{24}|01010\rangle;\ |01101\rangle = \hat{U}_{31}|00111\rangle$$

$$|10000\rangle = \hat{U}_{34}|01010\rangle;\ |10001\rangle = \hat{U}_{35}|01011\rangle$$

$$|01101\rangle = \hat{U}_{40}|01100\rangle;\ |10001\rangle = \hat{U}_{44}|10000\rangle$$

$$|10010\rangle = \hat{U}_{50}|01100\rangle;\ |10110\rangle = \hat{U}_{54}|10000\rangle$$

$$|10111\rangle = \hat{U}_{55}|10001\rangle;\ |10110\rangle = \hat{U}_{63}|10101\rangle$$

$$|10111\rangle = \hat{U}_{64}|10110\rangle;\ |11000\rangle = \hat{U}_{70}|10010\rangle$$

$$|11100\rangle = \hat{U}_{74}|10110\rangle;\ |11101\rangle = \hat{U}_{75}|10111\rangle$$

$$|11001\rangle = \hat{U}_{80}|11001\rangle;\ |11101\rangle = \hat{U}_{84}|11100\rangle$$

$$|11111\rangle = \hat{U}_{91}|11001\rangle$$

In the above equations, $\hat{U}$ is reversible operator. For example, we can easily get

$$|00000\rangle = \hat{U}_{00}^{-1}|00001\rangle \tag{22}$$

Assume the other transitions are impossible except the above transitions and corresponding inverse transitions. As shown in Fig. 4, suppose the target state is $|\psi_{target}\rangle = |\psi_e\rangle = |11100\rangle$. If the initial unknown quantum state $|\psi_{unknown}\rangle$ is measured through projective measurement and the five-qubit system collapses to an eigenstate $|\psi_j\rangle = |11111\rangle$. But the five-qubit system can not be driven from $|11111\rangle$ to $|11100\rangle$ using any control directly, which is marked with a dash line and a cross as shown in Fig. 4. Thus the following task is to find an optimal control sequence. The QRL method proposed previously is used to find the optimal control sequence to drive the five-qubit system from $|11111\rangle$ to $|11100\rangle$. The parameter settings for QRL algorithm are as follows: learning rate $\alpha = 0.08$, reward $r = -1$ for each state transition until reaching $|11100\rangle$, then a reward $r = 100$ is received.

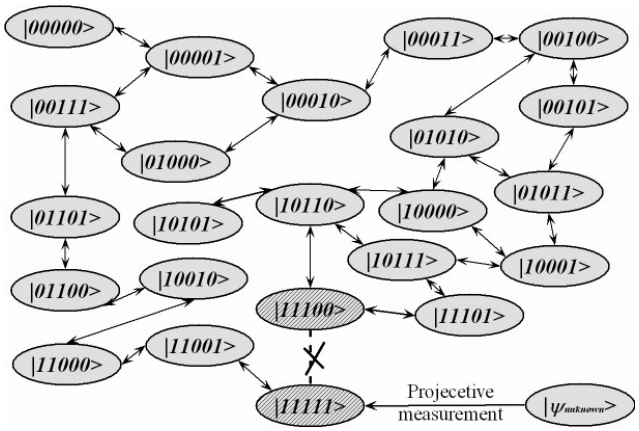

Figure 4. The quantum control problem of a five-qubit system

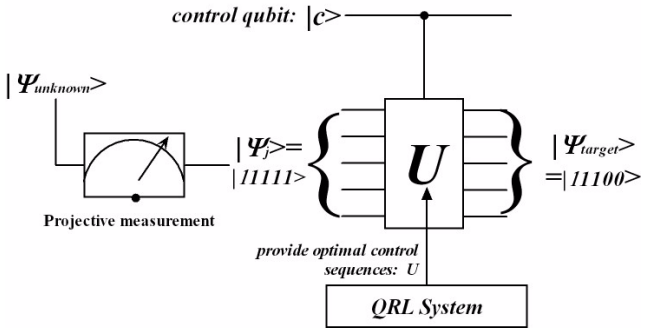

Figure 5. Quantum circuit implementation for the learning control of the five-qubit system

Fig. 5 shows a physical implementation using quantum circuits for the control of the five-qubit system using the approach presented above. After the projective measurement on an unknown quantum state $|\psi_{unknown}\rangle$, the control for the five-qubit system from $|\psi_j\rangle = |11111\rangle$ to $|\psi_{target}\rangle = |11100\rangle$ is carried out using a *Controlled-U* operation on five qubits. As long as the control qubit $|c\rangle = |1\rangle$, the *Controlled-U* operation will transit $|\psi_j\rangle = |11111\rangle$ to $|\psi_{target}\rangle = |11100\rangle$ using the optimal control sequence U learned by the QRL system.

The learning results are shown in Fig. 6. From the results, it is obvious that the algorithm steadily converges to 14 control steps after about 25 episodes of learning. More experiments also show that the control system can robustly find the optimal control sequence for the five-qubit system through learning and there are two optimal control sequences:

$$U = \{\hat{U}_{91}^{-1}, \hat{U}_{80}^{-1}, \hat{U}_{70}^{-1}, \hat{U}_{50}^{-1}, \hat{U}_{40}, \hat{U}_{31}^{-1}, \hat{U}_{21}, \hat{U}_{12}^{-1}, \hat{U}_{02}, \hat{U}_{03}, \hat{U}_{14}, \hat{U}_{34}, \hat{U}_{54}, \hat{U}_{74}\}$$

or

$$\{\hat{U}_{91}^{-1}, \hat{U}_{80}^{-1}, \hat{U}_{70}^{-1}, \hat{U}_{50}^{-1}, \hat{U}_{40}, \hat{U}_{31}^{-1}, \hat{U}_{11}^{-1}, \hat{U}_{01}, \hat{U}_{02}, \hat{U}_{03}, \hat{U}_{14}, \hat{U}_{34}, \hat{U}_{54}, \hat{U}_{74}\}$$

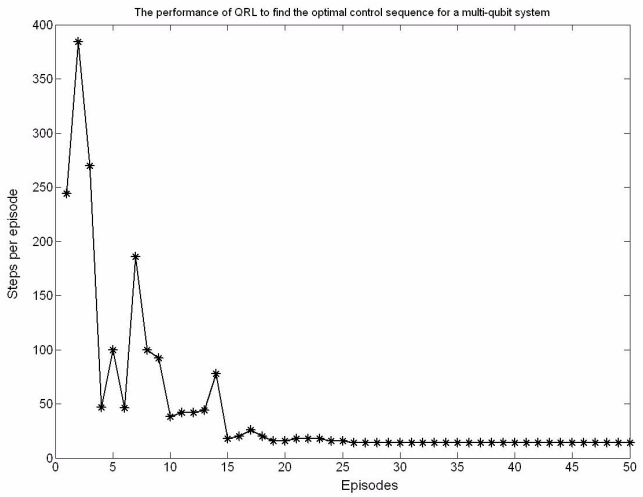

Figure 6. The performance of QRL for optimal control sequence

6. CONCLUSIONS

In this paper, the control problem of multi-qubit is studied using an incoherent control approach based on projective measurement and a quantum reinforcement learning algorithm is used to find an optimal control sequence for the multi-qubit systems. The example demonstrates that the presented approach is feasible and effective. It also provides an alternative strategy to the measurement based incoherent control and learning control of quantum systems.

REFERENCES

[1] M. A. Nielsen, I. L. Chuang, "Quantum Computation and Quantum Information", Cambridge University Press, 2000, ISBN: 7-04-013502-7.

[2] D. Y. Dong, C. L. Chen, Z. H. Chen, C. B. Zhang, "Control of Five-qubit System Based on Quantum Reinforcement Learning", Proc. the 2006 International Conference on Computational Intelligence and Security, Part I, Guangzhou, China, 2006, pp. 164-167.

[3] F. Albertini, D. D'Alessandro, "Notions of controllability for bilinear multilevel quantum systems", IEEE Transactions on Automatic Control, Vol. 48, 2003, pp. 1399-1403.

[4] Z. H. Chen, D. Y. Dong, C. B. Zhang, "Quantum Control Theory: An Introduction", University of Science and Technology of China Press, Hefei, China, 2005. (in Chinese).

[5] D. Y. Dong, Z. H. Chen, "Applications of quantum control theory in chemistry", Progress in Chemistry, Vol. 17, 2005, pp. 581-587.

[6] W. S. Warren, H. Rabitz, M. Dahleh, "Coherent control of quantum dynamics: The Dream Is Alive", Science, Vol. 259, 1993, pp. 1581-1589.

[7] S. Lloyd, "Coherent Quantum Feedback", Physical Review A, Vol. 62, No. 2-022108, 2000, pp. 1-12.

[8] D. D'Alessandro, M. Dahleh, "Optimal control of two-level quantum systems", IEEE Transactions on Automatic Control, Vol. 46, 2001, pp. 866-876.

[9] D. Y. Dong, C. B. Zhang, Z. H. Chen, C. L. Chen, "Information-technology approach to quantum feedback control", International Journal of Modern Physics B, Vol. 20, 2006, pp. 1304-1316.

[10] R. Van Handel, J. K. Stockton, H. Mabuchi, "Feedback control of quantum state reduction", IEEE Transactions on Automatic Control, Vol. 50, 2005, pp. 768-780.

[11] JD. Y. Dong, C. L. Chen, T. J. Tarn, A. Pechen, H. Rabitz, "Incoherent Control of Quantum Systems with Wavefunction Controllable Subspaces via Quantum Reinforcement Learning", IEEE Transactions on Systems, Man, and Cybernetics B, Vol. 38, No. 4, 2008, pp. 957-962.

[12] P. W. Shor, "Algorithms for quantum computation: discrete logarithms and factoring", Proc.35th Annual Symposium on Foundations of Computer Science, IEEE Press, 1994, pp. 124-134.

[13] L. K. Grover, "Quantum Mechanics Helps in Searching for a Needle in a Haystack", Physical Review Letters, Vol. 79, 1997, pp. 325-328.

[14] D. Y. Dong, C. L. Chen, H. X. Li, T. J. Tarn, "Quantum Reinforcement Learning", IEEE Transactions on Systems, Man, and Cybernetics, Part B: Cybernetics, to appear, 2008.

[15] D. Y. Dong, C. L. Chen, C. B. Zhang, Z. H. Chen, "Estimation-Based Information Acquisition in Quantum Feedback Control", Dynamics of Continuous, Discrete and Impulsive Systems-series B-Applications & Algorithms, Vol. 13, 2006, pp. 1204-1208.

[16] C. L. Chen, D. Y. Dong, "Quantum-inspired and Quantum Reinforcement Learning", Reinforcement Learning: Theory and Applications, C. Weber, M. Elshaw, N. M. Mayer (Eds), pp. 59-84, I-Tech Education and Publishing, Vienna, Austria, 2008, ISBN: 978-3-902613-14-1.

[17] D. Y. Dong, C. L. Chen, C. B. Zhang, Z. H. Chen, "Quantum robot: structure, algorithms and applications," Robotica, Vol. 24, 2006, pp. 513-521.

[18] R. Sutton, A. G. Barto, "Reinforcement Learning: An Introduction", MIT Press, Cambridge, MA, 1998, ISBN: 0-262-19398-1.

[19] C. Chen, D. Dong, Z. Chen, H. Wang, "Qualitative control for mobile robot navigation based on reinforcement learning and grey system", The Mediterranean Journal of Measurement and Control, Vol. 4, No. 1, 2008, pp. 1-7.

Biographies

Chunlin Chen (chunlin.chen@ieee.org) was born in Bozhou, Anhui province, China, in 1979. He received his B.S. degree and Ph.D. degree from University of Science and Technology of China in 2001 and 2006, respectively. Now he is a lecturer in the Department of Control and System Engineering of Nanjing University. His research interests include intelligent control, quantum computation and machine learning.

Zhangqing Zhu (zzq-hf@163.com) was born in Wuwei, Anhui province, China, in 1967. He is an associate professor in the Department of Control and System Engineering of Nanjing University. His research interests include network control and nonlinear system.

Xianzhong Zhou (zhouxz@nju.edu.cn) was born in Taixing, Jiangsu province, China, in 1962. He is a professor in the Department of Control and System Engineering of Nanjing University. His research interests include intelligent information processing, system engineering and machine learning.

Qiang Chen (chenqia0772@vip.sina.com) was born in Shanghai, China, in 1971. He received his Ph.D. degree from Nanjing University of Science and Technology in 2006. Now he is a lecturer in the Department of Control and System Engineering of Nanjing University. His research interests include pattern recognition and machine vision.

ESTIMATED FEEDBACK LINEARIZATION CONTROLLER WITH DISTURBANCE COMPENSATOR FOR ROBOTIC APPLICATIONS

A. Merabet *, J. Gu
Department of Electrical & Computer Engineering, Dalhousie University, Halifax, Canada

ABSTRACT

This paper aims to design a robust feedback linearization controller based on state estimation for rigid link robot. The trajectories' tracking for angular positions of the links is the objective to be achieved by this controller. The control law is carried out via a system linearization. The unknown external disturbances, unmodeled quantities and parametric uncertainties are taken into account by designing a disturbance observer. This observer is simplified from the feedback linearization control law and integrated in the control loop as a disturbance compensator. It contains an integral action, which eliminates the steady errors and enhances the robustness of the control scheme. A high gain observer is implemented to deal with robot state estimation. The global stability of the closed loop system (robot, controller, and state observer) and the robustness issue are proved analytically based on the Lyapunov stability theorem. Simulations are carried out for two link rigid robot to verify the performance of the proposed control scheme.

Keywords

Feedback Linearization, Disturbance Compensation, Rigid Link Robot, Disturbance Observer.

1. INTRODUCTION

Control of mobile robot is currently among the main subjects of scientific research in robotic area. Many strategies have been developed in last years for robot control. However, the standard technique PID, with its different combinations, is used for industrial and commercial robot arms. But the dynamic equations of a robot manipulator form a complex, nonlinear, and multivariable system. Suitable methods for control task, called model based controllers, can be derived from the mathematical model of the robot. The most common strategy of model based control is the computed torque control, widely used for industrial robot arms for its simplicity to implement [1-3]. However, it is weakened by the inaccuracies present in the robot model, where the performance of the computed torque control algorithm is not guaranteed. These inaccuracies can be defined as parametric uncertainties, unmodeled dynamics, and unknown external disturbances. To overcome the uncertainties' drawback, robust control can be a solution [4-7]. The goal of robust control is to maintain performance in terms of stability, tracking error, or other specifications despite inaccuracies present in the system.

The robust stabilization of the robotic system, which is uncertain and disturbed, has been considered as major topic for research in the field of control [8-19]. In [8], several approaches for the robust control of the robot motion, such as linear-multivariable, passivity, variable-structure, robust-adaptive, have been discussed with summarize of the available literature on the subject. In [9-11], a robust controller has been designed based on disturbance attenuation, which is included in the control loop. The artificial intelligence has been used in [12, 13] to design an intelligent robust controller. Sliding mode, which is known as a good tool to deal with uncertainties, has been applied successfully in robotic [14], [15]. In [16], the robust controller is designed based on parameters estimation. In [17], an adaptive approach is used to handle with uncertainties. Although these approaches give solutions for the problem of trajectory tracking, the research is open for more adequate control scheme in case of state estimation, considered known in all analysis, which is not always happens in practice.

Based on system inaccuracies compensation, the robust motion control can be decomposed in two parts: nominal part and disturbance compensation part. The nominal part of the control law depends on known nominal part of the system. There are several methods, based on process model, to deal with this kind of control as feedback linearization control [18-20]. The disturbance compensation part depends on total plant uncertainties. This problem can be solved by an estimation of the disturbance [21], which will be used in this work.

The feedback linearization control assumes that all state variables are available. It implies the presence of additional sensors in each joint such as velocity measurements. They are often obtained by means of tachometers, which are perturbed by noise, or moreover, velocity measuring equipment is frequently omitted due to the savings in cost, volume, and weight that can be obtained. Model-based observers are considered very well adapted for state estimation and allow, in most cases, a stability proof and a methodology to tune the observer gains, which guarantee a stable closed loop system [22]. In this work, high gain observer is used for state variables estimation. It is a powerful tool to handle with nonlinear and uncertain systems, which is the case of the robot manipulator [23, 24].

In this paper, we develop a robust tracking-control scheme with the use of a state observer without involving adaptations and velocity measurements of joint angles. Section 2 is

*Corresponding author: *E-mail:* Adel.Merabet@dal.ca

 ISSN: 1743-9310

dedicated to the robot modeling. In Section 3, the control task of the nominal model of the robot is carried out by a feedback linearization control law. Whereas, the robustness is guaranteed through compensation of the system inaccuracies, such as parametric uncertainties, unmodeled dynamics and unknown external disturbances. In Section 4, the state variables, needed for control computation, are obtained from the high gain observer. The closed loop system, containing robot, controller and state observer, is discussed in Section 5. Then, in Section 6, its stability is proved analytically by the theory of guaranteed stability of uncertain systems, which is based on Lyapunov's second method. Finally, simulation results are presented in Section 7.

2. ROBOT MODELING

The dynamic of n-link rigid robot manipulator is driven by the Euler-Lagrange equations as.

$$\mathrm{D}(\mathrm{q})\ddot{\mathrm{q}} + \mathrm{C}(\mathrm{q},\dot{\mathrm{q}})\dot{\mathrm{q}} + \mathrm{G}(\mathbf{q}) = \mathrm{u} \tag{1}$$

where $\mathbf{q}(t) \in \Re^n$ is the vector of the angular joint positions, which are the generalized coordinates and assumed available by measurement. $\mathbf{u}(t) \in \Re^n$ is the vector of the driving torques, which are the control inputs. $\mathbf{D}(\mathbf{q}) \in \Re^{n\times n}$, $\mathbf{D}(\mathbf{q}) = \mathbf{D}(\mathbf{q})^T > 0$ is the link inertia matrix. $\mathbf{C}(\mathbf{q}, \dot{\mathbf{q}})\dot{\mathbf{q}} \in \Re^n$ is the vector of the Coriolis and centripetal torques. $\mathbf{G}(t) \in \Re^n$ is the vector of gravitational torques. The outputs to be controlled are the angular positions.

In practical implementation of the control law, the various sources of uncertainties, such as modeling errors, parametric uncertainty, unknown load and computation errors, must be taken into consideration when modeling the robot. For more information about robot modeling, the reader is referred to [1-3].

The uncertainties of the system, error or mismatch represented by $\Delta(.)$, are added to the computed or nominal value, represented by $(.)_0$, to get the real value of system elements. Therefore, the matrices are rewritten as

$$\begin{cases} \mathrm{D}(\mathrm{q}) = \mathrm{D}_0(\mathrm{q}) + \Delta\mathrm{D} \\ \mathrm{C}(\mathrm{q},\dot{\mathrm{q}}) = \mathrm{C}_0(\mathrm{q},\dot{\mathrm{q}}) + \Delta\mathrm{C} \\ \mathrm{G}(\mathrm{q}) = \mathrm{G}_0(\mathrm{q}) + \Delta\mathrm{G} \end{cases} \tag{2}$$

Moreover, the friction $\mathbf{F_r}(t) \in \Re^n$, considered as an unmodeled quantity, and the external disturbances $\mathbf{b}(t) \in \Re^n$ are added to the robot model (1). It becomes

$$\begin{aligned} \left(\mathrm{D}_0(\mathrm{q}) + \Delta\mathrm{D}\right)\ddot{\mathrm{q}} + \left(\mathrm{C}_0(\mathrm{q},\dot{\mathrm{q}}) + \Delta\mathrm{C}\right)\dot{\mathrm{q}} + \\ \mathrm{G}_0(\mathbf{q}) + \Delta\mathrm{G} + \mathrm{F}_\mathrm{r} = \mathrm{u} + \mathrm{b} \end{aligned} \tag{3}$$

Then, after simplification, the dynamic model of the robot is given by

$$\mathrm{D}_0(\mathrm{q})\ddot{\mathrm{q}} + \mathrm{C}_0(\mathrm{q},\dot{\mathrm{q}})\dot{\mathrm{q}} + \mathrm{G}_0(\mathbf{q}) = \mathrm{u} + \eta(\ddot{\mathrm{q}},\dot{\mathrm{q}},\mathrm{q},\mathrm{b}) \tag{4}$$

η is called uncertainty, which is defined by

$$\eta = -\left\{\Delta\mathrm{D}\ddot{\mathrm{q}} + \Delta\mathrm{C}\dot{\mathrm{q}} + \Delta\mathrm{G} + \mathrm{F}_\mathrm{r} - \mathrm{b}\right\} \tag{5}$$

It includes unmodeled quantities, parametric uncertainties, and external disturbances.

3. CONTROL LAW SYNTHESIS

The control objective is to track some reference trajectories. The controller must be robust to parameters variations, unmodeled quantities and unknown disturbances.

The control law can be decomposed in two parts: nominal part $\mathbf{u}_{nom}$ and disturbance compensation part $\mathbf{u}_{cmp}$

$$\mathbf{u}(t) = \mathrm{u}_{nom}(t) + \mathrm{u}_{cmp}(t) \tag{6}$$

The nominal part of the control law depends on known nominal part of the system (4). It is carried out from the feedback linearization control.

The disturbance compensation part depends on total plant uncertainties:

$$\mathrm{u}_{cmp}(t) = -\eta(\mathrm{q},t) \tag{7}$$

3.1 Feedback Linearization Control

The feedback linearization control can be deduced from the nominal model of the robot, which is given by.

$$\ddot{\mathrm{q}} = -\mathrm{D}_0(\mathrm{q})^{-1}\left(\mathrm{C}_0(\mathrm{q},\dot{\mathrm{q}})\dot{\mathrm{q}} + \mathrm{G}_0(\mathbf{q})\right) + \mathrm{D}_0(\mathrm{q})^{-1}\mathrm{u}_{nom} \tag{8}$$

The principle is to get a linear system, where the output is influenced by an external input **v** only through a chain of two integrators as

$$\ddot{\mathrm{q}} = -\mathrm{D}_0(\mathrm{q})^{-1}\left(\mathrm{C}_0(\mathrm{q},\dot{\mathrm{q}})\dot{\mathrm{q}} + \mathrm{G}_0(\mathbf{q})\right) + \mathrm{D}_0(\mathrm{q})^{-1}\mathrm{u}_{nom} = \mathrm{v} \tag{9}$$

Then, the control law is carried out as

$$\mathrm{u}_{nom} = \mathrm{D}_0(\mathrm{q})\left(\mathrm{v} + \mathrm{D}_0(\mathrm{q})^{-1}\left(\mathrm{C}_0(\mathrm{q},\dot{\mathrm{q}})\dot{\mathrm{q}} + \mathrm{G}_0(\mathrm{q})\right)\right) \tag{10}$$

It is possible to realize a pole-placement by imposing **v** as

$$\mathrm{v} = \ddot{\mathrm{q}}_\mathrm{r} - K_2(\dot{\mathrm{q}} - \dot{\mathrm{q}}_\mathrm{r}) - K_1(\mathrm{q} - \mathrm{q}_\mathrm{r}) \tag{11}$$

where

$$K_1 = diag(k_{1i}),$$
$$K_2 = diag(k_{2i}),\ i = 1,...,n$$

Applying this control law, the tracking error $\mathbf{e_q}(t) = \mathbf{q} - \mathbf{q_r}$ satisfies the second linear equation

$$\ddot{\mathrm{e}}_\mathrm{q}(t) + K_2\dot{\mathrm{e}}_\mathrm{q}(t) + K_1\mathrm{e}_\mathrm{q}(t) = 0 \tag{12}$$

and, hence, the error dynamics are determined by the choice of K_2 and K_1, so that the characteristic equation is Hurwitz.

3.2 Disturbance Compensation

Usually, the uncertainties η are unknown. Therefore, estimation is required to compute accurately the control law and compensate their effects. In this case, the disturbance compensation becomes

$$\mathrm{u}_{cmp}(t) = -\eta_{est}(\mathrm{q}, t) \tag{13}$$

Using (10) and (13), the control law (6) becomes

$$\mathrm{u} = \mathrm{D}_0(\mathrm{q})\left(\mathrm{v} + \mathrm{D}_0(\mathrm{q})^{-1}\left(\mathrm{C}_0(\mathrm{q},\dot{\mathrm{q}})\dot{\mathrm{q}} + \mathrm{G}_0(\mathrm{q})\right)\right) - \eta_{est} \tag{14}$$

As there is no information about uncertainties variations, we can assume that $\dot{\eta}(t) = 0$. This assumption does not necessarily mean a constant variable, but that the changing rate in every sampling interval should be slow.

From the dynamic model of the robot (4), a disturbance observer [21] can be designed as

$$\begin{aligned}\dot{\eta}_{est} &= -P\mathrm{D}_0(\mathrm{q})^{-1}\eta_{est} \\ &+ P\left(\ddot{\mathrm{q}} + \mathrm{D}_0(\mathrm{q})^{-1}\mathrm{C}_0(\mathrm{q},\dot{\mathrm{q}})\dot{\mathrm{q}}\right. \\ &\left. + \mathrm{D}_0(\mathrm{q})^{-1}\mathrm{G}_0(\mathbf{q}) - \mathrm{D}_0(\mathrm{q})^{-1}\mathrm{u}(t)\right)\end{aligned} \tag{15}$$

where $P \in \Re^{n\times n}$ is a matrix gain, which can be chosen as

$$P = diag(p_i),\ i = 1,...,n$$

p_i is a positive constant.

Substituting the control law (14) in observer (15), we get

$$\dot{\eta}_{est}(t) = P\left(\ddot{\mathrm{e}}_{\mathrm{q}}(t) + K_2\dot{\mathrm{e}}_{\mathrm{q}}(t) + K_1\mathrm{e}_{\mathrm{q}}(t)\right) \tag{16}$$

Integrating the equation (16), the observation is defined by

$$\eta_{est}(t) = P\left(\dot{\mathrm{e}}_{\mathrm{q}}(t) + K_2\mathrm{e}_{\mathrm{q}}(t) + K_1\int \mathrm{e}_{\mathrm{q}}(t)dt\right) \tag{17}$$

The observer introduces an integral action, which allows achieving zero steady state error for constant reference inputs and disturbances [7, 18]. K_i (i = 1, 2) are determined following (12) therefore only P is used to tune the controller PID (17).

The control law, which is robust with respect to model uncertainties and external disturbances rejection, is given by

$$\begin{aligned}\mathrm{u} &= \mathrm{D}_0(\mathrm{q})\left(\mathrm{v} + \mathrm{D}_0(\mathrm{q})^{-1}\left(\mathrm{C}_0(\mathrm{q},\dot{\mathrm{q}})\dot{\mathrm{q}} + \mathrm{G}_0(\mathrm{q})\right)\right) \\ &- P\left(\dot{\mathrm{e}}_{\mathrm{q}}(t) + K_2\mathrm{e}_{\mathrm{q}}(t) + K_1\int \mathrm{e}_{\mathrm{q}}(t)dt\right)\end{aligned} \tag{18}$$

3.3 Closed Loop System

Substituting the control law (14) in the robot model (4), the tracking error dynamic is driven by the equation

$$\ddot{\mathrm{e}}_{\mathrm{q}}(t) + K_2\dot{\mathrm{e}}_{\mathrm{q}}(t) + K_1\mathrm{e}_{\mathrm{q}}(t) = \mathrm{D}_0(\mathrm{q})^{-1}\mathrm{e}_{\eta}(t) \tag{19}$$

where $e_{\eta}(t)$ is the error of uncertainties

$$\mathrm{e}_{\eta}(t) = \eta(t) - \eta_{est}(t) \tag{20}$$

From (4) and (15), with the condition $\dot{\eta}(t) = 0$, the tracking error of the disturbance observation is given by

$$\dot{\mathrm{e}}_{\eta}(t) + P\mathrm{D}_0(\mathrm{q})^{-1}\mathrm{e}_{\eta}(t) = 0 \tag{21}$$

Since $K_i > 0$, $p > 0$ and $\mathbf{D_0}(\mathbf{q}) > 0$, it is clear that the closed loop system, described by the dynamic errors (19) and (21), is asymptotically stable.

The control synthesis, given above, assumes that the angular positions and the velocities are known by measurement. However, in real implementation, it is practical to avoid sensors for velocity measurement [1, 23-25].

An estimated feedback controller based on high gain observer for state estimation is given in the next sections, where the stability analysis of the closed loop system and the robustness issue are discussed.

4. HIGH GAIN OBSERVER FOR STATE ESTIMATION

The equation of rigid robot (4) can be rewritten in a state space form as

$$\begin{cases}\dot{\mathrm{x}}_1 = \mathrm{x}_2 \\ \dot{\mathrm{x}}_2 = f(\mathrm{x}_1, \mathrm{x}_2) + g(\mathrm{x}_1)\mathrm{u} + g(\mathrm{x}_1)\eta \\ \mathrm{y} = \mathrm{x}_1\end{cases} \tag{22}$$

where $\mathbf{x}_1 = \mathbf{q}$; $\mathbf{x}_2 = \mathbf{q}$, $\mathbf{y}$ is the measurable position vector.

$$\begin{cases}f(\mathrm{x}_1, \mathrm{x}_2) = -\mathrm{D}_0(\mathrm{x}_1)^{-1}\left(\mathrm{C}_0(\mathrm{x}_1, \mathrm{x}_2)\mathrm{x}_2 + \mathrm{G}_0(\mathrm{x}_1)\right) \\ g(\mathrm{x}_1) = \mathrm{D}_0(\mathrm{x}_1)^{-1}\end{cases} \tag{23}$$

The high gain state observer for the system (22) is designed, to estimate angular positions and velocities, as

$$\begin{cases}\dot{\hat{\mathrm{x}}}_1 = \hat{\mathrm{x}}_2 + H_1(\mathrm{y} - \hat{\mathrm{x}}_1) \\ \dot{\hat{\mathrm{x}}}_2 = f(\hat{\mathrm{x}}_1, \hat{\mathrm{x}}_2) + g(\hat{\mathrm{x}}_1)\mathrm{u} + g(\hat{\mathrm{x}}_1)\hat{\eta}_{est} + H_2(\mathrm{y} - \hat{\mathrm{x}}_1)\end{cases} \tag{24}$$

where $\hat{\mathbf{x}}_i$ (i =1, 2) are the estimated states; $\hat{\eta}_{est}$ is the estimated disturbance carried out from (15) with estimated states.

The estimated nonlinear functions f(.) and g(.) are given by:

$$\begin{cases} f(\hat{x}_1, \hat{x}_2) = -D_0(\hat{x}_1)^{-1}\left(C_0(\hat{x}_1, \hat{x}_2)\hat{x}_2 + G_0(\hat{x}_1)\right) \\ g(\hat{x}_1) = D_0(\hat{x}_1)^{-1} \end{cases} \quad (25)$$

From (22) and (24), the dynamic of observer error is

$$\begin{cases} \dot{\tilde{x}}_1 = -H_1\tilde{x}_1 + \tilde{x}_2 \\ \dot{\tilde{x}}_2 = -H_2\tilde{x}_1 + \delta(q, \hat{q}, t) \end{cases} \quad (26)$$

where

$$\tilde{e} = \begin{bmatrix} \tilde{x}_1 = \tilde{e}_q \\ \tilde{x}_2 = \dot{\tilde{e}}_q \end{bmatrix} = \begin{bmatrix} q - \hat{q} \\ \dot{q} - \dot{\hat{q}} \end{bmatrix} \quad (27)$$

δ(.) is the disturbance term in the observer. It is given by

$$\delta(.) = f(.) - f(\hat{.}) + \left(g(.) - g(\hat{.})\right) u + g(.)\eta - g(\hat{.})\hat{\eta}_{est}$$

The observer gain is chosen such that

$$H = \begin{bmatrix} -H_1 & I_{n\times n} \\ -H_2 & 0_{n\times n} \end{bmatrix} \quad (29)$$

is a Hurwitz matrix.

where

$$H_1 = h_1 * I_{n\times n},\ H_2 = h_2 * I_{n\times n}$$

and h_1, h_2 are positive constants.

In the presence of δ, the observer gains are adjusted as

$$h_1 = \frac{\gamma_1}{\varepsilon},\quad h_2 = \frac{\gamma_2}{\varepsilon^2} \quad (30)$$

where, $0 < \varepsilon << 1$, and γ_1, γ_2 are positive constants.

This adjustment allows making the transfer function from δ to **e** small so that the estimation error is not sensitive to the modeling error [22-24].

5. ESTIMATED CONTROL LAW AND CLOSED LOOP SYSTEM

Integrating the state observer in the control loop, the control law is carried out with the state estimation [25]. Based on state observer (24), the control law (18) becomes

$$u = D_0(\hat{q})\left(\hat{v} + D_0(\hat{q})^{-1}\left(C_0(\hat{q}, \dot{\hat{q}})\dot{\hat{q}} + G_0(\hat{q})\right)\right) - \hat{\eta}_{est} \quad (31)$$

where

$$\hat{v} = \ddot{q}_r - K_2\dot{\hat{e}}_q(t) - K_1\hat{e}_q(t)$$

$$\hat{\eta}_{est}(t) = P\left(\dot{\hat{e}}_q(t) + K_2\hat{e}_q(t) + K_1\int \hat{e}_q(t)dt\right)$$

$$\hat{e}_q = \hat{q} - q_r$$

Substituting the control law (31) in the second equation of (24), we get the dynamic of the tracking error as

$$\ddot{\tilde{e}}_q(t) + K_2\dot{\tilde{e}}_q(t) + K_1\tilde{e}_q(t) = H_2'\tilde{e}(t) \quad (32)$$

where

$$H_2' = \begin{bmatrix} H_2 & 0_{n\times n} \end{bmatrix}$$

In term of tracking error

$$\hat{e} = \begin{bmatrix} \hat{e}_q \\ \dot{\hat{e}}_q \end{bmatrix} = \begin{bmatrix} \hat{q} - q_r \\ \dot{\hat{q}} - \dot{q}_r \end{bmatrix} \quad (33)$$

We can write equations (32) and (33) in state space form as

$$\dot{\hat{e}}(t) = A\hat{e}(t) + B\tilde{e}(t) \quad (34)$$

where

$$A = \begin{bmatrix} 0_{n\times n} & I_{n\times n} \\ -K_1 & -K_2 \end{bmatrix},\ B = \begin{bmatrix} 0_{n\times n} & 0_{n\times n} \\ H_2 & 0_{n\times n} \end{bmatrix}$$

The disturbance observer (15) can be designed from state observation as

$$\begin{aligned} \dot{\hat{\eta}}_{est} = &-PD_0(\hat{q})^{-1}\hat{\eta}_{est} \\ &+ P\left(\ddot{\hat{q}} + D_0(\hat{q})^{-1}C_0(\hat{q}, \dot{\hat{q}})\dot{\hat{q}}\right. \\ &+ D_0(\hat{q})^{-1}G_0(\hat{q}) \\ &\left. - D_0(\hat{q})^{-1}u(t)\right) \end{aligned} \quad (35)$$

From the second equation of (24), and the assumption ($\dot{\eta}(t) = 0$), the error dynamic of the disturbance observer is given by

$$\dot{\hat{e}}_\eta(t) = -PH_2'\tilde{e}(t) \quad (36)$$

where $\hat{e}_\eta(t)$ is the error of uncertainties based on state estimation.

$$\hat{e}_\eta(t) = \eta(t) - \hat{\eta}_{est}(t) \quad (37)$$

and

$$H_2' = [H_2 \quad 0_{n\times n}]$$

The error dynamic of the state observer is driven by the equation (26). In matrix form, it can be written as

$$\dot{\tilde{\mathrm{e}}}(t) = H\tilde{\mathrm{e}}(t) + W\delta(t) \tag{38}$$

where

$$W = \begin{bmatrix} 0_{n\times n} \\ I_{n\times n} \end{bmatrix}$$

Adding the term ($\mathbf{q}$ – $\mathbf{q_r}$) and its derivatives in (32), the tracking error, for the actual angular positions, is given by

$$\dot{\mathrm{e}}(t) = A\mathrm{e}(t) + \bar{B}\tilde{\mathrm{e}}(t) + W\delta(t) \tag{39}$$

where,

$$\mathrm{e} = \begin{bmatrix} \mathrm{q} - \mathrm{q_r} \\ \dot{\mathrm{q}} - \dot{\mathrm{q}}_\mathrm{r} \end{bmatrix},\ \bar{B} = \begin{bmatrix} 0_{n\times n} & 0_{n\times n} \\ -K_1 & -K_2 \end{bmatrix}$$

6. STABILITY ANALYSIS AND ROBUSTNESS ISSUE

The robustness issue, global stability and boundedness of tracking errors for the complete system (system, controller, state observer, and disturbance observer) are discussed in this section. The theory of guaranteed stability of uncertain systems, which is based on Lyapunov's second method, is used in this work.

The propriety of boundedness of the model elements of the robot are given from [1].

- Since $\mathbf{D}_0(\mathbf{q})$ > 0, it can be assumed that $\underline{\mathbf{D}} \le \left\|\mathbf{D}_0(\mathbf{q})^{-1}\right\| \le \overline{\mathbf{D}}$, where $\underline{\mathbf{D}}$, $\overline{\mathbf{D}}$ are positive constants.
- The matrix $\mathbf{C}_0(\mathbf{q}, \dot{\mathbf{q}})$ is linear on $\dot{\mathbf{q}}(t)$ and bounded on **qt.**). Therefore,

$$\left\|\mathrm{C}_0(\mathrm{q},\dot{\mathrm{q}})\right\| \le \alpha_1 \left\|\dot{\mathrm{q}}\right\|;\ \alpha_1 \in \Re^+.$$

- The vector $\mathbf{G}_0(\mathbf{q})$ satisfies $\left\|\mathbf{G}_0(\mathbf{q})\right\| \le \alpha_2$; $\alpha_2 \in \Re^+$.
- All variations Δ(.) are bounded.
- The signals $\dot{\mathbf{q}}_\mathbf{r}$, $\ddot{\mathbf{q}}_\mathbf{r}$ are bounded.
- The vector function $f(\mathbf{x}_1, \mathbf{x}_2)$ is Lipschitz with respect to $\mathbf{x}_2$. Thus, there exists $\kappa > 0$ such that

$$\left\|f(\mathrm{x}_1,\mathrm{x}_2) - f(\mathrm{x}_1,\dot{\mathrm{q}}_{ref})\right\| \le \kappa\left\|\mathrm{x}_2 - \dot{\mathrm{q}}_{ref}\right\| = \kappa\left\|\mathrm{e}_2\right\|;$$
$$\forall(\mathrm{x}_1,\mathrm{x}_2) \in \Re^n \times \Re^n$$

From the error dynamic of the state observer (38), the matrix H is Hurwitz because $h_i > 0$. Then, for any symmetric positive define matrix **Q**, there exists a symmetric positive defined matrix **P** satisfying the Lyapunov equation

$$H^T\mathrm{P} + \mathrm{P}H = -\mathrm{Q} \tag{40}$$

Lets define the function

$$V_1 = \tilde{\mathrm{e}}^T\mathrm{P}\tilde{\mathrm{e}} \tag{41}$$

Its derivative is given by

$$\dot{V}_1 = -\tilde{\mathrm{e}}^T\mathrm{Q}\tilde{\mathrm{e}} + 2\tilde{\mathrm{e}}^T\mathrm{P}W\delta \tag{42}$$

Using the relationship

$$\lambda_{\min}(\mathrm{Q})\left\|\tilde{\mathrm{e}}\right\|^2 \le \tilde{\mathrm{e}}^T\mathrm{Q}\tilde{\mathrm{e}} \le \lambda_{\max}(\mathrm{Q})\left\|\tilde{\mathrm{e}}\right\|^2 \tag{43}$$

where $\lambda_{min}(\mathbf{Q})$, $\lambda_{max}(\mathbf{Q})$ denote the minimum and the maximum eigenvalues, respectively, of the matrix **Q**.

We have

$$\dot{V}_1 \le -\lambda_{\min}(\mathrm{Q})\left\|\tilde{\mathrm{e}}\right\|^2 + 2\left\|\delta\right\|\ \left\|W\right\|\ \left\|\mathrm{P}\right\|\ \left\|\tilde{\mathrm{e}}\right\| \tag{44}$$

The adjustment of the state observer gains (30) allows neglecting the effect of δ on estimation error $\tilde{\boldsymbol{e}}$. Moreover, from the Lipschitz propriety of $f(\mathbf{x}_1, \mathbf{x}_2)$, it can be considered that

$$\delta \le \gamma\left\|\tilde{\mathrm{e}}\right\| \tag{45}$$

Therefore,

$$\begin{aligned} \dot{V}_1 &\le -\lambda_{\min}(\mathrm{Q})\left\|\tilde{\mathrm{e}}\right\|^2 + 2\gamma\lambda_{\max}(\mathrm{P})\ \left\|\tilde{\mathrm{e}}\right\|^2 \\ &\le -\left(\lambda_{\min}(\mathrm{Q}) - 2\gamma\lambda_{\max}(\mathrm{P})\right)\left\|\tilde{\mathrm{e}}\right\|^2 \end{aligned} \tag{46}$$

which is definite negative if

$$\gamma < \frac{\lambda_{\min}(\mathrm{Q})}{2\lambda_{\max}(\mathrm{P})}$$

Therefore, by LaSalle's invariance theorem, the origin is asymptotically stable.

For the tracking error dynamic (34), since K_i > 0, the same Lyapunov method can be used.

The function to be chosen is

$$V_2 = \hat{\mathrm{e}}^T\overline{\mathrm{P}}\hat{\mathrm{e}} \tag{47}$$

Its derivative is given by

$$\dot{V}_2 = -\hat{\mathrm{e}}^T \bar{\mathrm{Q}} \hat{\mathrm{e}} + 2\hat{\mathrm{e}}^T \bar{\mathrm{P}} B \tilde{\mathrm{e}} \tag{48}$$

Then,

$$\dot{V}_2 \le -\lambda_{\min}(\bar{\mathrm{Q}}) \left\|\hat{\mathrm{e}}\right\|^2 + 2\left\|\tilde{\mathrm{e}}\right\| \ \left\|B\right\| \ \left\|\bar{\mathrm{P}}\right\| \ \left\|\hat{\mathrm{e}}\right\| \tag{49}$$

Since $\tilde{e}$ converge to the origin, we can conclude, using the same analysis as above, that the origin is asymptotically stable for trajectory tracking of estimated state.

For the tracking error (39), the candidate function is chosen as

$$V_3 = \mathrm{e}^T \bar{\mathrm{P}} \mathrm{e} \tag{50}$$

Using the same method, described earlier, we have

$$\dot{V}_3 \le -\lambda_{\min}(\bar{\mathrm{Q}}) \left\|\mathrm{e}\right\|^2 + 2\left(\left\|\tilde{\mathrm{e}}\right\| \ \left\|\bar{B}\right\| \ + \left\|\delta\right\| \ \left\|W\right\|\right) \ \left\|\bar{\mathrm{P}}\right\| \ \left\|\mathrm{e}\right\| \tag{51}$$

Therefore, the asymptotic stability can be demonstrated LaSalle's invariance theorem.

For the disturbance observer (36), the function chosen is

$$V_4 = e_\eta \tag{52}$$

Its derivative is given by

$$\dot{V}_4 = \dot{e}_\eta = -PH_2' \tilde{\mathrm{e}} \tag{53}$$

Since $P > 0$, $H' > 0$ and $\|\tilde{e}\|$ is bounded, the derivative satisfies

$$\dot{V}_4 < 0 \tag{54}$$

To prove the global stability of the closed loop system, let define the Lyapunov function candidate

$$V = V_1 + V_2 + V_3 + V_4 \tag{55}$$

It follows from the asymptotic stability of each sub system that the global asymptotic stability of the complete closed loop system is guaranteed.

Fig. 1 shows the block diagram of the estimated feedback linearization control for a robot manipulator.

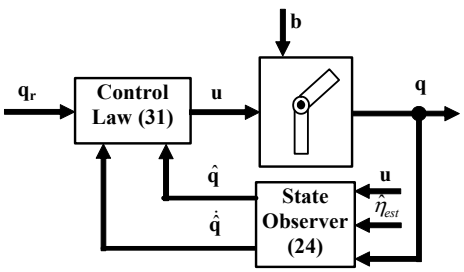

Figure 1. Estimated feedback linearization control for a robot manipulator

7. SIMULATION RESULTS

Simulations are conducted for a two-link rigid robot to test the performance of the proposed control strategy. The elements of the robot model are given by [1]

$$D_{11} = m_1 l_{c1}^2 + m_2 (l_1^2 + l_{c2}^2 + 2 l_1 l_{c2} \cos q_2) + I_1 + I_2$$
$$D_{12} = D_{21} = m_2 (l_{c2}^2 + l_1 l_{c2} \cos q_2) + I_2$$
$$D_{22} = m_2 l_{c2}^2 + I_2$$
$$C_{11} = -(m_2 l_1 l_{c2} \sin q_2) \dot{q}_2$$
$$C_{12} = -(\dot{q}_1 + \dot{q}_2) m_2 l_1 l_{c2} \sin q_2$$
$$C_{21} = (m_2 l_1 l_{c2} \sin q_2) \dot{q}_1$$
$$C_{22} = 0$$
$$G_1 = (m_1 l_{c1} + m_2 l_1) g \cos q_1 + m_2 l_{c2} g \cos(q_1 + q_2)$$
$$G_2 = m_2 l_{c2} g \cos(q_1 + q_2)$$

For i = 1, 2, q_i denotes the joint angle; m_i denotes the mass of link i; l_i denotes the length of link i; l_{ci} denotes the distance from the previous joint to the center of mass of link i; and I_i denotes the moment of inertia of link i.

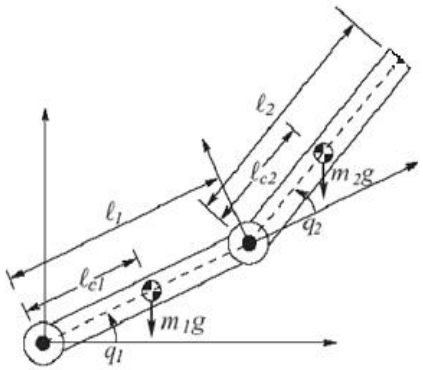

Figure 2. Two-link rigid robot

The values of robot parameters are:

Link 1: $m1$ = 10 kg, l_1 = 1 m, l_{c1} = 0.5 m, I_1 = 10/12 kg-m^2.

Link 2: $m2$ = 5 kg, l_2 = 1 m, l_{c2} = 0.5 m, I_2 = 5/12 kg-m^2.

The initial angular positions and velocities are chosen as:

$$q_1(0) = q_2(0) = 0 \text{ rad}; \ \dot{q}_1(0) = \dot{q}_2(0) = 0 \text{ rad/s}$$
$$\hat{q}_1(0) = \hat{q}_2(0) = 0.1 \text{ rad}; \ \dot{\hat{q}}_1(0) = \dot{\hat{q}}_2(0) = 0 \text{ rad/s}$$

The controller parameters (K_1, K_2), the disturbance observer gains (p_1, p_2) and the state observer gains (h_1, h_2) are chosen by trial and error in order to achieve a satisfactory tracking performance. The choice of values is: K_1 = [400 0; 0 80], K_2 = [800 0; 0 150], $p_1 = p_2$ = 90; h_1 = 104, h_2 = 108.

The simulations are carried out to verify the rejection of an external disturbance and the tracking performance in case of

mismatched model. First, the robot model is affected by a step signal disturbance of value 5 Nm. The disturbance is injected, in the link 1, after 1.5 sec, and after 3 sec in the link 2. Fig. 3 represents the angular positions of joints (1) and (2) under feedback controller without compensation action. It can be seen from the results that steady errors occur in tracking responses. Fig. 4 shows the responses in case of control law with disturbance compensator. It can be noticed that steady errors are eliminated. It is known in control theory that an integral action allows achieving zero steady state error for constant reference inputs and disturbances. However, some overshoots are observed on responses, which can be explained by the PID structure of the disturbance compensator. The output responses are faster compared with results of Fig. 3. The estimation of angles is included in both figures. Fig. 5 gives the estimation of the angular velocity for each joint. It can be seen from estimation results that the state observer gives a good estimation for angle and velocity. Overall, the tracking performances are achieved successfully and the effect of disturbance is well rejected.

In case of mismatched model, the friction includes Coulomb and viscous friction components. It is given by:

$$\mathrm{F_r}(\dot{\mathrm{q}}) = \mathrm{F_c}\,sign(\dot{\mathrm{q}}) + \mathrm{F_v}\dot{\mathrm{q}}$$

where $F_c = F_v = 5\times I_{2\times 2}$ Nm.

Furthermore, we assume that an unknown load is carried by the robot, then the link 2 parameters m2, lc2 and I2 will change with variations: $\Delta m_2 = 2.5$, $\Delta l_{c2} = 0.175$, $\Delta I_2 = 1/12$.

These variations are added only in robot model. The control law (31) and state observer (24) are computed with the nominal values. The same parameters values, as above, are used in this simulation. It can be observed from the Fig. 6 that the outputs (angles) track their reference trajectories, after a while, with zero steady state error. The transient responses are affected by the uncertainties, where the overshoots are bigger than the case of external disturbance rejection. However, their affects are vanished in steady state. These results show that this control strategy is robust against the modeling uncertainties and disturbances.

The simulation results show that responses converge to their references with zero steady errors, which has been verified through the mathematical analysis in the article.

In [1], the robust controller, which is frequently used in literature, is designed by studying the guaranteed stability of uncertain system, based on Lyapunov's second method. The uncertainty is carried out using the angle error and/or its derivative. However, in our case, an integral action is used as part of the disturbance structure, which gives more accuracy for disturbance rejection.

This control strategy combines between feedback linearization control and PID control, which is the contribution of this work. This permits the guarantee of the system stability, elimination of the steady state error and disturbance rejection. Furthermore, the Lyapunov theory is carried out in this work to prove the global stability of the estimated version of this controller applied to the robot manipulator.

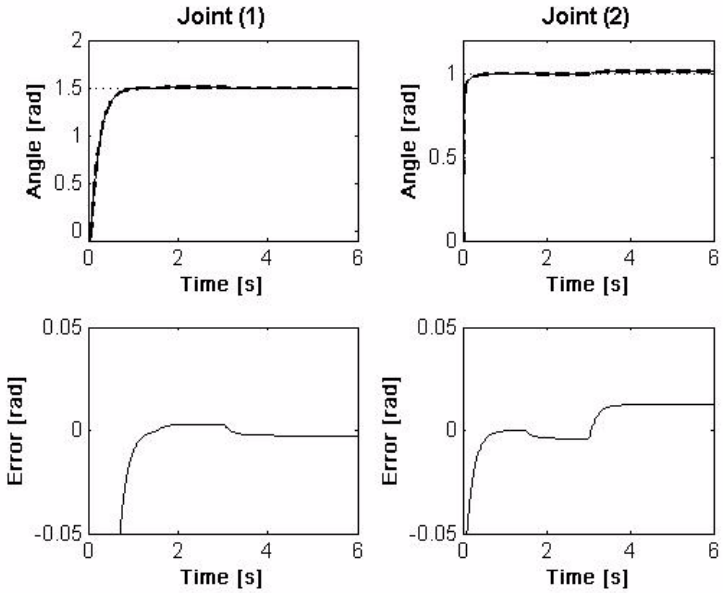

Figure 3. Angular positions of joints (1) and (2) under feedback controller without compensation action (…..) desired, (----) estimate, (___) actual

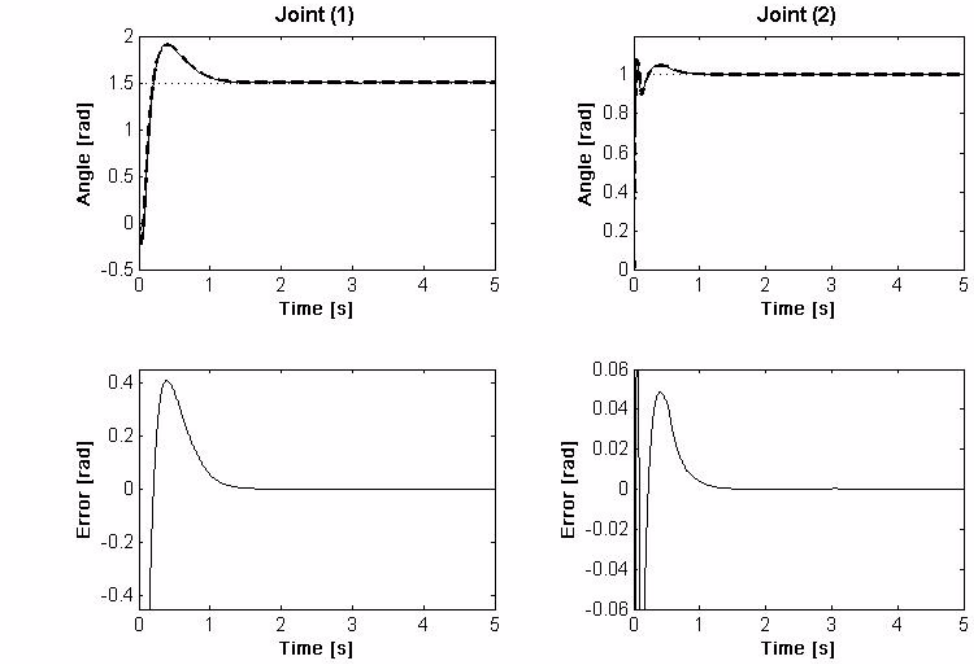

Figure 4. Angular positions of joints (1) and (2) under feedback controller with compensation action (…..) desired, (----) estimate, (——) actual

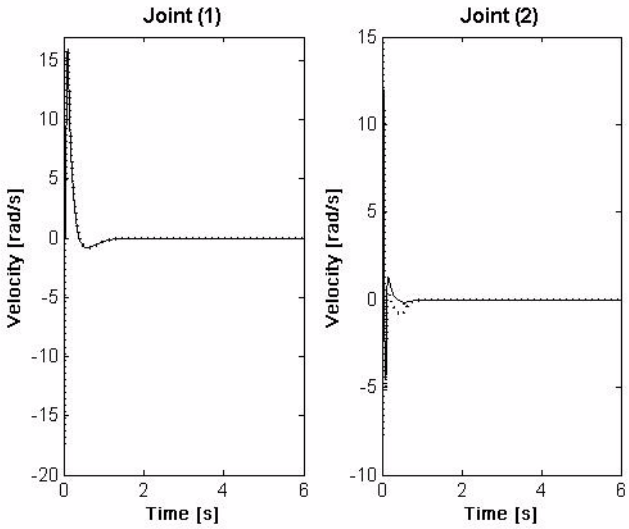

Figure 5. Angular velocities of joints (1) and (2) (…..) estimate, (——) actual

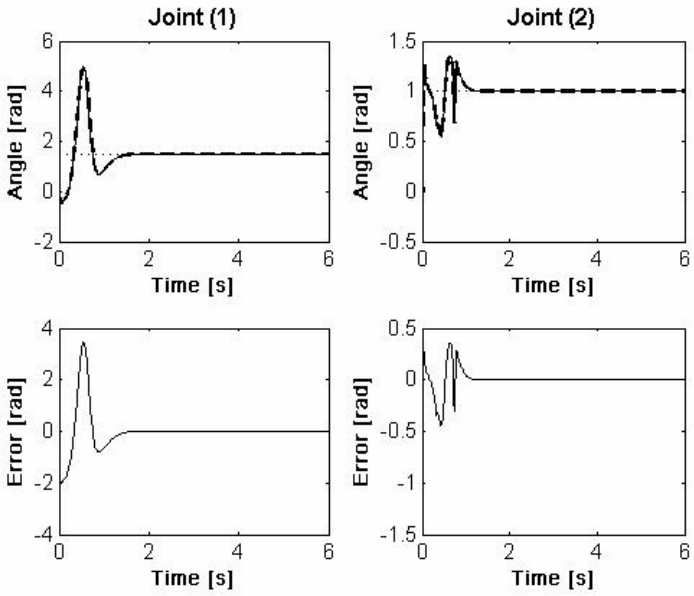

Figure 6. Angular positions of joints (1) and (2) of mismatched model under feedback controller with compensation action ….. desired, ---- estimate, (—) actual

8. CONCLUSIONS

A robust feedback linearization controller based on state estimation for rigid robot is presented in this work. The controller is robust with respect to modeling errors, very effective in disturbance rejection, and gives no steady state error caused by either parameters uncertainties or external disturbances. The robustness is guaranteed by a disturbance compensator, which is designed from the feedback linearization control law. The control synthesis and the stability of the closed loop system are studied for measured positions and velocities. Then, the same study is carried out with estimated quantities. The velocities, needed in control calculation, are estimated by means of a high gain nonlinear observer. The control law is computed with the estimation of the positions and velocities. It has been shown analytically that the global asymptotic stability of the closed loop system (robot, controller, and state observer) is guaranteed. Results were given to illustrate the link position tracking performance of the proposed robust feedback linearization controller based on state estimation.

REFERENCES

[1] M. W. Spong, S. Hutchinson, M. Vidyasagar, "Robot modeling and control", John Wiley & Sons, USA, 2006, ISBN: 978-0-471-64990-8.

[2] E. Dombre, W. Khalil, "Robots manipulators: Modeling, Performances, analysis and control", Wiley-ISTE, London, UK, 2007, ISBN: 978-1-905209-10-1.

[3] H. Asada, J. J. E. Slotine, "Robot analysis and control", John Wiley & Sons, NY, USA, 1986, ISBN: 978-0-471-83029-0.

[4] B. Xian, D. M. Dawson, M. S. De Queiroz, J. Chen, "A continuous asymptotic tracking control strategy for uncertain nonlinear systems", IEEE Transactions on Automatic Control, Vol. 49, No. 7, 2004, pp. 1206-1211.

[5] F. Lin, R. D. Brandt, J. Sun, "Robust control of nonlinear systems: compensating for uncertainty", International Journal of Control, Vol. 56, No. 6, 1992, pp. 1453-1459.

[6] Y. F. Peng, C. M. Lin, "RCMAC-based adaptive control for uncertain nonlinear systems", IEEE Transactions on Systems, Man, and Cybernetics-Part B: Cybernetics, Vol. 37, No. 3, 2007, pp. 651-666.

[7] A. Cavallo, G. De Maria, P. Nistri, "Robust control design with integral action and limited rate control", IEEE Transactions on Automatic Control, Vol. 44, No. 8, 1999, pp. 1569-1572.

[8] C. H. C. Abdallah, D. M. Dawson, P. Dorato, M. Jamshidi, "Survey of the robust control of robots", IEEE Control Systems Magazine, Vol. 11, No. 2, 1991, pp. 24-30.

[9] C. H. Choi, N. Kwak, "Disturbance attenuation in robot control", Proc. of IEEE International Conference on robotics & Automation, Seoul, Korea, 2001, pp. 2560-2565.

[10] P. Tomei, "Tracking control of flexible joint robots with uncertain parameters and disturbances", IEEE Transactions on Automatic Control, Vol. 39, No. 5, 1994, pp. 1067-1072.

[11] C. H. Choi, N. Kwak, "Robust control of robot manipulator by model-based disturbance attenuation", IEEE/ASME Transactions on Mechatronics, Vol. 8, No. 4, 2003, pp. 511-513.

[12] A. Hamzaoui, N. Essounbouli, K. Benmahammed, J. Zaytoon, "State observer based robust adaptive fuzzy controller for nonlinear uncertain and perturbed systems", IEEE Transactions on Systems, Man, and Cybernetics-Part B: Cybernetics, Vol. 34, No. 2, 2004, pp. 942-950.

[13] Y. C. Chang, "Intelligent robust control for uncertain nonlinear time-varying systems and its application to robotic

systems", IEEE Transactions on Systems, Man, and Cybernetics-Part B: Cybernetics, Vol. 35, No. 6, 2005, pp. 1108-1119.

[14] B. Curk, K. Jezernik, "Sliding mode control with perturbation estimation: Application on DD robot mechanism", Robotica, Vol. 19, No. 10, 2001, pp. 641-648.

[15] A. C. Huang, Y-C. Chen, "Adaptive sliding control for single-link flexible-joint robot with mismatched uncertainties," IEEE Transactions on Control Systems, Vol. 12, No. 5, 2004, pp. 770-775.

[16] K. M. Koo, J. H. Kim, "Robust control of robot manipulators with parametric uncertainty," IEEE Transactions on Automatic Control, Vol. 39, No. 6, 1994, pp. 1230-1233.

[17] Z. Li, S.S. Ge, H. A. Ming, "Adaptive robust motion/force control of holonomic-constrained nonholonomic mobile manipulators", IEEE Transactions on Systems, Man, and Cybernetics-Part B: Cybernetics, Vol. 37, No. 3, 2007, 2007, pp. 607-616.

[18] J. P. Corriou, "Process control: Theory and applications", Springer, London, UK, 2004, ISBN 1-85233-776-1.

[19] K. Mitobe, N. Mori, K. Aida, Y. Nasu, "Nonlinear feedback control of a biped walking robot", Proc. IEEE International Conference on Robotics and Automation, Nagoya, Aichi, Japan, 1995, pp. 2865-2870.

[20] X. Yun, Y. Yamamoto, "On feedback linearization of mobile robots," Technical Reports (CIS), Department of Computer & Information Science, University of Pennsylvania, USA, 1992.

[21] W. H. Chen, D. J. Balance, P. J. Gawthrop, J. O'Reilly, "A nonlinear disturbance observer for robotic Manipulators", IEEE Transactions on Industrial Electronics, Vol. 47, No. 4, 2000, pp. 932-938.

[22] W. Wang, Z. Gao "A comparison study of advanced state observer design techniques", Proc. American Control Conference, Denver, Colorado, USA, 2003, pp. 4754-4759.

[23] H. K. Khalil, "High-gain observers in nonlinear feedback control. New directions in nonlinear observer design", (Lecture Notes in Control and Information Sciences), Vol. 24, No. 4, 1999, pp. 249-68.

[24] J. A. Heredia, W. Yu, "A high-gain observer-based PD control for robot manipulator" Proc. American Control Conference, Chicago, Illinois, USA, 2000, pp. 2518-2522.

[25] A. Rodriguez-Angeles, H. Nijmeijer, "Synchronizing tracking control for flexible joint robots via estimated state feedback", ASME Journal of Dynamic Systems, Measurement and Control, Vol. 126, 2004, pp. 162-172.

Biographies

Adel Merabet received his Ingeniorat d'etat degree in Electrical Engineering from Annaba University, Algeria, in 1998. DEA degree in Automatic and Applied Computer from Ecole Centrale de Nantes, France, in 2002. Ph.D. degree in Electrical Engineering from University of Quebec at Chicoutimi, Canada, in 2007. He is currently a postdoctoral fellow in Department of Electrical & Computer Engineering at Dalhousie University, Halifax, Canada. His areas of interest include process control, robotics, artificial intelligence, electric machines and drives.

Jason Gu received his bachelor's degree from Electrical Engineering and Information Science at the University of Science and Technology of China in 1992 and his Master's degree from Biomedical Engineering at Shanghai Jiaotong University in 1995 and Ph.D. degree from the University of Alberta in Canada in Electrical and Computer Engineering in 2001. He is currently an associate professor in Electrical and Computer Engineering at Dalhousie University in Canada. He is also a cross-appointed professor in School of Biomedical Engineering and Faculty of Computer Science for his multidisciplinary research work. Dr. Gu's research areas include robotics, biomedical engineering, rehabilitation engineering, neural networks, and control. Dr. Gu was a recipient of best paper award in ICCSE 2003. He also was awarded Faculty of Engineering Teaching award in 2003, the outstanding IEEE Student Branch Councillor award in 2004 and Discovery Award of the Province of Nova Scotia in Canada in 2005, and faculty of Engineering Research award in 2006. Dr. Gu is a member of American Society of Engineering Education, a senior member of IEEE.

LINEAR FRACTIONAL TRANSFORMATION BASED H-INFINITY OUTPUT STABILIZATION FOR TAKAGI-SUGENO FUZZY MODELS

M. Zerar, K. Guelton, N. Manamanni *
Universite de Reims Champagne-Ardenne, CReSTIC - URCA, 51687 Reims Cedex, France

ABSTRACT

In this paper, a global stabilization and robust Dynamic Output Feedback Controller (DOFC) design methodology for Takagi-Sugeno (T-S) fuzzy systems is proposed. Based on a standard robust control structure, one rewrites an original nonlinear model as an extended nonlinear model with exogenous inputs. The latter contains control objectives that are classically introduced in terms of linear weighting functions in robust control theory. In order to point out the interconnection between the extended nonlinear model and the designated DOFC, unsolvable stability conditions are derived using Linear Fractional Transformation (LFT) and H_∞ tools. Based on the universal approximator properties of T-S modeling, the obtained nonlinear stability conditions are then transformed into Linear Matrix Inequalities (LMI) to allow the design of a dedicated Full Parallel Distributed Compensation (FPDC) DOFC. In that case, when a solution is tractable from the proposed LMI conditions, the synthesized controller guarantees the prescribed stability performances. Finally, a numerical example is used to illustrate the validity of the designed approach.

Keywords

Takagi-Sugeno Fuzzy Models, Robust Control, Linear Fractional Transformation (LFT), Linear Matrix Inequalities (LMI), H-Infinity.

1. INTRODUCTION

In the past few years, considerable attention has been devoted to the stability and controller design of fuzzy control systems. Among nonlinear control theory, the Takagi-Sugeno (T-S) fuzzy model [1] is becoming popular since it is able of universal approximations of a wide class of nonlinear systems [2, 3]. Moreover, some recent studies have shown their practicability; see e.g. [4, 5]. Therefore, the T-S fuzzy models are intensively used for analyzing stability problems related to fuzzy systems [6, 7]. Several corresponding control schemes have been developed, in the literature, to solve the problem of the T-S fuzzy models stabilization and control since early nineties (see for instance [8, 9] and references therein). The typical approach for controller design is carried out via the so-called Parallel Distributed Compensation (PDC) method [10, 11].

Since the stability and performance are two essential problems in control theory, many improved results have been proposed such as state feedback [11-13], and robust static output feedback controller design [14]. Note that these approaches remain static state feedback which leads to lower computational cost when implementing real time systems. Nevertheless, as the compensation to the nonlinear dynamics of the controlled system remains on a simple state feedback, it can be shown that static state feedback are less powerful when specified performances are desired with respect to the transient response [15, 16].

To improve the closed-loop dynamic control laws' performances, robust control based on Dynamic Output Feedback Controller (DOFC) has been extensively studied in various kinds of linear systems (Linear Time Invariant (LTI), Linear Parameter Varying (LPV), Linear Time Varying (LTV) [15-17]. These techniques are often based on the H_∞ criteria [16, 18] and on the Linear Fractional Transformation (LFT) paradigm [21]. Dealing with T-S fuzzy models, DOFC design has been proposed in [20, 27, 28]. Let us point out that, in the author's best knowledge, LFT based approaches are scarcely used in T-S fuzzy approaches.

In this paper, we propose an H_∞ / LFT based DOFC design methodology for T-S fuzzy models that can be summarized as follows: after introducing the control objectives in terms of linear weighting functions, an extended nonlinear model with exogenous inputs can be obtained from the nonlinear model. Then, nonlinear T-S fuzzy output feedback dynamic control law can be obtained using a finite set of Linear Matrix Inequalities (LMI) with H_∞ criteria optimization [16].

The rest of this paper is organized as follows: After the nonlinear control problem statement, a recall of T-S modeling, lower LFT representations and the proposed nonlinear T-S control design methodology will be presented in Section 2. In Section 3, the efficiency of the proposed approach is illustrated through a numerical example. Finally in Section4, we concluded our work of this paper.

2. NONLINEAR CONTROL PROBLEM STATEMENT

Let us consider the following class of nonlinear systems:

$$\begin{cases} \dot{x}(t) = A(x(t))x(t) + B(x(t))u(t) \\ y(t) = C(x(t))x(t) \end{cases} \quad (1)$$

*Corresponding author: *E-mail:* noureddine.manamanni@univ-reims.fr

 ISSN: 1743-9310

where $x(t) \in \Re^n$ is the state vector, $u(t) \in \Re^m$ is the control vector, $y(t) \in \Re^q$ is the measured output vector, $A(.) \in \Re^{n \times n}$, $B(.) \in \Re^{n \times m}$ and $C(.) \in \Re^{q \times n}$ are the state, input and output nonlinear matrices, respectively.

The objective is to design a DOFC given by the following nonlinear state space representation:

$$\begin{cases} \dot{x}^c(t) = A^c\left(x(t)\right)x^c(t) + B^c\left(x(t)\right)y(t) \\ u(t) = C^c\left(x(t)\right)x^c(t) + D^c\left(x(t)\right)y(t) \end{cases} \quad (2)$$

where $x^c(t) \in \Re^{n_c}$ is the controller state vector, $A^c(.) \in \Re^{n_c \times n_c}$, $B^c(.) \in \Re^{n_c \times q}$, $C^c(.) \in \Re^{m \times n_c}$ and $D^c(.) \in \Re^{m \times q}$ are the controller matrices.

To design such controller, performance control objectives can be introduced in terms of linear weighting functions. This can be achieved using the standard control structure depicted in Fig. 1 [22, 23].

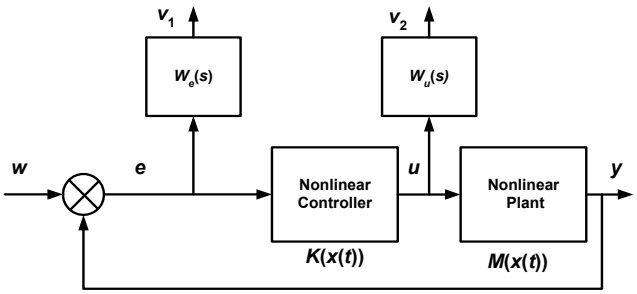

Figure 1. Standard control structure diagram

Within this structure, $w(.) \in \Re^q$ represent an exogenous input vector, $e(.) \in \Re^q$ is the error vector and $v(.) = [v_1(.)^T, v_2(.)^T]^T \in \Re^{q+m}$ is the controlled output vector. The different objectives are specified in terms of linear weighting functions $W_e(s)$ and $W_u(s)$ on the sensitivity ($S(s)$ transfer) and controls inputs ($KS(s)$ transfer) respectively (Fig. 1). The weighting functions are defined in order to remove the fast variation of the error signal and to bound variations of the control signal $u(t)$. The choice of these weighting functions is done following the methodology presented in [22, 23].

Thus, the linear tracking weighting function is given by the following linear state space representation:

$$\begin{cases} \dot{x}_e(t) = A_e x_e(t) + B_e e(t) \\ v_1(t) = C_e x_e(t) + D_e e(t) \end{cases} \quad (3)$$

In the same way, the linear control weighting function is given as follows:

$$\begin{cases} \dot{x}_u(t) = A_u x_u(t) + B_u u(t) \\ v_2(t) = C_u x_u(t) + D_u u(t) \end{cases} \quad (4)$$

where $x_e(.) \in \Re^q$ and $x_u(.) \in \Re^m$ are the W_e and W_u state vector respectively. $A_e \in \Re^{n_e \times n_e}$, $B_e \in \Re^{n_e \times q}$, $C_e \in \Re^{q \times n_e}$, $D_e \in \Re^{q \times q}$, $A_u \in \Re^{n_u \times n_u}$, $B_u \in \Re^{n_u \times m}$, $C_u \in \Re^{m \times n_u}$ and $D_u \in \Re^{m \times m}$ are constant matrices.

Combining (1), (3) and (4), an extended nonlinear model with exogenous inputs can be written as follows:

$$\begin{cases} \dot{\tilde{x}}(t) = \tilde{A}\left(x(t)\right)\tilde{x}(t) + \tilde{B}_1 w(t) + \tilde{B}_2\left(x(t)\right)u(t) \\ v(t) = \tilde{C}_1\left(x(t)\right)\tilde{x}(t) + \tilde{D}_{11} w(t) + \tilde{D}_{12} u(t) \\ y(t) = \tilde{C}_2\left(x(t)\right)\tilde{x}(t) \end{cases} \quad (5)$$

where $\tilde{x}(t) = \left[x_e^T\ x_u^T\ x^T\right]^T$ is the extended state vector, and

$$\tilde{A}\left(\tilde{x}(t)\right) = \begin{bmatrix} A_e & 0 & -B_e C\left(x(t)\right) \\ 0 & A_u & 0 \\ 0 & 0 & A\left(x(t)\right) \end{bmatrix},$$

$$\tilde{B}_1 = \begin{bmatrix} B_e \\ 0 \\ 0 \end{bmatrix},\ \tilde{B}_2\left(\tilde{x}(t)\right) = \begin{bmatrix} 0 \\ B_u \\ B\left(x(t)\right) \end{bmatrix},$$

$$\tilde{D}_{11} = \begin{bmatrix} D_e \\ 0 \end{bmatrix},\ \tilde{D}_{12} = \begin{bmatrix} 0 \\ D_u \end{bmatrix},$$

$$\tilde{C}_1\left(\tilde{x}(t)\right) = \begin{bmatrix} C_e & 0 & -D_e C\left(x(t)\right) \\ 0 & C_u & 0 \end{bmatrix}$$

$$\tilde{C}_2\left(\tilde{x}(t)\right) = \left[0\ 0\ C\left(x(t)\right)\right]$$

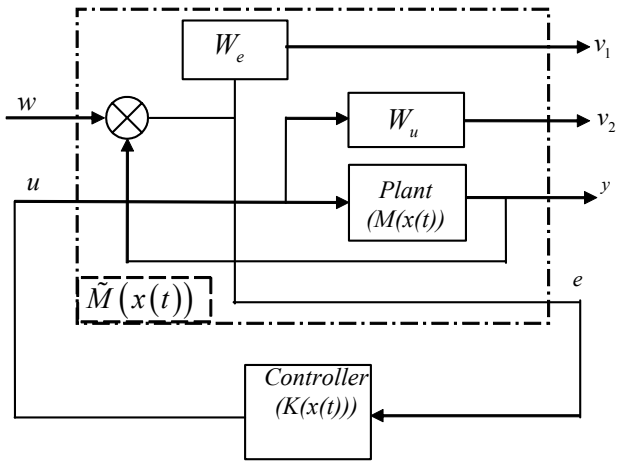

Figure 2. Lower LFT diagram

Let us recall that a convenient way to run to the closed loop formulation from (5) and (2) is to consider the well-known LFT tools. Note that, since the striking pioneer work of Redheffer [21], this tool play an important role in robust control system design [15, 24]. The LFT algebra arises naturally when one describes a so-called "well-posed" feedback system as shown by the block diagram depicted in Fig. 2 where $\tilde{M}(x(t))$ and $K(x(t))$ are the system's matrices realizations of (5) and (2) respectively defined as:

$$\tilde{M}\left(x(t)\right)=\left(\begin{array}{c|cc}\tilde{A}\left(x(t)\right) & \tilde{B}_1 & \tilde{B}_2\left(x(t)\right)\\ \hline \tilde{C}_1\left(x(t)\right) & \tilde{D}_{11} & \tilde{D}_{12}\\ \tilde{C}_2\left(x(t)\right) & 0 & 0\end{array}\right) \quad (6)$$

$$K\left(x(t)\right)=\left(\begin{array}{c|c}A^c\left(x(t)\right) & B^c\left(x(t)\right)\\ \hline C^c\left(x(t)\right) & D^c\left(x(t)\right)\end{array}\right) \quad (7)$$

From Fig. 2, the resulting input/output relation can be represented as,

$$v(t)=F_l\left(\tilde{M}\left(x(t)\right),K\left(x(t)\right)\right)w(t)$$

where $F_l(.)$ is said to be the lower LFT of $\tilde{M}(x(t))$ on $K(x(t))$. Then, the corresponding closed loop system's matrix realization $F_l(\tilde{M}(x(t)),K(x(t)))$ is given using the Redhefer star product of $\tilde{M}(x(t))$ and $K(x(t))$ defined by (8) [15, 21]:

$$\begin{aligned}F_l\left(\tilde{M}\left(x(t)\right),K\left(x(t)\right)\right)&=\left(\begin{array}{c|c}A_{cl}\left(x(t)\right) & B_{cl}\\ \hline C_{cl}\left(x(t)\right) & D_{cl}\end{array}\right)\\ &=\left(\begin{array}{cc|c}\tilde{A}\left(x(t)\right)+\tilde{B}_2\left(x(t)\right)D^c\left(x(t)\right)\tilde{C}_2\left(x(t)\right) & \tilde{B}_2\left(x(t)\right)C^c\left(x(t)\right) & \tilde{B}_1\\ B^c\left(x(t)\right)\tilde{C}_2\left(x(t)\right) & A^c\left(x(t)\right) & 0\\ \hline \tilde{C}_1\left(x(t)\right)+\tilde{D}_{12}D^c\left(x(t)\right)\tilde{C}_2\left(x(t)\right) & \tilde{D}_{12}C^c\left(x(t)\right) & \tilde{D}_{11}\end{array}\right)\end{aligned} \quad (8)$$

Once the closed-loop dynamics (8) being defined, the goal is now to provide conditions ensuring to find a DOFC of the form (2) so that the closed loop system is stable. To address this problem, the direct Lyapunov methodology can be employed. Thus, let us consider the following candidate quadratic Lyapunov function:

$$V\left(\tilde{x}(t)\right)=\tilde{x}(t)^T\,P\tilde{x}(t)\geq 0,\ P=P^T>0 \quad (9)$$

The problem is to design a nonlinear DOFC (2) stabilizing the closed loop nonlinear system (8) and satisfying the following H_∞ constraints:

$$\sup_{\|w(t)\|_2\neq 0}\frac{\|v(t)\|_2}{\|w(t)\|_2}=\left\|F_l\left(\tilde{M}\left(x(t)\right),K\left(x(t)\right)\right)\right\|_\infty<\gamma \quad (10)$$

where $\|.\|_2$ is defined as the L_2 norm and γ is a positive scalar performance level to be minimized to ensure the best dynamics of the closed-loop system.

Then (10) can be rewritten as:

$$\int_0^\infty\left(v(t)^T\,v(t)-\gamma^2 w(t)^T\,w(t)\right)dt<0 \quad (11)$$

In the sequel, when there is no ambiguity, the time variable t and the parameters of the nonlinear matrices $\bullet(x(t))$ will be omitted for more clarity of the mathematical expressions.

The decrease of (9) can be constrained by (11), it yields:

$$\dot{\tilde{x}}^T P\tilde{x}+\tilde{x}^T P\dot{\tilde{x}}+v^T v-\gamma^2 w^T w<0 \quad (12)$$

From (8), we have

$$\dot{\tilde{x}}=A_{cl}\tilde{x}+B_{cl}w,\ v=C_{cl}\tilde{x}+D_{cl}w$$

so (12) can be rewritten as:

$$\begin{aligned}&\tilde{x}^T\left(A_{cl}{}^T P+PA_{cl}\right)\tilde{x}+w^T B_{cl}{}^T P\tilde{x}\\ &+\tilde{x}^T PB_{cl}w+\tilde{x}^T C_{cl}{}^T v\\ &+w^T D_{cl}{}^T v+v^T C_{cl}\tilde{x}+v^T D_{cl}w\\ &-v^T v-\gamma^2 w^T w<0\end{aligned} \quad (13)$$

That is to say,

$$\begin{pmatrix}\tilde{x}\\ w\\ v\end{pmatrix}^T\begin{pmatrix}A_{cl}{}^T P+PA_{cl} & (*) & (*)\\ B_{cl}{}^T P & -\gamma^2 I & (*)\\ C_{cl} & D_{cl} & -I\end{pmatrix}\begin{pmatrix}\tilde{x}\\ w\\ v\end{pmatrix}<0 \quad (14)$$

It is obvious that (14) holds if:

$$\begin{pmatrix}A_{cl}{}^T P+PA_{cl} & (*) & (*)\\ B_{cl}{}^T P & -\gamma^2 I & (*)\\ C_{cl} & D_{cl} & -I\end{pmatrix}<0 \quad (15)$$

Let us consider

$$L=P^{-1}=\begin{bmatrix}Q_1 & Q_2\\ Q_2{}^T & Q_3\end{bmatrix}>0,\ L^{-1}=P=\begin{bmatrix}P_1 & P_2\\ P_2{}^T & P_3\end{bmatrix}>0$$

such that:

$$L = L_1 L_2 = \begin{bmatrix} Q_1 & I \\ Q_2^{\,T} & 0 \end{bmatrix} \begin{bmatrix} I & P_1 \\ 0 & P_2^{\,T} \end{bmatrix}^{-1} \tag{16}$$

Since $LL^{-1} = I$, we have the following constraint $Q_2 P_2^T = I - Q_1 P_1$ and the $P > 0$ condition is equivalent (see [19]) to:

$$\begin{bmatrix} Q_1 & I \\ I & P_1 \end{bmatrix} > 0$$

Multiplying respectively left and right by

$$\begin{pmatrix} L & 0 & 0 \\ 0 & I & 0 \\ 0 & 0 & I \end{pmatrix} \text{and} \begin{pmatrix} L & 0 & 0 \\ 0 & I & 0 \\ 0 & 0 & I \end{pmatrix}^T$$

we obtain,

$$\begin{pmatrix} L_2^{\,T} L_1^{\,T} A_{cl}^{\,T} + A_{cl} L_1 L_2 & (*) & (*) \\ B_{cl}^{\,T} & -\gamma^2 I & (*) \\ C_{cl} L_1 L_2 & D_{cl} & -I \end{pmatrix} < 0 \tag{17}$$

then, multiplying left by

$$\begin{pmatrix} L_2^{\,-1} & 0 & 0 \\ 0 & I & 0 \\ 0 & 0 & I \end{pmatrix}^T$$

and multiplying right by

$$\begin{pmatrix} L_2^{\,-1} & 0 & 0 \\ 0 & I & 0 \\ 0 & 0 & I \end{pmatrix}$$

we obtain,

$$\begin{pmatrix} L_1^{\,T} A_{cl}^{\,T} L_2^{\,-1} + L_2^{\,-T} A_{cl} L_1 & (*) & (*) \\ B_{cl}^{\,T} L_2^{\,-1} & -\gamma^2 I & (*) \\ C_{cl} L_1 & D_{cl} & -I \end{pmatrix} < 0 \tag{18}$$

Substituting (8) and (16) in (18), an equivalent nonlinear inequality (NLI) can be obtained and given in the following extended form:

$$\begin{pmatrix} \Psi_{11}(x(t)) & (*) & (*) & (*) \\ \Psi_{21}(x(t)) & \Psi_{22}(x(t)) & (*) & (*) \\ \tilde{B}_1^{\,T} & \tilde{B}_1^{\,T} P_1 & -\gamma^2 I & (*) \\ \Psi_{41}(x(t)) & \Psi_{42}(x(t)) & \tilde{D}_{11} & -I \end{pmatrix} < 0 \tag{19}$$

where

$$\begin{aligned} \Psi_{11}(x(t)) = {} & Q_1^{\,T} \tilde{A}(x(t))^T + \tilde{A}(x(t)) Q_1 \\ & + Q_1^{\,T} \tilde{C}_2(x(t))^T D^c(x(t))^T \tilde{B}_2(x(t))^T \\ & + \tilde{B}_2(x(t)) D^c(x(t)) \tilde{C}_2(x(t)) Q_1 \\ & + Q_2 C^c(x(t))^T \tilde{B}_2(x(t))^T \\ & + \tilde{B}_2(x(t)) C^c(x(t)) Q_2^{\,T} \end{aligned}$$

$$\begin{aligned} \Psi_{21}(x(t)) = {} & \tilde{A}(x(t))^T \\ & + \tilde{C}_2(x(t))^T D^c(x(t))^T \tilde{B}_2(x(t))^T \\ & + P_1^T \tilde{A}(x(t)) Q_1 \\ & + P_2 B^c(x(t)) \tilde{C}_2(x(t)) Q_1 \\ & + P_2 A^c(x(t)) Q_2^{\,T} \\ & + P_1^T \tilde{B}_2(x(t)) D^c(x(t)) \tilde{C}_2(x(t)) Q_1 \\ & + P_1^T \tilde{B}_2(x(t)) C^c(x(t)) Q_2^{\,T} \end{aligned}$$

$$\begin{aligned} \Psi_{22}(x(t)) = {} & \tilde{A}(x(t))^T P_1 + P_1^T \tilde{A}(x(t)) \\ & + \tilde{C}_2(x(t))^T D^c(x(t))^T \tilde{B}_2(x(t))^T P_1 \\ & + P_1 \tilde{B}_2(x(t)) D^c(x(t)) \tilde{C}_2(x(t)) \\ & + \tilde{C}_2(x(t))^T B^c(x(t))^T P_2^T \\ & + P_2 B^c(x(t)) \tilde{C}_2(x(t)) \end{aligned}$$

$$\begin{aligned} \Psi_{41}(x(t)) = {} & \tilde{C}_1(x(t)) Q_1 \\ & + \tilde{D}_{12} D^c(x(t)) \tilde{C}_2(x(t)) Q_1 \\ & + \tilde{D}_{12} C^c(x(t)) Q_2^{\,T} \end{aligned}$$

$$\Psi_{42}(x(t)) = \tilde{C}_1(x(t)) + \tilde{D}_{12} D^c(x(t)) \tilde{C}_2(x(t))$$

Remark 1: The nonlinear model (1), with the tracking and control performances (3) and (4), is stable via the output feedback control law (2) under H_∞ performances (10), if there exist the matrices $P_1 = P_1^T > 0$, $P_2 = P_2^T > 0$, $Q_1 = Q_1^T > 0$, $Q_2 = Q_2^T > 0$, $A^c(x(t))$, $B^c(x(t))$, $C^c(x(t))$, $D^c(x(t))$ regulars with appropriate dimensions and a scalar $\gamma > 0$ such that the NLI (19) is fulfilled.

Notice that, there are no direct tools to solve this NLI. Therefore, in the next section, one proposes to use a fuzzy T-S modeling approach in order to provide LMI stability conditions able to overcome this problem.

3. LMI STABILITY FORMULATION BASED ON T-S MODELLING

Let us recall that, over the past two decades, there has been rapidly growing interest in approximating a nonlinear system by a T-S fuzzy model [1, 6, 25]. The fuzzy modelling approach provides a powerful tool for modelling complex nonlinear systems. Unlike conventional modelling approaches, where a single model is used to describe the global behaviour of a system, T-S modelling approach considers local LTI systems combined by membership functions to describe the global behaviour of the nonlinear system [1]. Indeed, a continuous time nonlinear system of the form (1) can be approximated by a T-S fuzzy model constituted by the r following IF-THEN rules:

Plant Rule i: **IF** $z_1(t)$ is M_1^i and … and $z_p(t)$ is M_p^i, **THEN**

$$\begin{cases} \dot{x}(t) = A_i x(t) + B_i u(t) \\ y(t) = C_i x(t) \end{cases}, \; i = 1, 2, ..., r \qquad (20)$$

where $z_1(t) \ldots z_p(t)$ are the premise variables, M_j^i $(j = 1, \ldots, p)$ are fuzzy sets, $x(t) \in \Re^n$ is the state vector, $u(t) \in \Re^m$ is the input vector, $y(t) \in \Re^q$ is the controlled output vector, $A_i \in \Re^{n \times n}$, $B_i \in \Re^{n \times m}$ and $C_i \in \Re^{q \times n}$ are constant matrices and r is the number of IF-THEN rules. Then, using the barycentric defuzzification method [8], the fuzzy model is inferred as:

$$\begin{cases} \dot{x}(t) = \sum_{i=1}^{r} h_i(z(t)) \left(A_i x(t) + B_i u(t) \right) \\ y(t) = \sum_{i=1}^{r} h_i(z(t)) \left(C_i x(t) \right) \end{cases} \qquad (21)$$

with

$$z(t) = \left[z_1(t), \ldots, z_p(t) \right]^T, w_i(z(t)) = \prod_{j=1}^{p} M_j^i(z(t))$$

$$h_i(z(t)) = \frac{w_i(z(t))}{\sum_{i=1}^{r} w_i(z(t))}$$

where $M_j^i(z_j(t))$ is the fuzzy membership grade of $z_j(t)$ in M_j^i. Note that, $w_i(z(t)) \geq 0$, $\sum_{i=1}^{r} w_i(z(t)) > 0$. Therefore, the following convex property holds:

$$h_i(z(t)) \geq 0 \text{ and } \sum_{i=1}^{r} h_i(z(t)) = 1$$

Note that (21) can obviously be rewritten, when considering the weighting functions (3) and (4), in the form of an exogenous input (5). That is to say, by the following exogenous T-S model:

$$\begin{cases} \dot{\tilde{x}}(t) = \sum_{i=1}^{r} h_i(z(t)) \left(\tilde{A}_i \tilde{x}(t) + \tilde{B}_{2i} u(t) \right) + \tilde{B}_1 w(t) \\ v(t) = \sum_{i=1}^{r} h_i(z(t)) \tilde{C}_{1i} \tilde{x}(t) + \tilde{D}_{11} w(t) + \tilde{D}_{12} u(t) \\ y(t) = \sum_{i=1}^{r} h_i(z(t)) \tilde{C}_{2i} \tilde{x}(t) \end{cases} \qquad (22)$$

where $\tilde{A}_i$, $\tilde{B}_1$, $\tilde{B}_{2i}$, $\tilde{C}_{1i}$, $\tilde{C}_{2i}$, $\tilde{D}_{11}$ and $\tilde{D}_{12}$ are the LTI system state matrices defined as:

$$\tilde{A}_i = \begin{bmatrix} A_e & 0 & -B_e C_i \\ 0 & A_u & 0 \\ 0 & 0 & A_i \end{bmatrix}, \tilde{B}_1 = \begin{bmatrix} B_e \\ 0 \\ 0 \end{bmatrix},$$

$$\tilde{B}_{2i} = \begin{bmatrix} 0 \\ B_u \\ B_i \end{bmatrix}, \tilde{C}_{1i} = \begin{bmatrix} C_e^T & 0 \\ 0 & C_u^T \\ -C_i^T D_e^T & 0 \end{bmatrix}^T$$

$$\tilde{D}_{11} = \begin{bmatrix} D_e \\ 0 \end{bmatrix}, \tilde{D}_{12} = \begin{bmatrix} 0 \\ D_u \end{bmatrix}$$

Let us also recall that the most commonly used control scheme for T-S fuzzy model is the so-called Parallel Distributed Compensation (PDC) [11]. The meaning of such control laws is the use of the same membership functions as the one used by the T-S model to be stabilized. Thus, after checking (19) with the fuzzy blending of (22), one can propose the following PDC control law using a summation structure chosen in order to fully compensate the nonlinear stability condition (19):

$$\begin{cases} \dot{x}^c(t) = \sum_{i=1}^{r} \sum_{j=1}^{r} \sum_{k=1}^{r} h_i h_j h_k A_{ijk}^c x^c(t) \\ \qquad + \sum_{j=1}^{r} \sum_{k=1}^{r} h_j h_k B_{jk}^c y(t) \\ u(t) = \sum_{j=1}^{r} \sum_{k=1}^{r} h_j h_k C_{jk}^c x^c(t) + \sum_{k=1}^{r} h_k D_k^c y(t) \end{cases} \qquad (23)$$

where A_{ijk}^c, B_{jk}^c, C_{jk}^c and D_k^c are constant matrices with appropriate dimensions to be synthesized. Thus, substituting (22) and (23) in (19), the NLI can be rewritten as (24):

$$\sum_{i=1}^{r}\sum_{j=1}^{r}\sum_{k=1}^{r} h_i h_j h_k \begin{pmatrix} \Psi_{11}^{ijk} & (*) & (*) & (*) \\ \Psi_{21}^{ijk} & \Psi_{22}^{ijk} & (*) & (*) \\ \tilde{B}_1^{\,T} & \tilde{B}_1^{\,T} P_1 & -\eta I & (*) \\ \tilde{C}_{1i} Q_1 + \tilde{D}_{12} D_k^c \tilde{C}_{2i} Q_1 + \tilde{D}_{12} C_{ik}^c Q_2^{\,T} & \tilde{C}_{1i} + \tilde{D}_{12} D_k^c \tilde{C}_{2i} & \tilde{D}_{11} & -I \end{pmatrix} < 0 \tag{24}$$

where

$$\Psi_{11}^{ijk} = Q_1^{\,T} \tilde{A}_i^{\,T} + \tilde{A}_i Q_1 + Q_1^{\,T} \tilde{C}_{2i}^{\,T} D_k^{cT} \tilde{B}_{2j}^{\,T} + \tilde{B}_{2j} D_k^c \tilde{C}_{2i} Q_1 + Q_2 C_{ik}^{c\,T} \tilde{B}_{2j}^{\,T} + \tilde{B}_{2j} C_{ik}^c Q_2^{\,T}$$

$$\Psi_{21}^{ijk} = \tilde{A}_i^{\,T} + \tilde{C}_{2i}^{\,T} D_k^{cT} \tilde{B}_{2j}^{\,T} + P_1^T \tilde{A}_i Q_1 + P_1^T \tilde{B}_{2j} D_k^c \tilde{C}_{2i} Q_1 + P_1^T \tilde{B}_{2j} C_{ik}^c Q_2^{\,T} + P_2 B_{jk}^c \tilde{C}_{2i} Q_1 -$$

$$\Psi_{22}^{ijk} = \tilde{A}_i^{\,T} P_1 + P_1^T \tilde{A}_i + \tilde{C}_{2i}^{\,T} D_k^{cT} \tilde{B}_{2j}^{\,T} P_1 + P_1 \tilde{B}_{2j} D_k^c \tilde{C}_{2i} + \tilde{C}_{2i}^{\,T} B_{jk}^{c\,T} P_2^T + P_2 B_{jk}^c \tilde{C}_{2i}$$

Using the following change of variables:

$$G_{1ik} = D_k^c C_{2i} Q_1 + C_{ik}^c Q_2,\ G_{2jk} = P_1^T \tilde{B}_{2j} D_k^c + P_2 B_{jk}^c,$$
$$G_{3ijk} = P_1^T \left(\tilde{A}_i + \tilde{B}_{2j} D_k^c \tilde{C}_{2i} \right) Q_1 + P_2 B_{jk}^c \tilde{C}_{2i} Q_1 + P_1^T \tilde{B}_{2j} C_{ik}^c Q_2^{\,T} + P_2 A_{ijk}^c Q_2^{\,T},$$
$$\gamma^2 = \eta$$

the inequality (24) becomes:

$$\sum_{i=1}^{r}\sum_{j=1}^{r}\sum_{k=1}^{r} h_i h_j h_k \Upsilon_{ijk} < 0 \tag{25}$$

$$\Upsilon_{ijk} = \begin{pmatrix} A_i Q_1 + Q_1 A_i^{\,T} + B_{2j} G_{1ik} + G_{1ik}^{\,T} B_{2j}^{\,T} & (*) & (*) & (*) \\ A_i^{\,T} + G_{3ijk} + C_{2i}^{\,T} D_k^{cT} B_{2j}^{\,T} & P_1 A_i + A_i^{\,T} P_1 + G_{2jk} C_{2i} + C_{2i}^{\,T} G_{2jk}^{\,T} & (*) & (*) \\ B_{1i}^{\,T} & B_{1i}^{\,T} P_1 & -\eta & (*) \\ C_{1i} Q_1 + D_{12i} G_{1ik} & C_{1i} + D_{12} D_k^c C_{2i} & D_{11} & -I \end{pmatrix}$$

Note that, a convenient way to obtain LMI stability conditions from (25) is to search the decision variables considering that each $\gamma_{ijk} < 0$, for all combination of $i, j, k = 1, \ldots, r$ [10, 11]. Obviously, these conditions are conservative. In order to relax LMI stability conditions, one proposes to extend the well-known relaxation scheme introduced in [6] to the case of a triple summation structure as appearing in (25). Let us consider the following proprieties [6]:

$$\sum_{i=1}^{r}\sum_{j=1}^{r} h_i(z) h_j(z) \varphi_{ij} = \sum_{i=1}^{r} h_i^2(z) \varphi_{ii} + \sum_{i=1}^{r}\sum_{\substack{j=1 \\ j<i}}^{r} h_i(z) h_j(z) \left(\varphi_{ij} + \varphi_{ji} \right) \tag{26}$$

Therefore, applying twice (26) on (25) one has:

$$\sum_{i=1}^{r} h_i^3 \Upsilon_{iii} + \sum_{i=1}^{r}\sum_{\substack{j=1 \\ j<i}}^{r} h_i h_j^{\,2} \left(\Upsilon_{ijj} + \Upsilon_{jii} \right) + \sum_{i=1}^{r}\sum_{j=1}^{r}\sum_{\substack{k=1 \\ k<j}}^{r} h_i h_j h_k \left(\Upsilon_{ijk} + \Upsilon_{ikj} \right) < 0 \tag{27}$$

Obviously (27) holds if the conditions summarized in the following theorem are satisfied.

Theorem 1: The T-S fuzzy model with exogenous inputs given by (22) is stable via the control law (23) with H_∞ quadratic performances, if there exist matrices $P_1 = P_1^T > 0$, $Q_1 = Q_1^T > 0$, D_k^c, G_{1ik}, G_{2jk}, G_{3ijk} regulars with appropriate dimensions and a scalar $\eta > 0$ such that the following LMIs are satisfied:

$$\text{for } i=1,...,r,\ \Upsilon_{iii}<0 \tag{28}$$

$$\text{for } i=1,...,r,\ j=1,...,r \text{ and } j<i,\ \Upsilon_{ijj}+\Upsilon_{jii}<0 \tag{29}$$

$$\text{for } i=1,...,r,\ k=1,...,r, \text{ and } k<j,\ \Upsilon_{ijk}+\Upsilon_{ikj}<0 \tag{30}$$

with Υ_{ijk} defined in (25)

Remark 2: For a particular numerical example, when there exist a solution to **Theorem 1** from LMIs (28), (29) and (30), the fuzzy controller matrices defined in (23) stabilizing the fuzzy system (21) with respect to the performances objectives introduced by (3) and (4) under $\gamma^2 = \eta$, are obtained using the bijective change of variables

$$\begin{aligned}
C_{ik}^c &= \left(G_{1ik} - D_k^c C_{2i} Q_1\right) Q_2^{-1} \\
A_{ijk}^c &= P_2^{-1}\Big(G_{3ijk} - P_1^T\left(\tilde{A}_i + \tilde{B}_{2j} D_k^c \tilde{C}_{2i}\right) Q_1 \\
&\quad - P_2 B_{jk}^c \tilde{C}_{2i} Q_1 - P_1^T \tilde{B}_{2j} C_{ik}^c Q_2^T\Big) Q_2^{-T} \\
B_{jk}^c &= P_2^{-1}\left(G_{2jk} - P_1^T \tilde{B}_{2j} D_k^c\right)
\end{aligned}$$

Remark 3: Note that other relaxations are available in the literature, see e.g. [29-31]. The objective of this study is not dwelling on the subject of relaxing more and more the proposed stability condition. Nevertheless, In case where is it required by any practical application, these relaxation schemes can obviously be employed together with condition (25) without loss of generality.

4. SIMULATION RESULTS

To illustrate the efficiency of the above proposed controller design methodology, let us consider the following numerical example:

$$\begin{cases} \dot{x}(t) = A\left(x(t)\right)x(t) + B\left(x(t)\right)u(t) \\ y(t) = C\,x(t) \end{cases} \tag{31}$$

where $x(t) = [x_1^T(t), x_2^T(t)]^T$ is the state vector, $u(t)$ is the input vector, $y(t) = x_1(t)$ is the measured output vector and

$$A\left(x(t)\right) = \begin{bmatrix} \sin^2\left(x_1(t)\right) & 3 \\ 1 & 1 \end{bmatrix}$$

$$B\left(x(t)\right) = \begin{bmatrix} 1+\sin^2\left(x_1(t)\right) \\ 1 \end{bmatrix}$$

$$C = \begin{bmatrix} 1 \\ 0 \end{bmatrix}^T$$

The desired performance specifications on control system are defined in terms of frequency low-pass filter W_e and high-pass filter W_u (respectively defined in (3) and (4)) to remove the fast variation of the error signal $e(t)$ and to bound variations of the control signal $u(t)$. In order to show the influence of these weighting functions on the whole nonlinear system behavior, two cases are considered with different parameters (bandwidth, cut-off frequency and static gain). These are given by:

- **Case 1:**

$$\begin{aligned}
W_e &: \begin{cases} \dot{x}_e = -0.5 x_e + 0.5 e \\ v_1 = 0.9\, x_e \end{cases} \\
W_u &: \begin{cases} \dot{x}_u = -1000 x_u - 99.49 u \\ v_2 = 99.49 x_u + 10 u \end{cases}
\end{aligned} \tag{32}$$

- **Case 2:**

$$\begin{aligned}
W_e &: \begin{cases} \dot{x}_e = -0.0025 x_e - 0.4985 e \\ v_1 = -0.4985\, x_e + 0.1 e \end{cases} \\
W_u &: \begin{cases} \dot{x}_u = -1000 x_u - 99.49 u \\ v_2 = 99.49 x_u + 10 u \end{cases}
\end{aligned} \tag{33}$$

Combining (31), (32) (or (33)) and considering $\tilde{x} = [x_e^T\ x_u^T\ x_1^T\ x_2^T]^T$, for each cases, the obtained nonlinear model with exogenous inputs can be represented as:

$$\begin{cases} \dot{\tilde{x}}(t) = \tilde{A}\left(x(t)\right)\tilde{x}(t) + \tilde{B}_1 w(t) + \tilde{B}_2\left(x(t)\right)u(t) \\ v(t) = \tilde{C}_1\left(x(t)\right)\tilde{x}(t) + \tilde{D}_{11} w(t) + \tilde{D}_{12} u(t) \\ y(t) = \tilde{C}_2\left(x(t)\right)\tilde{x}(t) \end{cases} \tag{34}$$

where

$$\tilde{C}_2 = \begin{bmatrix} 0 & 0 & C \end{bmatrix},\ \tilde{A}\left(\tilde{x}(t)\right) = \begin{bmatrix} A_e & 0 & -B_e C \\ 0 & A_u & 0 \\ 0 & 0 & A\left(x(t)\right) \end{bmatrix}$$

$$\tilde{B}_1 = \begin{bmatrix} B_e \\ 0 \\ 0 \end{bmatrix},\ \tilde{B}_2\left(\tilde{x}(t)\right) = \begin{bmatrix} 0 \\ B_u \\ B\left(x(t)\right) \end{bmatrix}$$

$$\tilde{D}_{11} = \begin{bmatrix} D_e \\ 0 \end{bmatrix},\ \tilde{D}_{12} = \begin{bmatrix} 0 \\ D_u \end{bmatrix},\ \tilde{C}_1 = \begin{bmatrix} C_e & 0 & -D_e C \\ 0 & C_u & 0 \end{bmatrix}$$

The nonlinear model (34) contains one nonlinearity ($\sin^2(x_1(t))$). Thus, according to the well know sector nonlinearity approach [8], an exact T-S fuzzy representation of (34) can be obtained considering:

$$\begin{aligned}
&\sin^2(x_1) = (1)\left(\sin^2(x_1)\right) + (0)\left(1-\sin^2(x_1)\right)\\
&h_1(x_1) = \sin^2(x_1)\\
&h_2(x_1) = 1 - h_1(x_1)
\end{aligned} \tag{35}$$

In that case, one has the following 2 rules T-S fuzzy model:

$$\begin{cases}
\dot{\tilde{x}}(t) = \sum_{i=1}^{2} h_i(x_1(t))\left(\tilde{A}_i\tilde{x}(t) + \tilde{B}_{2i}u(t)\right) + \tilde{B}_1 w(t)\\
v(t) = \tilde{C}_1\tilde{x}(t) + \tilde{D}_{12}u(t)\\
y(t) = \tilde{C}_2\tilde{x}(t)
\end{cases} \tag{36}$$

with

$$\tilde{A}_1 = \begin{bmatrix} A_e & 0 & -B_eC \\ 0 & A_u & 0 \\ 0 & 0 & A_1 \end{bmatrix}, \tilde{A}_2 = \begin{bmatrix} A_e & 0 & -B_eC \\ 0 & A_u & 0 \\ 0 & 0 & A_2 \end{bmatrix},$$

$$\tilde{B}_1 = \begin{bmatrix} B_e \\ 0 \\ 0 \end{bmatrix}, \tilde{B}_{21} = \begin{bmatrix} 0 \\ B_u \\ B_1 \end{bmatrix}, \tilde{B}_{22} = \begin{bmatrix} 0 \\ B_u \\ B_2 \end{bmatrix},$$

$$\tilde{C}_1 = \begin{bmatrix} C_e & 0 & -D_eC \\ 0 & C_u & 0 \end{bmatrix}, \tilde{C}_2 = \begin{bmatrix} 0 \\ 0 \\ C \end{bmatrix}^T, \tilde{D}_{12} = \begin{bmatrix} 0 \\ D_u \end{bmatrix}$$

and where

$$A_1 = \begin{bmatrix} 0 & 3 \\ 1 & 1 \end{bmatrix}, A_2 = \begin{bmatrix} 1 & 3 \\ 1 & 1 \end{bmatrix},$$

$$B_1 = \begin{bmatrix} 1 \\ 1 \end{bmatrix}, B_2 = \begin{bmatrix} 2 \\ 1 \end{bmatrix}$$

Then, the goal is now to design a DOFC controller such as:

$$\begin{cases}
\dot{x}^c(t) = \sum_{i=1}^{2}\sum_{j=1}^{2}\sum_{k=1}^{2} h_i h_j h_k A_{ijk}^c x^c(t) + \sum_{j=1}^{2}\sum_{k=1}^{2} h_j h_k B_{jk}^c y(t)\\
u(t) = \sum_{j=1}^{2}\sum_{k=1}^{2} h_j h_k C_{jk}^c x^c(t) + \sum_{k=1}^{2} h_k D_k^c y(t)
\end{cases} \tag{37}$$

The LMI conditions proposed in theorem 1 are solved via the MATLAB™ LMI Control Toolbox [26] twice for case 1 and case 2. For each of these two cases, the whole closed loop system has been simulated through MATLAB/SIMULINK™ with the initial state $x(0) = [1\ -1]^T$. The comparison of the performances is shown in Fig. 3. where it can be noticed that stabilization in case 1 is better than the one in case 2.

For the reader's information, the solutions of **Theorem 1** in the case 1 are given by the matrices:

$$A_{111}^c \simeq A_{121}^c \simeq \begin{bmatrix} -1 & -46 & 63 & -1 \\ 3 & -79 & 79 & 1134 \\ 1 & 24 & -79 & -18643 \\ 0 & 0 & 0 & -87 \end{bmatrix},$$

$$A_{112}^c \simeq A_{122}^c \simeq \begin{bmatrix} -4 & 175 & -245 & -4 \\ 4 & -106 & 117 & 1134 \\ 2 & 2 & -49 & -18644 \\ 0 & 0 & 0 & -87 \end{bmatrix},$$

$$A_{211}^c \simeq A_{221}^c \simeq \begin{bmatrix} 0 & -50 & 63 & -1 \\ 3 & -79 & 79 & 1134 \\ 1 & 25 & -79 & 18643 \\ 0 & 0 & 0 & 87 \end{bmatrix},$$

$$A_{212}^c \simeq A_{222}^c \simeq \begin{bmatrix} -4 & 171 & -245 & 4 \\ 4 & -106 & 117 & 1133 \\ 2 & 3 & -49 & -18644 \\ 0 & 0 & 0 & -87 \end{bmatrix},$$

$$B_{11}^c \simeq B_{12}^c \simeq B_{21}^c \simeq B_{22}^c$$

$$\simeq \begin{bmatrix} 159.4 & -5205 & -3739 & -27.1 \end{bmatrix}^T,$$

$$C_{11}^c \simeq C_{12}^c \simeq C_{21}^c \simeq C_{22}^c$$

$$\simeq \begin{bmatrix} -0.0036 & 0.2387 & -0.3325 & 0.0064 \end{bmatrix},$$

$$D_1^c \simeq D_2^c \simeq 0,$$

$$P_1 \simeq \begin{bmatrix} 1.80 & 0 & -0.0001 & 0.0005 \\ 0 & 174631.80 & 0 & 0 \\ -0.0001 & 0 & 30345386.18 & -35325781.03 \\ 0.0005 & 0 & -35325781.03 & 43554724.33 \end{bmatrix},$$

$$Q_1 \simeq \begin{bmatrix} 2.05 & 0.09 & 5.51 & -1.21 \\ 0.09 & 46.11 & 20.86 & 14 \\ 5.51 & 20.86 & 32.04 & -1.57 \\ -1.21 & 14 & -1.57 & 33.21 \end{bmatrix}$$

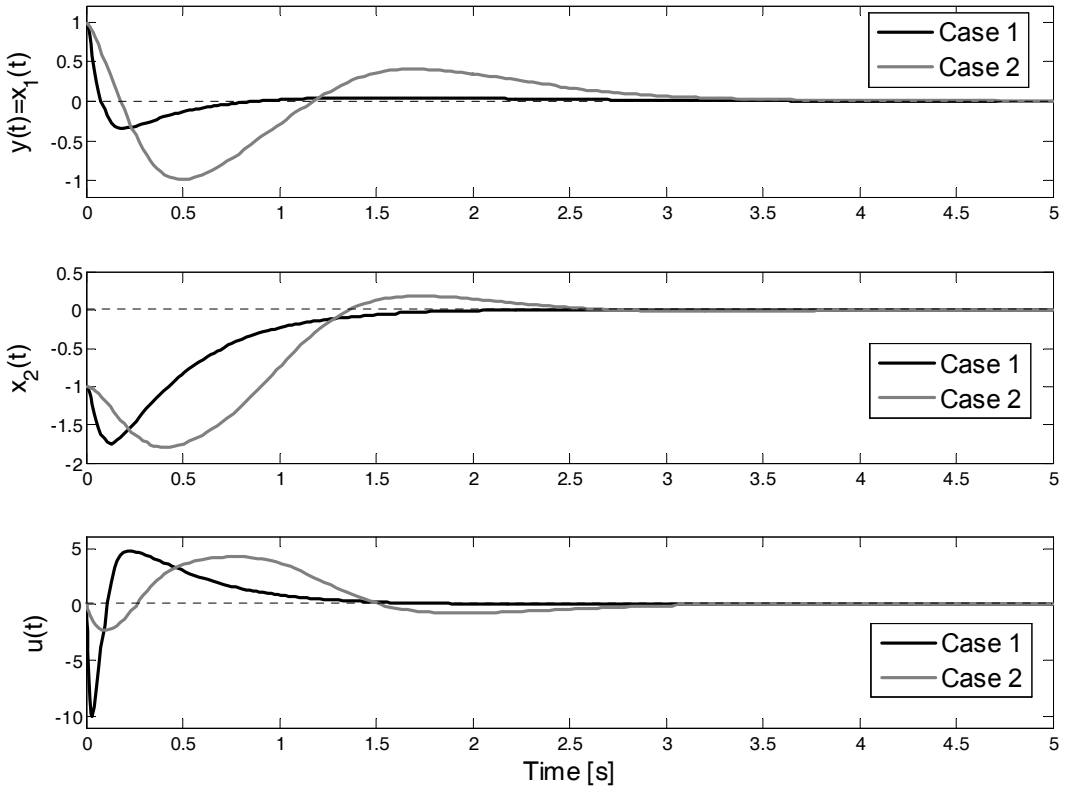

Figure 3. Stabilization, state and control signals, comparison between case 1 and case 2

5. CONCLUSIONS

In this paper, a general framework for Takagi-Sugeno (T-S) fuzzy models LFT based output feedback robust control has been proposed. Thus, adapted from classical linear robust control theory [15-17], an extended model, combining the nonlinear one and the considered weighting function has been derived. Then a bounded real lemma has been obtained in the general case of nonlinear systems. A way to solve the nonlinear control problem, a fuzzy T-S modeling approach is used to derive LMI stability conditions. Indeed, the proposed control methodology remains to H_∞/LFT dynamic output feedback controller synthesis for Takagi-Sugeno systems. That one allows setting stability performances of the closed-loop system. Finally, simulation results and a comparison between two sets of weighting functions have been presented and conclude to the efficiency of the proposed nonlinear control synthesis.

ACKNOWLEDGEMENT

The authors would like to thank the GIS 3SGS for his financial support within the project COSMOS and Mr. Elie Maille for his valuable technical comments.

REFERENCES

[1] T. Takagi, M. Sugeno, “Fuzzy Identification of Systems and its Application to Modelling and Control. IEEE Trans”, Syst., Man and Cyber., Vol. 1115, 1985, pp. 116-132.

[2] H. Ying, “Sufficient conditions on general fuzzy systems as function approximators. Automatica”, Vol. 30. No. 3, 1994, pp. 521-525.

[3] K. Zeng, N. Y. Zhang, W. L. Xu, “A comparative study on sufficient conditions for Takagy Sugeno fuzzy systems as universal approximations”, IEEE Trans. Fuzzy syst, 2000, Vol 8, pp. 773-780.

[4] H. Schulte, K. Guelton, “Modelling and simulation of two-link robot manipulators based on Takagi Sugeno fuzzy descriptor systems”, Proc. IEEE ICIT’06, International Conference on Industrial Technology, Mumbai, December 15-17, 2006, pp. 2692-2697.

[5] K. Guelton, S. Delprat, T. M. Guerra, “An alternative to inverse dynamics joint torques estimation in human stance based on a Takagi-Sugeno unknown inputs observer in the descriptor form”, Control Engineering Practice, Vol. 16, No 12, 2008, pp. 1414-14262.

[6] K. Tanaka, M. Sugeno, “Stability analysis and design of fuzzy control systems”, Fuzzy Sets and Systems, Vol. 42, 1992, pp. 135-156.

[7] K. Tanaka, M. Sano, “A robust stabilisation problem of fuzzy control systems and its application to backing up control of a truck-trailer”, IEEE Trans. Fuzzy syst., Vol. 2, 1994, pp. 119-133.

[8] K. Tanaka, H.O. Wang, “Fuzzy control systems design and analysis: a linear matrix inequality approach”, John Wiley &

Son Eds, New York, Wiley-Interscience, 2001, ISBN 0-471-32324-190000.

[9] A. Sala., T. M. Guerra, R. Babuska, "Perspectives of fuzzy systems and control", Fuzzy Sets and Systems (Special Issue: 40th Anniversary of Fuzzy Sets), 153 (3), 2005, pp. 432-444.

[10] H. O. Wang, K. Tanaka, M. Griffin, "Parallel Distributed Compensation of Nonlinear Systems by Takagi-Sugeno Fuzzy Model", Proc. FUZZ-IEEE/IFES'95, International Conference on Fuzzy Systems, 1995, pp. 531-538.

[11] H.O. Wang, K. Tanaka, M. Griffin, "An approach to fuzzy control of nonlinear systems: Stability and design issues", IEEE Transactions on Fuzzy Systems, Vol. 11, No. 4, 1996, pp 14-23.

[12] S. G. Cao, N. W. Rees, G. Feng, "H-infinity control of uncertain fuzzy continuos-time systems", Fuzzy Sets and Systems, Vol. 115, 2000, pp 171-190.

[13] F. Zheng, Q. G. Wang, T. H. Lee, X. Huang, "Robust PI controller Design for Nonlinear systems via Fuzzy Modeling Approach", IEEE Trans. Syst. Man & Cybern. Part A: Systems and Humans, Vol. 31, 2001, pp. 666-675.

[14] D. Huang, S. K. Nguang, "Robust H static out feedback control of fuzzy systems: An ILMI approach", IEEE Trans. Syst., Man, Cybern. B, Vol. 36, No. 1, Feb. 2006, pp. 216-222.

[15] C. Doll, "La robustesse de lois de commande pour des structures flexibles en aeronautique et espace", These de doctorat, Ecole nationale Superieure de l'Aeronautique et de l'Espace SUPAERO, 2001.

[16] K. Zhou, J Doyle, K. Glover, "Robust and Optimal Control", Prentice Hall, New Jersey, pp. 596, 1996, ISBN-10: 0134565673.

[17] P. Apkarian, J. M. Biannic, P. Gahinet, "Self-Scheduled Control of a Missile via Linear Matrix Inequalities", Journal of Guidance Control and Dyn., Vol. 18, No. 3, Dec. 1993, pp. 532-538.

[18] G. Zames, "Feedback optimal sensitivity: model preference transformation. Multiplicative seminorms and approximate inverses", IEEE Trans. on Automatic Control, AC-26:301-320, 1981.

[19] J. Li, H. O. Wang, D. Niemann, K. Tanaka, "Dynamic parallel distributed compensation for Takagi-Sugeno fuzzy systems: An LMI approach", Information Sciences 123: 201-221, 2000.

[20] W. Chang, J. B. Park, Y. H. Joo, G. Chen, "Output Feedback Fuzzy Control for Uncertain Nonlinear Systems", Journal of Dynamic Systems, Measurement, and Control, December 2003, Vol. 125, No. 4, pp. 521-530.

[21] R. M. Redheffer, "On a certain linear fractional transformation", J. Math. And Phys., 1960, (39):269-286.

[22] G. Duc, S. Font, "Commande H_∞ et μ-analyse, collection pedagogique d'automatique", Hermes, ISBN 2-7462-0041-4, 1999.

[23] S. Font, "Methodologie pour prendre en compte la robustesse des systemes asservis: Optimisation H_∞ et approche symbolique de la forme standard", These de Doctorat, Université Paris XI et Supelec, 1995.

[24] A. Packard, "Gain scheduling via linear fractional transformations", Sys. Control Lett., Vol. 22, 1994, pp. 79-92.

[25] L. X. Wang, "A course in fuzzy systems and control", Upper Saddle River. NJ: Prentice Hall. 1997.

[26] P. Gahinet, A. Nemirovskii, A. J. Laub, M. Chilali, "The LMI Control Toolbox for Use with Matlab", The Mathworks Inx., 1995.

[27] S. K. Nguang, P.Shi, "Robust H_∞ Output Feedback Control Design for Takagi-Sugeno Systems with Markovian Jumps: A Linear Matrix Inequality Approach. Journal of Dynamic Systems, Measurement, and Control. September 2006. Volume 128, Issue 3, pp. 617-625.

[28] K. Guelton, T. Bouarar, N. Manamanni, "Fuzzy Lyapunov LMI based output feedback stabilization of Takagi Sugeno systems using descriptor redundancy", Proc. FUZZ-IEEE, International Conference on Fuzzy Systems, Hong Kong, June 1-6, 2008, pp. 1212-1218.

[29] E. Kim, H. Lee, "New approaches to relaxed quadratic stability condition of fuzzy control systems," IEEE Trans. Fuzzy Systems, Vol.8. No 5, 2000.

[30] H. D. Tuan, P. Apkarian, T. Narikiyo, Y. Yamamoto, "Parametrized linear matrix inequality techniques in fuzzy control design", IEEE Trans. Fuzzy Systems, Vol. 9(2), 2001, pp. 324-332.

[31] X. Liu, Q. Zhang, "New approaches to H_∞ controller design based on fuzzy observers for fuzzy T-S systems via LMI, Automatica", Vol 39 (9), 2003, pp. 1571-1582.

Biographies

Madjid Zerar received his M.S. degree in Automatic control and robotics from the University of Franche-Comte in 2002 and his Ph.D. in Automatic control from the University of Bordeaux 1 in 2006. From 2002 to 2006 he was with the "Laboratoire de l'Integration du Materiau au Systeme", University of Bordeaux 1 as a research assistant and then moved to the "Centre de Recherche en Sciences et Techniques de l'Information et de la Communication", University of Reims Champagne-Ardenne as Post-Doctoral Fellows. Since 2008, he serves as research & development engineer at EMC France Company. Dr. Zerar is a member of GDR MACS. His research interests are in nonlinear control, fuzzy control and their application to aerospace vehicle and engine control.

Kevin Guelton received his M.S. degree in 2000 and his Ph.D. in 2003 both in Human and Industrial Automatic Control from the University of Valenciennes, France. In 2000, he also received the French Diploma of Engineering School (M.Eng.) from the "Ecole d'Ingénieurs en Génie Informatique et Productique". From 2003 to 2005, he serves as an assistant professor in Human and Industrial Automatic Control at the "Ecole Nationale Supérieure d'Ingenieurs en Informatique Automatique Mecanique Energetique Electronique" of Valenciennes and was affiliated with both the Biomechanics team and the Fuzzy Systems team of the "Laboratoire d'Automatique et de Mécanique Industrielles et Humaines". Since 2005 he is an Associate Professor in automatic control at

the University of Reims Champagne-Ardenne and is affiliated with the "Centre de Recherche en Sciences et Techniques de l'Information et de la Communication". Dr. Guelton is a member of the IFAC Technical Committee on Modelling and Control of Biomedical Systems (TC 8.2), member of the IEEE Haptics Committee and member of the IEEE Control System Society. He is an IPC member of IFAC MCBMS'06-'09 and IEEE CICA'09; a SSC-TC member and special session organizer at FUZZ IEEE'2008, NOC vice chair of IFAC MCBMS'06, NOC member of IFAC CHAOS'06 and JD/JN MACS'07. His research interests are in nonlinear control, fuzzy control and their application to robotic, biomedical and biomechanical systems.

Prof. Noureddine Manamanni was born in Annaba, Algeria in January 1967. He received the Electrical engineering diploma (M. Eng.) in 1990 from the University of Annaba, and in 1998 the Ph.D. degree in robotics and automation from Universite Pierre et Marie Curie – Paris VI in France. From 1999 to 2005 he serves as an Associate Professor in automatic control at the University of Reims Champagne-Ardenne and is affiliated with the CReSTIC "Centre de Recherche en Sciences et Techniques de l'Information et de la Communication". Since, 2006 he is a full Professor in automatic control at URCA. Prof. Manamanni is a member of two IFAC Technical Committees: Control Design (TC-2.1.) since 2005 and Modelling and Control of Biomedical Systems (TC-8.2.) since 1999. He is an IPC member of IFAC MCBMS'03-'06-'09, IFAC ADHS'05, IFAC CHAOS'06, a TC member of FUZZ-IEEE'2008. He was Editor of IFAC CHAOS'06, JDMACS'07 and NOC vice chair of MCBMS'06. He is also member of the IEEE Control System Society. His research interest includes non linear control, fuzzy control non linear observer's synthesis, hybrid dynamical systems, control of robotic systems, control of biomedical systems.

ADAPTIVE STABILIZATION OF NETWORKED CONTROL SYSTEMS WITH DATA-PACKET DROPOUT

A. H. Tahoun *, F. Hua-Jing
Department of Control Science and Engineering, Huazhong University of Science and Technology, China

ABSTRACT

Since data-packet dropout might be potential source to instability and poor performance of networked control systems, the main objective of this paper is to design an adaptive stabilizing controller for networked systems with data-packet dropout. With the continuous-time approach, the case of state feedback is studied in which a new adaptive control model in the presence of data-packet dropout is proposed. The problem is to find upper bounds on the sampling period and the transmission packet dropout, to guarantee stability of the overall adaptive networked control systems. The resulting upper bounds are time varying and can be estimated online. Rigorous mathematical proofs are established, that relies heavily on Lyapunov's stability criterion and its extensions. Illustrative example is given to illustrate the effectiveness of our design approach.

Keywords

Networked Control Systems, Sampling, Packet Dropout, Adaptive Control, Lyapunov's Stability.

1. INTRODUCTION

Networked control systems are systems whose sensors, actuators, estimator units, and control units are connected through data networks. This type of system has the advantage of greater flexibility with respect to traditional control systems. Also, it allows for reduced wiring, as well as a lower installation cost. It also permits greater agility in diagnosis and maintenance procedures. Examples of such systems can be seen in aircrafts or manufacturing plants.

Conventional control theories suppose ideal assumptions, such as no drops and no delays from sensors to actuators. On the other hand, the network-induced data-packet dropouts and delays can degrade the performance of control systems designed without considering them, and can even destabilize the system. So, conventional control theories must be reevaluated before they can be applied to NCSs. Specifically, the data-packet dropout that occurs while exchanging data among devices.

*Corresponding author: *E-mail:* alitahoun@yahoo.com

 ISSN: 1743-9310

Recently, much attention has been paid to the study of stability analysis and control design of NCSs. Under the assumption that the network is modeled as a switch the stability analysis of NCSs was investigated in [1] and [2], with constant delay less than the sampling period. The method they used derives from the stability analysis for asynchronous dynamic systems. The case of model-based NCS was studied in [3], with constant time intervals and constant sensor-to-controller delay. In [4] and [5], a new model of NCSs was provided under consideration of both the network-induced delay and the data packet dropout in the transmission and no discretization of the continuous-time plant was needed for modeling. With packet-loss rate known and constant, the NCS was formulated in [6], as a Markovian jump system. A dynamic output feedback controller design method was proposed such that the NCS is mean square stable and has H8 gain below certain value in terms of linear matrix inequalities (LMIs). Moreover, in [7], the packet-loss process was modeled as an arbitrary but finite switching signal. This enables to apply the theory from switched systems to stabilize the NCS. An iterative approach to model networked control systems (NCSs) with arbitrary but finite data packet dropout and network delays as switched linear systems was proposed in [8]. The results obtained in [8] suggest that one may drop data packet at a certain rate to save network bandwidth while preserving the stability of the NCS. This is of practical importance in industrial applications. The stabilization problem of NCSs with bounded packet losses was studied in [9]. Two types of networked controller design methods were proposed. One ensures the networked control system is asymptotically stable in the presence of the arbitrary packet losses. The other ensures the mean square stability in the presence of the Markovian packet losses.

The problem of optimal LQG control when one sensor and the controller are communicating across a packet erasure channel was considered in [10]. The information that the sensor should provide to the controller to obtain the optimal LQG performance was identified. This can be viewed as constructing an encoder for the channel. Also, the decoder that uses the information it receives across the link to construct an estimate of the state of the plant was designed. The proposed algorithm is recursive yet optimal irrespective of the packet-drop pattern.

A collection of results to determine the closed- loop stability of NCSs in the presence of network sampling, delays, and packet dropouts are covered in [11], [12], and [13] and references therein. Many of the results presented rely on Lyapunov based techniques and only provide sufficient conditions for stability of the NCS.

The adaptive control problem of NCSs was firstly discussed in [14] and [15]. In [14], the stability of adaptive control of networked systems was considered with network inserted between sensors and the controller only, which was extended

in [15] with network inserted between sensors and the controller and between the controller and actuators but without delay and packet dropouts. In [16], an adaptive control model of NCSs in the presence of time-varying network-induced delays was proposed. In this paper, we propose a new adaptive model of NCS in the presence of data-packet dropouts. The analysis in this paper is more complex because we deal with the adaptation technique to estimate the gain matrix k(t) online, the data-packet dropouts. Here, k(t) is time varying, so the resulting upper bounds of sampling period and packet dropout are also time varying that can be estimated online.

The rest of the paper is organized as follows: the problem is formulated in Section 2. The modeling of the packet dropout is discussed in Section 3. The main result is given in Section 4. Section 5 presents an illustrative example. Finally we present our conclusions in Section 6.

2. FORMULATION OF THE PROBLEM

In the NCS shown in Fig. 1, we make the following assumptions:

(A1) The sensor is clock-driven and both controller and actuator are event driven.

(A2) The data are transmitted in a single packet at each time step.

(A3) No delay exists in the transmission channel.

(A4) The data packets reach the controller and the actuators by their original transmitting sequence if they are not lost.

Remark 1: Assumptions (A1) is standard in NCSs design, assumptions (A2) and (A3) may be extended in future work, assumption (A4) is needed to guarantee that no more sensor updates are sent out until the current one is received by the controller.

Also, we assume that there exist positive constant η and such that, $\eta \le (k+1)h - (k-i_k)h$, where h is the sampling period, i_k is the number of packets dropped out at time kh.

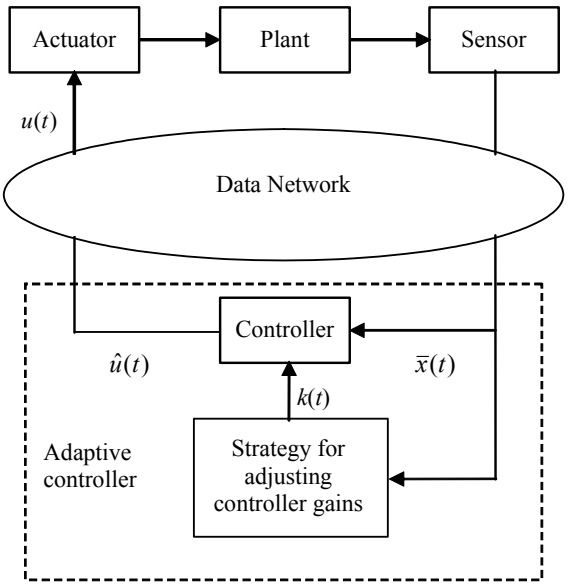

Figure 1. The block diagram of adaptive NCS

In Fig. 1, a class of linear time-invariant plants is described as

$$\dot{x}(t) = Ax(t) + bu(t), \quad t \in [kh, (k+1)h), k = 0,1,2,\ldots, \tag{1}$$

where $x(t) \in R^n$ is a state vector, $u(t) \in R$ is a piecewise continuous control input vector. In Eq. (1), the pair (A, b) is controllable and A, b are unknown matrices with compatible dimensions.

Our objective is to design an adaptive control stabilizer for the networked system and to find upper bounds on the time sampling period, h, and the data-packet dropout such that the NCS is still stable.

To meet this adaptive control objective, we assume

(A5) There exist a constant vector $k^* \in R^n$ and a nonzero constant scalar $k_1^* \in R$ such that the following equations are satisfied:

$$\bar{A} = A + bk^{*T}, \bar{b} = k_1^* b$$

where $\bar{A}$ and $\bar{b}$ are known constant matrices, $\bar{A}$ is Hurwitz matrix satisfying that $\bar{A}^T P + P\bar{A} = -Q$, P and Q are symmetric and positive-definite matrices, and T denotes transpose.

(A6) The sign of k_1^*, $sign[k_1^*]$ is known.

Remark 2: Assumptions (A5) and (A6) are standard in adaptive control design, and assumption (A1) is the so-called matching condition [17], in which if A and b were known, the controller

$$u(t) = k^{*T} x(t)$$

would led to the network-free closed-loop system for $t \ge 0$

$$\dot{x}(t) = Ax(t) + bk^{*T} x(t) = \bar{A}x(t)$$

whose state vector $x(t)$ is exponentially stable, achieving the control objective.

As A, b are unknown, the adaptive controller for the considered networked system will be chosen as

$$u(t) = k^T(t)\bar{x}(t), \quad t \in [kh, (k+1)h), k = 0,1,2,\ldots, \tag{2}$$

where $k(t)$ is the estimates of k^*, $\bar{x}(t)$ is the output of the sensor-controller network part.

3. MODELING OF THE PACKET DROPOUT

As the controller is time varying, the network can be considered as double switches (S1 and S2) rather than a single switch as in [1], [2], and [8], see Fig. 2. When the switch (S1 or S2) is closed (in position 1), network packet is transmitted, whereas when it is open (in position 2), the packet is lost and the old data packet is used

The modeling of the packet dropout between sensors and the controller can be expressed as follows:

With no packet dropout at time *kh*:

$$\bar{x}(t) = x(kh)$$

With one packet dropout at time *kh*:

$$\bar{x}(t) = x((k-1)h)$$

With two packets dropout at time *kh*:

$$\bar{x}(t) = x((k-2)h)$$
$$\vdots$$

With packets dropout at time *kh*:

$$\bar{x}(t) = x((k-\ell_k)h)$$

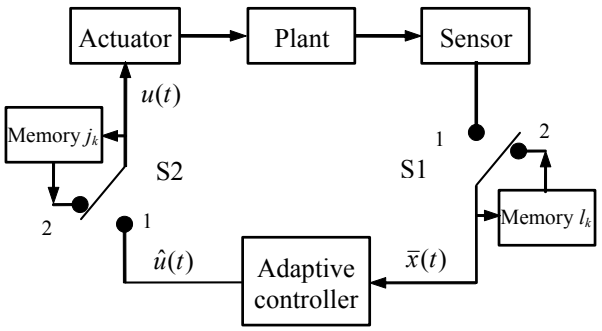

Figure 2.

The quantity of dropped packets between sensors and the controller is accumulated from the latest time when $\bar{x}(t)$ has been updated.

The modeling of the packet loss between sensors and the actuators can be expressed, with j_k packets dropout at time *kh*, as follows:

With no packet dropout between sensors and controller:

$$u(t) = k^T((k-j_k)h)x((k-\max(0,\ell_{k-j_k}+j_k,j_k))h)$$

With one packet dropout between sensors and controller:

$$u(t) = k^T((k-j_k)h)x((k-\max(1,\ell_{k-j_k}+j_k,j_k))h)$$

With two packet dropout between sensors and controller:

$$u(t) = k^T((k-j_k)h)x((k-\max(2,\ell_{k-j_k}+j_k,j_k))h)$$
$$\vdots$$

In general, the modeling of the packet loss between sensors and the actuators with ℓ_k packets dropout between sensors and controller and j_k packets dropout between the controller and the actuators can be summarized at time *kh*, as follows:

$$u(t) = k^T((k-j_k)h)x((k-i_k)h) \tag{3}$$

where

$$i_k = \max(\ell_k, \ell_{k-j_k}+j_k, j_k)$$

Again, the quantity of dropped packets between the controller and the actuators is accumulated from the latest time when $u(t)$ has been updated.

Remark 3: When $\ell_k = j_k$, it means the packet is dropped between sensors and controller and between the controller and the actuators in the same transmission period. In this case, $u(t)$ is replaced by

$$u(t) = k^T((k-\ell_k)h)x((k-\ell_k)h)$$

Remark 4: When $\ell_k, j_k = 0$, it means no packet is dropped or rejected in the transmission. In this case, $u(t)$ is replaced by

$$u(t) = k^T(kh)x(kh).$$

Thus, from Eq. (1) and (3), we get

$$\begin{aligned}\dot{x}(t) &= Ax(t) + bk^T((k-j_k)h)x((k-i_k)h),\\ &\quad t \in [kh,(k+1)h),\\ &\quad k = 0,1,2,\ldots, \quad i_k \in \{0,1,2,3,.....\}\\ x(t) &= x(0), t \in [0,i_0)\end{aligned}$$

Then, the system can be expressed as

$$\dot{x}(t) = \bar{A}x(t) - bk^{*T}x(t) + bk^T((k-j_k)h)x((k-i_k)h) \tag{4}$$

Define $\phi(t) = k(t) - k^*$ as the control parameter error vector, and $e(t) = x(t) - x((k-i_k)h)$ as the transmission error, Eq. (4) can be rewritten as

$$\dot{x}(t) = \bar{A}x(t) + b\phi^T((k-j_k)h)x((k-i_k)h) - bk^{*T}e(t) \tag{5}$$

4. MAIN RESULT

In order to obtain the upper bounds on the sampling period, h, and the data-packet dropout to guarantee stability of the overall adaptive NCS described by Eq. (1) and (3), the following Lemma play an important role.

Lemma 1: The transmission error $e(t)$ of the overall NCS is bounded between two successive transmissions by

$$\|e(t)\| \le \gamma \|x((k-i_k)h)\| + (\gamma+1)\int_{t-\eta}^{t} \|\dot{x}(s)\| ds \tag{6}$$

where

$$\gamma = \frac{A_{upp} + \left\| bk^T((k-j_k)h) \right\|}{A_{upp}} (e^{A_{upp}(t-kh)} - 1)$$

A_{upp} is an upper bound on A such that; $\|A\| \le A_{upp}$.

Proof: Since the following formula holds

$$x(kh) = x((k-i_k)h) + \int_{(k-i_k)h}^{kh} \dot{x}(s)ds, \qquad (7)$$

it can be found that

$$e(t) = e_1(t) + \int_{(k-i_k)h}^{kh} \dot{x}(s)ds$$

where $e_1(t) = x(t) - x(kh)$, and $x(kh)$ only changes value at instants kh, and kept constant until next control update is received at time $(k+1)h$ (realized by a zero-order hold (ZOH)). From Eq. (4), for $t \in [kh, (k+1)h)$, $k = 0, 1, 2, \ldots$, we get

$$\dot{e}_1(t) = Ae_1(t) + Ax(kh) + bk^T((k-j_k)h)x((k-i_k)h)$$

Taking the integral on both sides, taking into account, $e_1(t) = 0$ at $t = kh$, we have

$$e_1(t) = [Ax(kh) + bk^T((k-j_k)h)x((k-i_k)h)](t-kh) + \int_{kh}^{t} Ae_1(s)ds$$

Therefore,

$$\left\|e_1(t)\right\| \le \|A\| \left\|x((k-i_k)h)\right\| (t-kh) + \left\|bk^T((k-j_k)h)\right\| \left\|x((k-i_k)h)\right\| \times (t-kh) + \int_{kh}^{t} \|A\| \left\|e_1(s)\right\| ds$$

Applying Bellman-Gronwall Lemma [2], yields

$$\left\|e_1(t)\right\| \le \frac{b_{upp} \left\|k^T((k-j_k)h)\right\|}{A_{upp}} (e^{A_{upp}(t-kh)} - 1) \left\|x((k-i_k)h)\right\| + (e^{A_{upp}(t-kh)} - 1) \left\|x(kh)\right\|$$

where, $\|A\| \le A_{upp}$ and $\|b\| \le b_{upp}$.

From Eq. (7), and using,

$$\int_{(k-i_k)h}^{kh} \left\|\dot{x}(s)\right\| ds \le \int_{t-\eta}^{t} \left\|\dot{x}(s)\right\| ds, t \in [kh, (k+1)h), \quad k = 0, 1, 2, \ldots$$

where, $\eta \le (1 + i_k)h$, we have

$$\left\|e_1(t)\right\| \le \left(\frac{A_{upp} + b_{upp} \left\|k^T((k-j_k)h)\right\|}{A_{upp}} \cdot (e^{A_{upp}(t-kh)} - 1) \left\|x((k-i_k)h)\right\| \right) + (e^{A_{upp}(t-kh)} - 1) \int_{t-\eta}^{t} \left\|\dot{x}(s)\right\| ds$$

By choosing

$$\gamma = \frac{A_{upp} + b_{upp} \left\|k^T((k-j_k)h)\right\|}{A_{upp}} (e^{A_{upp}(t-kh)} - 1)$$

we get

$$\left\|e(t)\right\| \le \gamma \left\|x((k-i_k)h)\right\| + (\gamma + 1) \int_{t-\eta}^{t} \left\|\dot{x}(s)\right\| ds$$

At $t = (k+1)h$, by choosing $A_{upp} \ge 1$, it can be found that, $h \le \gamma$, then $\eta \le (1 + i_k)\gamma$.

We are now in a position to develop our controller design method for the current situation.

Theorem 1: The NCS with linear time-invariant plant (1) and an adaptive stabilizer (3) is globally stable if the adaptive control law takes the form [17]

$$\dot{\phi}(t) = -sign[k_1^*] \alpha \, \bar{x}(t) \bar{x}^T(t) P \bar{b}, \quad t \in [kh, (k+1)h), k = 0, 1, 2, \qquad (8)$$

and the sampling period satisfies $h < \min\{h_1, h_2, h_3\}$, where, α is an $n \times n$ symmetric positive-definite adaptation gain matrix, and

$$h_1 = \frac{1}{A_{upp}} \ln\left(1 + \frac{\gamma_{\max} A_{upp}}{A_{upp} + b_{upp}\left\|k^T((k-j_k)h)\right\|}\right)$$

$$h_2 = \frac{1}{A_{upp}} \ln\left(1 + \frac{\beta\lambda_{\min}(Q) A_{upp}}{\zeta}\right)$$

$$h_3 = \frac{1}{A_{upp}} \ln\left(1 + \frac{(1-3\beta) A_{upp}}{A_{upp} + b_{upp}\left\|k^T((k-j_k)h)\right\|}\right)$$

where

$$\zeta = \left(A_{upp} + b_{upp}\left\|k^T((k-j_k)h)\right\|\right)(1+\xi),$$

$$\xi = 2\|P\|\Upsilon_2 + \sigma_1\|P\|^4\|\alpha\|^2 b_{upp}^2\|x((k-i_k)h)\|^4 + \sigma_2(1+i_k)MA_{upp}^2 + \sigma_3\Upsilon_1 + \frac{(\gamma_{\max}+1)^2(1+i_k)}{\sigma_5}\|P\|^2\Upsilon_2 + (1+i_k)Mb_{upp}^2\left\|k^T((k-i_k)h)\right\|^2,$$

$$M = \sigma_4\Upsilon_1 + \sigma_5\Upsilon_2,\ \Upsilon_1 = \left\|\bar{A}\right\| + A_{upp},$$

$$\Upsilon_2 = b_{upp}\left\|k^T(t)\right\| + \left\|\bar{A}\right\| + A_{upp},$$

for positive constants β, γ_{max}, σ_i, i = 1, 2, 3, 4, 5.

Proof: Consider a positive-definite Lyapunov function $V(t)$ of the form

$$V(t) = V_1(t) + V_2(t) + V_3(t) \tag{9}$$

where

$$V_1(t) = x^T(t)Px(t) + \frac{1}{\left|k_1^*\right|}\phi^T(t)\alpha^{-1}\phi(t)$$

$$V_2(t) = \int_{(k-i_k)h}^{t} x(s)Rx(s)ds$$

$$V_3(t) = M\int_{t-\eta}^{t}\int_{s}^{t}\dot{x}(v)\dot{x}(v)dvds$$

Differentiating $V_i(t)$, i =1, 2, 3, with respect to t, for $t \in [kh, (k+1)h)$, k = 0, 1, 2, … , we have

$$\dot{V}_1(t) = \dot{x}^T(t)Px(t) + x^T(t)P\dot{x}(t) + \frac{2}{\left|k_1^*\right|}\dot{\phi}^T(t)\alpha^{-1}\phi(t)$$

$$\dot{V}_2(t) = x^T(t)Rx(t) - x^T((k-i_k)h)Rx((k-i_k)h)$$

$$\dot{V}_3(t) = \eta M\dot{x}^T(t)\dot{x}(t) - M\int_{t-\eta}^{t}\dot{x}^T(s)\dot{x}(s)ds$$

Substituting Eq. (5) and (8), taking into account $sign[k_1^*]\left|k_1^*\right| = k_1^*$ there results

$$\begin{aligned}\dot{V}_1(t) = {} & x^T(t)\bar{A}Px(t) + x^T(t)P\bar{A}x(t) \\ & + 2x^T(t)Pb\phi^T((k-j_k)h)x((k-i_k)h) \\ & - 2x^T(t)Pbk^{*T}e(t) \\ & - 2x^T((k-i_k)h)Pb\phi^T(t)x((k-i_k)h)\end{aligned} \tag{10}$$

and

$$\begin{aligned}\dot{V}_3(t) = {} & \eta Mx^T(t)A^TAx(t) \\ & + \eta Mx^T((k-i_k)h)k((k-j_k)h)b^Tb \\ & + 2\eta Mx^T(t)A^Tbk^T((k-j_k)h)x((k-i_k)h) \\ & \times k^T((k-i_k)h)x((k-i_k)h) - M\int_{t-\eta}^{t}\dot{x}^T(s)\dot{x}(s)ds\end{aligned}$$

Rearranging Eq. (10), yields

$$\begin{aligned}\dot{V}_1(t) = {} & -x^T(t)Qx(t) - 2x^T(t)Pbk^{*T}e(t) \\ & + 2x^T(t)Pb\Delta k^T(t)x((k-i_k)h) \\ & + 2e^T(t)Pb\phi^T(t)x((k-i_k)h)\end{aligned} \tag{11}$$

where

$$\Delta k^T(t) = k^T(t) - k^T((k-j_k)h)$$

Using (6) and the well-known inequality [18]

$$\pm 2a^Tb \le \frac{1}{\sigma}a^Ta + \sigma b^Tb \tag{12}$$

for any a, $b \in R^n$ and scalar $\sigma > 0$, becomes bounded from above as

$$\dot{V}(t) \le -\lambda_{\min}(Q)\|x(t)\|^2 + \frac{\gamma}{\sigma_1}\|x(t)\|^2 + \frac{\eta}{\sigma_2} M \left\|bk^T((k-j_k)h)\right\|^2 \|x(t)\|^2 + 2\gamma\|P\|\left\|bk^{*T}\right\|\|x(t)\|\|x((k-i_k)h)\| + 2(\gamma+1)\|P\|\left\|bk^{*T}\right\|\|x(t)\| \int_{t-\eta}^{t} \|\dot{x}(s)\|ds + \sigma_1\|P\|^2\left\|b\Delta k^T(t)\right\|^2\|x((k-i_k)h)\|^2 + 2\gamma\|P\|\left\|b\phi^T(t)\right\|\|x((k-i_k)h)\|^2 + 2(\gamma+1)\|P\|\left\|b\phi^T(t)\right\|\|x((k-i_k)h)\| \int_{t-\eta}^{t} \|\dot{x}(s)\|ds + x^T(t)Rx(t) - x^T((k-i_k)h)Rx((k-i_k)h) + \sigma_2\eta\|A\|^2 M\|x((k-i_k)h)\|^2 + \eta M\left\|bk^T((k-j_k)h)\right\|^2\|x((k-i_k)h)\|^2 + \eta M x^T(t)A^T Ax(t) - M\int_{t-\eta}^{t} \dot{x}^T(s)\dot{x}(s)ds$$

By choosing $\gamma < \gamma_{max}$ and $\gamma_{max} > 1$, we have $h < h_1$, where

$$h_1 = \frac{1}{A_{upp}} \ln\left(1 + \frac{\gamma_{\max} A_{upp}}{A_{upp} + b_{upp}\left\|k^T((k-j_k)h)\right\|}\right) \quad (13)$$

From Eq. (8), it can be found that

$$\left\|\Delta k(t)\right\| \le \|\alpha\|\|b\|\|x((k-i_k)h)\|^2\|P\|\gamma$$

Again, using (12), and the inequality [18]

$$\left(\int_{t-\eta}^{t} x(s)ds\right)^T \left(\int_{t-\eta}^{t} x(s)ds\right) \le \eta\int_{t-\eta}^{t} x^T(s)x(s)ds$$

we get

$$\dot{V}(t) \le \Big[-\lambda_{\min}(Q)(1-\gamma) + \frac{\gamma}{\sigma_1} + R + \eta\|A\|^2 M + \frac{\gamma}{\sigma_3}\|P\|^2\left\|bk^{*T}\right\| + \frac{\eta}{\sigma_2} M\left\|bk^T((k-j_k)h)\right\|^2 + \frac{\eta(\gamma+1)^2}{\sigma_4}\|P\|^2\left\|bk^{*T}\right\|\Big]\|x(t)\|^2 + 2\gamma\|P\|\left\|b\phi^T(t)\right\|\|x((k-i_k)h)\|^2 + \sigma_2\eta\|A\|^2 M\|x((k-i_k)h)\|^2 + \sigma_1\gamma^2\|P\|^4\|\alpha\|^2\|b\|^2\|x((k-i_k)h)\|^4\|x((k-i_k)h)\|^2 + \frac{\eta(\gamma+1)^2}{\sigma_5}\|P\|^2\left\|b\phi^T(t)\right\|\|x((k-i_k)h)\|^2 + \eta M\left\|bk^T((k-j_k)h)\right\|^2\|x((k-i_k)h)\|^2 + \sigma_3\gamma\left\|bk^{*T}\right\|\|x((k-i_k)h)\|^2 - x^T((k-i_k)h)Rx((k-i_k)h) + (\sigma_4\left\|bk^{*T}\right\| + \sigma_5\left\|b\phi^T(t)\right\|)\int_{t-\eta}^{t}\|\dot{x}(s)\|^2 ds - M\int_{t-\eta}^{t}\dot{x}^T(s)\dot{x}(s)ds$$

Rearranging, $\dot{V}(t)$ becomes

$$\dot{V}(t) \le \Big[-\lambda_{\min}(Q)(1-\gamma) + \gamma\left(\frac{1}{\sigma_3} + \frac{(1+i_k)(\gamma+1)^2}{\sigma_4}\right)\|P\|^2 \Upsilon_1 + \frac{\gamma}{\sigma_1} + R + (1+i_k)\gamma A_{upp}^2 M + \frac{(1+i_k)\gamma}{\sigma_2} M b_{upp}^2 \left\|k^T((k-j_k)h)\right\|^2 \Big] \|x(t)\|^2 + \sigma_1 \gamma^2 \|P\|^4 \|\alpha\|^2 b_{upp}^2 \|x((k-i_k)h)\|^4 \|x((k-i_k)h)\|^2 + \sigma_2(1+i_k)\gamma A_{upp}^2 M \|x((k-i_k)h)\|^2 + \sigma_3 \gamma \Upsilon_1 \|x((k-i_k)h)\|^2 + \frac{\gamma(1+i_k)(\gamma+1)^2}{\sigma_5}\|P\|^2 \Upsilon_2 \|x((k-i_k)h)\|^2 + (1+i_k)\gamma M b_{upp}^2 \left\|k^T((k-j_k)h)\right\|^2 \|x((k-i_k)h)\|^2 + 2\gamma\|P\| \Upsilon_2 \|x((k-i_k)h)\|^2 - x^T((k-i_k)h) R x((k-i_k)h) + (\sigma_4 \Upsilon_1 + \sigma_5 \Upsilon_2) \int_{t-\eta}^{t} \|\dot{x}(s)\|^2 ds - M \int_{t-\eta}^{t} \dot{x}^T(s)\dot{x}(s) ds$$

where

$$\Upsilon_1 = \left\|\bar{A}\right\| + A_{upp}, \Upsilon_2 = b_{upp}\left\|k^T(t)\right\| + \left\|\bar{A}\right\| + A_{upp}.$$

Choosing

$$M = \sigma_4 \Upsilon_1 + \sigma_5 \Upsilon_2,$$
$$R = \gamma\xi$$

where

$$\xi = 2\|P\| \Upsilon_2 + \sigma_1 \|P\|^4 \|\alpha\|^2 b_{upp}^2 \|x((k-i_k)h)\|^4 + \sigma_2(1+i_k)MA_{upp}^2 + \sigma_3 \Upsilon_1 + \frac{(\gamma_{\max}+1)^2(1+i_k)}{\sigma_5}\|P\|^2 \Upsilon_2 + (1+i_k)Mb_{upp}^2 \left\|k^T((k-i_k)h)\right\|^2,$$

we get

$$\dot{V}(t) \le \Big[-\lambda_{\min}(Q)(1-\gamma) + \frac{\gamma}{\sigma_1} + \gamma\xi + \gamma(1+i_k)A_{upp}^2 M + \gamma\left(\frac{1}{\sigma_3} + \frac{(1+i_k)(\gamma+1)^2}{\sigma_4}\right)\|P\|^2 \Upsilon_1 + \frac{(1+i_k)\gamma}{\sigma_2} M b_{upp}^2 \left\|k^T((k-j_k)h)\right\|^2 \Big] \|x(t)\|^2 \quad (14)$$

If we choose

$$\gamma < \frac{\beta\lambda_{\min}(Q)}{1+\xi}, \ 0 < \beta < 0.5$$

we have $h < h_2$, where

$$h_2 = \frac{1}{A_{upp}} \ln\left(1 + \frac{\beta\lambda_{\min}(Q)A_{upp}}{\zeta}\right) \quad (15)$$

$$\zeta = \left(A_{upp} + b_{upp}\left\|k^T((k-j_k)h)\right\|\right)(1+\xi)$$

With the appropriate choice of σ_i, i = 1, 2, 3, 4, 5, and substituting for γ in (14), we get

$$\dot{V}(t) \le \lambda_{\min}(Q)\|x(t)\|^2 [-(1-\gamma) + 2\beta]$$

Finally, by choosing, $\gamma < 1 - 2\beta$, we have $h < h_3$, where

$$h_3 = \frac{1}{A_{upp}} \ln\left(1 + \frac{(1-2\beta)A_{upp}}{A_{upp} + b_{upp}\left\|k^T((k-j_k)h)\right\|}\right) \quad (16)$$

Finally, we can conclude that $\dot{V}(t) < 0$, if h satisfies $h < \min\{h_1, h_2, h_3\}$ defined in Eq. (13), (15), and (16), respectively. Therefore, $x(t)$, $\phi(t)$, and $V(t)$ are bounded for all $t \ge t_0$ and the over all system is globally stable. We therefore obtained the desired result.

5. ILLUSTRATIVE EXAMPLE

Consider the following unstable system:

$$A = \begin{bmatrix} -0.8 & -0.01 \\ 1 & 0.1 \end{bmatrix}, \quad b = \begin{bmatrix} 0.4 \\ 0.1 \end{bmatrix}$$

Assume the desired system parameters

$$\bar{A} = \begin{bmatrix} -1 & 0 \\ 0 & -2 \end{bmatrix}$$

Let

$$P = \begin{bmatrix} 1 & 0 \\ 0 & 1 \end{bmatrix}, \quad Q = \begin{bmatrix} 2 & 0 \\ 0 & 4 \end{bmatrix}$$

Assume A and b are unknown but only A_{upp} and b_{upp} are known (take A_{upp} = 2, b_{upp} = 0.5), $x(0) = [1\ 1]^T$, α = 0.1I (I = identity matrix), β = 0.4, γ_{max}=0. 05, σ_1 =1, σ_2 = 1, σ_3 = 1, σ_4 = 0.3, σ_5 =0.2, and $k(0) = [0\ 0]^T$. With no packet loss, the sampling period h that guarantees the stability of the over all adaptive NCS is estimated on line to be $1.7*10^{-2}$s. With 10% packet loss, h is estimated on line to be $1.1*10^{-2}$s. With 70% packet loss, h is estimated on line to be $0.32*10^{-2}$s. For the considered system, the relationship between sampling period h and data-packet dropout for the NCS are illustrated in Fig. 3, from which we can see that with the sampling period increased, the data packet dropout has to be decreased in order to guarantee the stability of the NCS.

Remark 5: The results established in this paper can be applied to NCSs without packet loss to obtain the maximum allowable sampling period.

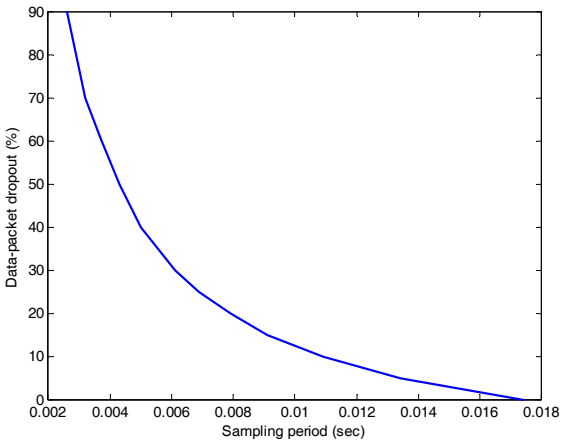

Figure 3. The relationship between sampling period and data-packet dropout

6. CONCLUSIONS

The paper addresses the adaptive stabilization problem of NCSs with data-packet dropout. A new adaptive model of NCS in the presence of data-packet dropout was proposed. The results established in this paper can be applied to NCSs without packet loss to obtain the maximum allowable sampling period. Rigorous mathematical proofs are established relies heavily on Lyapunov's stability criterion. Illustrative example was given to illustrate the effectiveness of the design approach. Much work should be done for adaptive NCSs with both network-induced delays and data-packet dropouts. This is the direction of the future research work.

ACKNOWLEDGEMENT

This work is supported by National Natural Science Foundation of China, Grant #60574088 and #60274014.

REFERENCES

[1] W. Zhang, M. S. Branicky, S. M. Phillips, "Stability of networked control systems", IEEE Control. Syst. Mag., Vol. 21, 2001, pp. 84-99.

[2] W. Zhang, "Stability analysis of networked control systems", PhD Thesis, Case Westem Reserve University, 2001.

[3] L. A Montestruque, P. Antsaklis, "On the model-based control of networked systems", Automatica, Vol. 39, 2003, pp. 1837-1843.

[4] D. Yue, Q. Han, C. Peng, "State Feedback Controller Design of Networked Control Systems", IEEE Trans. Circuits and Systems-II: Express Briefs, Vol. 51, 2004, pp. 640-644.

[5] L. Hu, T. Bai, P. Shi, Z. Wu, "Sampled-Data Control of Networked Linear Control Systems", Automatica, Vol. 43, 2007, pp. 903-911.

[6] P. Seiler, R. Sengupta, "An H_∞ approach to networked control", IEEE Trans. Automat. Contr., Vol. 50, No. 3, 2005, pp. 356-364.

[7] M. Yu, L. Wang, T. Chu, G. Xie, "Stabilization of networked control systems with data packet dropout and network delays via switching system approach", 43rd IEEE conference on decision and control, 2004, pp. 3539-3544.

[8] M. Yu, L.Wang, T. Chu, F. Hao, "An LMI Approach to Networked Control Systems with Data Packet Dropout and Transmission Delays", 43rd IEEE Conference on Decision and Control, 2004, pp. 3545-3550.

[9] J. Xiong, J. Lam, "Stabilization of linear systems over networks with bounded packet loss", Automatica, Vol. 43, 2007, pp. 80-877.

[10] V. Gupta, B. Hassibi, R. M. Murray, "Optimal LQG Control Across Packet-Dropping Links", Systems & Control Letters, Vol. 56, pp. 439 -446, 2007.

[11] Y. Jianyong, Y. Shimin, W. Haiqing, "Survey on the Performance Analysis of Networked Control Systems", IEEE International Conference on Systems, Man and Cybernetics, 2004, pp. 5068-5073.

[12] J. Baillieul, P. J. Antsaklis, "Control and Communication Challenges in Networked Control Systems", IEEE Control Syst. Mag., Vol. 95, 2007, pp. 9-28.

[13] J. P. Hespanha, P. N. Naghshtabrizi, Y. Xu, "A Survey of Recent Results in Networked Control Systems, IEEE Control Syst. Mag., Vol. 95, 2007, pp. 138-162.

[14] A. H. Tahoun, Hua-Jing Fang, "A Novel Approach to Adaptive Control of Networked Systems", Ubiquitous Computing and Communication Journal, Vol. 2, No. 4, 2007, pp 79-84.

[15] A. H. Tahoun, Hua-Jing Fang, "Adaptive Stabilization of Networked Control Systems", Journal of Applied Sciences, Vol., 7 No. 22, 2007, pp. 3547-3551.

[16] A. H. Tahoun, Hua-Jing Fang, "Adaptive Stabilization of Networked Control Systems with Network-Induced Delay", The Mediterranean Journal of Measurement and Control, Vol. 3, No. 4, 2007, pp. 183-190.

[17] G. Tao, "Adaptive Control Design and Analysis", John Wiley & Sons, Inc., New Jersy, 2003, ISBN: 978-0-471-27452-0.

[18] Y. S. Moon, P. Park, W. H. Kwon, "Robust stabilization of uncertain input-delayed systems using reduction method", Automatica, Vol. 37, 2001, pp. 307-312.

Biographies

A. H. Tahoun was born in 1976, He received his B.Sc. in electrical engineering in 1999, (distinction with honors), and his M.Sc. in control engineering in 2005 from Tanta University, Egypt. He is now doing his Ph.D. in Department of Control Science and Engineering, Huazhong University of Science and Technology, Wuhan, China. His research interests include adaptive control, networked control system, control system fault diagnosis, robust and fault-tolerant control.

Fang Hua-Jing received the B.Sc., M.Sc. and Ph.D. degree in Control Theory and Engineering from the Huazhong University of Science and Technology in 1982, 1984 and 1991, respectively. He is working with the Department of Control Science and Engineering, Huazhong University of Science and Technology, China, where he is a professor since 1994, and also serves as the director of the Institute of Control Theory, the vice director of the Center for Nonlinear and Complex Systems. He is the member of Fault Detection, Supervision and Safety of Technical Processes Committee and Education Committee of the Chinese Automation Association, Associate Editor of the Journal of Control Theory and Applications. His research interests include Complex networked control system, control system fault diagnosis, robust and fault-tolerant control, dynamics and control of autonomous vehicle's swarm.

TRANSIT POWER CONTROL USING THYRISTOR CONTROLLED SERIES CAPACITORS (TCSC)

F. Lakdja [1,*], F. Z. Gherbi [2]

[1] Department of Electrical Engineering University of Saida, Algeria

[2] Intelligent Control and Electrical Power System Laboratory, University of Sidi-Bel-Abbes, Algeria

ABSTRACT

The power transportation networks can be improved by multiplying or creating new lines. However, this is not always the case for various technical and commercial reasons. The series capacitors controlled by SCRs (Silicon Controlled Rectifiers) represent a good alternative to optimize the existing or the new electric links, because they permit the increase of the dynamic stability, the damping of the power oscillations, while balancing the loads between the parallel circuits. This paper presents an effective method for power distribution by inserting the TCSC (Thyristor controlled Series Capacitors) transit controller in the network. The insertion of the TCSC devices has given satisfying results that are, an increase of the transmitted active power, reduction of active losses, and improvement of the angular stability and the voltage stability without decreasing the transportation capacity.

Keywords

FACTS Devices, TCSC, Power Flow, Transit Power, Power Networks.

1. INTRODUCTION

The need for more efficient electricity systems management has given rise to innovative technologies in power generation and transmission. The combined cycle power station is good example of a new development in power generation and flexible AC transmission systems, FACTS (Flexible AC Transmission System) as they are generally known, are new devices that improve transmission systems.

In interconnected power systems, the actual transfer of power from one region to another might take unintended routes depending on impedances of the transmission lines connecting the areas. Controlled series compensation is a useful means for optimizing power flow between regions for varying loading and network configurations. It becomes possible to control power flows in order to achieve a number of goals:

- Minimizing of system losses.
- Reduction of loop flows.
- Elimination of line overloads.
- Optimizing of load sharing between parallel circuits.
- Directing of power flows along contractual paths.

Thyristor controlled series capacitor (TCSC) is one of generation FACTS controllers which control the effective line reactive by connecting a variable reactance in series with line. The variable reactance is obtained using FC-TCR (Fixed Capacitors/thyristor - Controlled Reactor) combination with mechanically switched capacitor sections in series.

In load flow studies the TCSC can be represented in many forms, in this paper we are going to aim for three objective: 1) the proper insertion of the TCSC in the electric network, 2) the use of one of the four regulating TCSC models which is the *"firing angle power flow model"*, 3) minimization of the power losses in power lines regulated by TCSC [1-4].

This paper is organized as follows: Section 2 introduces the FACTS devices and their connection schemes. Section 3 presents the Controlled Series Capacitor (CSC) Applications.

2. FACTS DEVICE

The FACTS (Flexible AC Transmission System) program was elaborated by Electric Power Research Institute (EPRI) of Palo Alto, California, with the collaboration of equipment manufacturers and electricity companies.

The FACTS (Flexible AC Transmission System) devices used today can be classified by three connection schemes:

- Shunt scheme.
- Series scheme.
- Combined shunt - series scheme.

The static devices such as TCSC (Thyristor controlled Series Capacitors) or SVC (Static Var Compensateur) became key players in electrical distribution grid systems and industrial networks. As they improve the voltage and the network behavior stability, limit the line losses by reducing the reactive power transport, and increase the transport capacity. For the industrial networks which are characterized by the strong and fast fluctuations of the reactive power, they reduce the disturbing influences such as the flicker effect and the important voltage drop. Therefore, it is now possible to implement several control schemes simultaneously that make it possible to obtain a better safety of service of the network and thus an increase in efficiency.

The compensator has good dynamic performances (fast time response of some tenth of a second). It is however, an expensive device as well as in investment or in exploitation, because of the power losses it causes and the low frequency

*Corresponding author: *E-mail:* flakdja@yahoo.fr

 ISSN: 1743-9310

harmonics that it generates. These harmonics can cause serious problems such as the amplification of the voltage network by the resonance phenomenon. Thus, it is necessary to install passive filters and take into account the regulation [4].

The universal power flow controller (UPFC) remains the more sophisticated FACTS device. This is essentially due to the various control techniques that give it the advantage of flexibility, during an unspecified disturbance, while acting with compensation effect of series or parallel type.

2.1 The Shunt Scheme

In this category we quote the static reactive power compensator (SVC Static Var Compensator) with thyristors which is widely used in electrical transmission systems for fast voltage and reactive power regulation. There are more than 20000 MVARs reactive power controller are in use at present [5]. Indeed, all the parallel compensators inject current in the network via the connection point. When a variable impedance is connected in parallel on a network, it consumes (or injects) a variable current. This current injection modifies the active and reactive powers which flow in the line.

Fig. 1 gives a single-phase diagrammatic representation of a shunt static compensator. It is composed of a condenser with reactance X_c where the provided reactive power can be completely engaged or completely started, and an induction coil with inductive reactance X_L whose absorptive reactive power is ordered between zero and its maximum value by thyristors assembled in head to tail to ensure very fast inversions of the current.

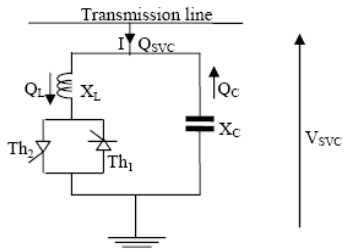

Figure 1. Single-phase diagrammatic representation of a static compensator

2.2 The series Scheme

In this scheme the series compensator commutated by TCSC is a series FACTS, used in the network in the form of a variable element quickly adjustable by thyristors. It is especially used to distribute the power flow between the parallel lines and to improve the transitory stability of alternators, by modifying the total line reactance where it is installed [6, 7]. Fig. 2 gives a diagrammatic representation of a series compensator circuit commutated by thyristors [8].

The circuit is composed of a series capacity assembled in parallel with an inductance coil whose reactance is gated by thyristors assembled in head to tail (gradator). The circuit includes also a safety device to shunt the compensator during the only moments where the over voltage exceeds the acceptable level for the condensers.

This safety device is a nonlinear zinc oxide (ZnO) resistance, called also varistor or "MOR" (Metal Oxide Resistor). The circuit is shunted by a circuit breaker. The group of condensers is connected with a TCR which allow current impulses to circulate in phase with the current line. This increases the condenser voltage beyond the voltage which can be obtained by the current line alone. Each thyristor is gated once per cycle and with a conducting time lower than a half-cycle of the applied fundamental frequency. If the added voltage, created by the flow of the current impulses, is controlled to be proportional to the line current, the electrical supply network sees the TCSC as a reactance which increases beyond the physical reactance of the condensers. Because of the interval conduction of the thyristors, current harmonics will be injected into the condensers. The current harmonics increase with the increase of the over voltage degree. The TCSC characteristics are:

- The material design is adapted to the maximum voltage to be supported.
- The MVar flow of the condenser group is proportional to the maximum voltage produced and the corresponding maximum current.
- An advanced control, particularly for the attenuation mode of Sub-Synchronous Resonances (SSR).
- An unrestricting number of operations and sequences.
- A precise configuration of a compensation degree.
- A frequent adjustment of the compensation degree for the attenuation of SSRs and the damping of the current oscillations.

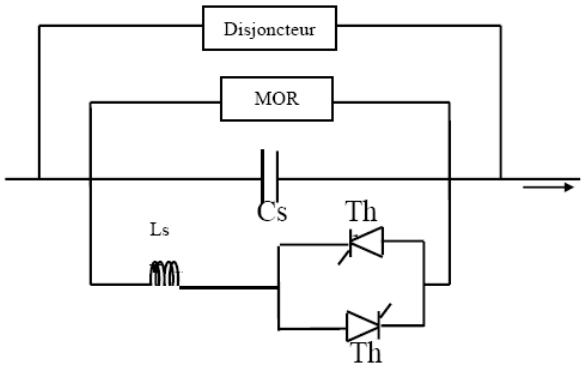

Figure 2. Diagrammatic representation of a single-phase TCSC, With Ls Series inductance and Cs Series capacitor

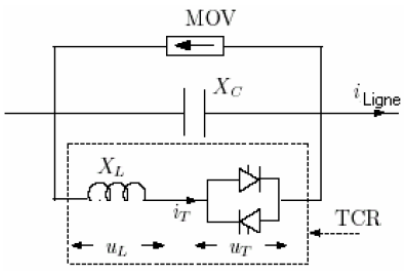

Figure 3. a TCSC diagram

The "TCSC" module represented in the Fig. 2, contains the following three operating modes [9]:

- The first mode is the "blocked Thyristors" mode; its impedance is a capacitive reactance Fig 4.
- The second mode is the "short-circuited Thyristors" mode; the equivalent impedance is inductive and low

because the totality of the line current flows through the thyristors branch Fig. 5.

- The last mode is based on partial conduction of the thyristors, i.e., if the Th1 thyristor is conducting, the Th2 thyristor is blocked and vice versa, when Th1 conducts the equivalent impedance is inductive as shown in Fig. 6, and if Th2 is conducting, the equivalent impedance is capacitive as shown in Fig. 7.

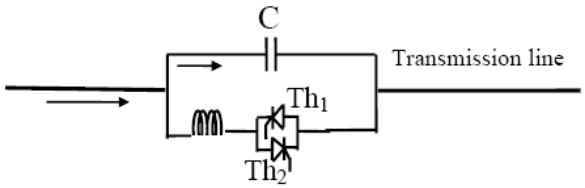

Figure 4. "Blocked Thyristors" operating mode

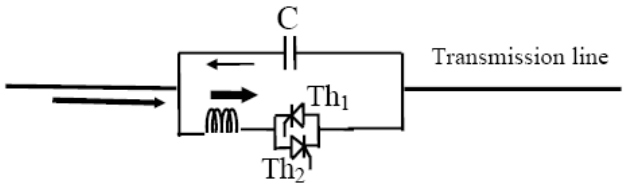

Figure 5. "Short-Circuited Thyristors" operating mode

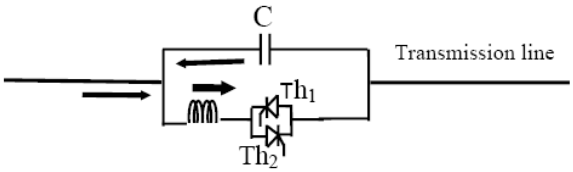

Figure 6. Operating mode with Th1 conducting

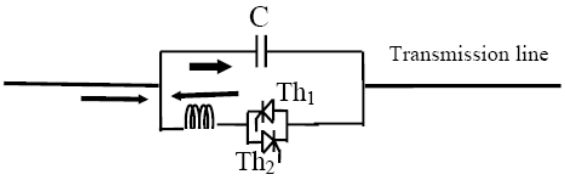

Figure 7. Operating mode with Th2 conducting

3. THE CONTROLLED SERIES CAPACITOR (CSC) APPLICATIONS

The series compensation is the best currently known technique to increase the power transfer capacity of the transmission line. The series condensers operate by inserting a voltage source in series with the transmission line with an opposite polarity to that of the line voltage drop. The apparent effect is the reduction in the apparent transmission line reactance. The various modes of the series condensers control can be suitable solutions for the following objectives:

3.1 A high degree of the series compensation

The series condensers increase the transfer capacity of the transmission lines. The maximum compensation degree in a transmission network is limited by the potential risk of interaction between the closest series condensers and the turbo alternators. This phenomenon is known under the term of sub-synchronous resonance (SSR). If a condenser with a reactance X_C is connected in series with the transmission line as shown in Fig. 8, the impedance becomes $(X_L\text{-}X_C)$. Then the power transmitted through this line is given by:

$$P_t = \frac{E_S E_R}{X_L - X_C} \sin\delta \qquad (1)$$

The maximum power transmitted is increased by $(X_L/X_C - X_L)$ compared to the non compensated line, if the condenser is provided with an inspecting device, the ratio $(X_L/X_C - X_L)$ becomes variable, and the transferred power could be controllable.

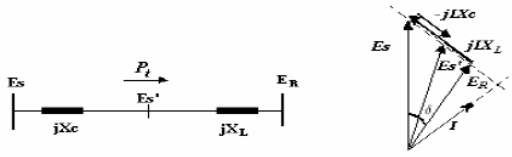

Figure 8. Series Compensation

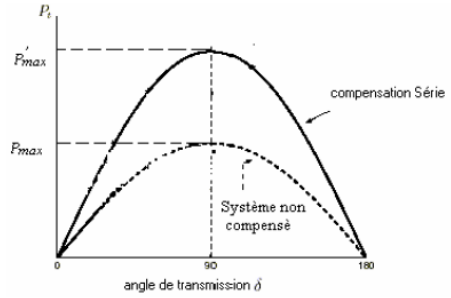

Figure 9. Effect of the compensation on the transmitted power

3.2 Damping of the power oscillations

Several non damped current oscillations with frequencies going from 0.2 to 2.0 Hz appear for high power levels in the long transmission lines.The CSCs (Controlled Series Capacitor) can damp these oscillations and thus allow a transfer of a power high level on long distances. Moreover, the CSCs can offer a significant support for the network when significant defaults happened by making it to find its synchronous operation.

3.3 Interconnections

Two or several electrical supply networks are often inter-connected to allow between them an economic power transfer, to share their stocks when necessary and to increase their profitability and reliability. The CSCs (Controlled Series Capacitor) are an effective means of interconnection to benefit a regular economical power exchange when the points of interconnections are electrically weak.

3.4 Power Flow Control

The CSCs (Controlled Series Capacitor) allow to the operators a better manage of the power flow through a transmission line. This is useful especially when an irregular power distribution

between various transmission circuits leads to an overload and forces the operator to reduce the use capacity of certain lines.

3.5 Control of loading capacity of the transmission lines

The CSCs are an effective means to improve the transfer capacity of the transmission lines. The degree of compensation can be controlled to minimize the system losses during its normal operation. Analyze of a TCSC circuit and its principal functionalities. Since the fundamental components of the voltage and the current are controllable, the TCSC becomes similar to a controllable impedance, which is the result of the parallelization of the equivalent reactance of a TCR component and a capacity.

Let us note:

$$Z_{TCSC} = jX_{TCSC} \tag{2}$$

The TCR equivalent impedance with

$$Z_{TCR} = jX_{TCR} = j\frac{X_L \pi}{2(\pi-\alpha)+\sin 2\alpha} \tag{3}$$

and the capacity impedance by

$$Z_C = -jX_C \tag{4}$$

we can write

$$Z_{TCSC} = Z_C // Z_{TCR} = \frac{-jX_C \cdot jX_{TCR}}{-jX_C + jX_{TCR}}$$

$$= \frac{-jX_C \cdot jX_{TCR}}{-jX_C + jX_{TCR}}$$

$$= j\frac{X_C X_L}{\frac{X_C}{\pi}(2(\pi-\alpha)+\sin 2\alpha) - X_L}$$

and

$$X_{TCSC}(\alpha) = \frac{X_C X_L}{\frac{X_C}{\pi}(2(\pi-\alpha)+\sin 2\alpha) - X_L} \tag{5}$$

4. TCSC DESIGN IN THE POWER FLOW MANAGEMENT

Assume that a TCSC device is placed between two nodes *k* and *m* as illustrated in Fig. 10. If the losses are neglected, the power *P* injected into the TCSC starting from the generation node *k* is equal to that injected by the TCSC in the load node *m*. The TCSC model represented in Fig. 10 is described by the system of Eq. 6 [10]:

$$\begin{aligned} P &= -V_k V_m B_e \sin(\theta_k - \theta_m) \\ Q_k &= V_k V_m B_e \cos(\theta_k - \theta_m) - V_k^2 B_e \\ Q_m &= V_k V_m B_e \cos(\theta_k - \theta_m) - V_m^2 B_e \\ B_e &= \frac{1}{X_C} - \frac{(2(\pi-\alpha)+\sin 2\alpha)}{\pi X_L} \\ \sqrt{P^2+Q^2} &= IV_k \\ \theta_k &= \theta_m + \delta_t \end{aligned} \tag{6}$$

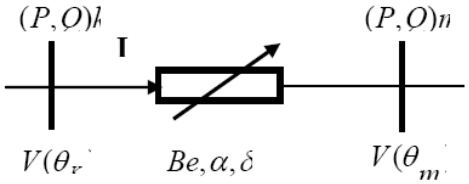

Figure 10. The TCSC Model in a Power Flow

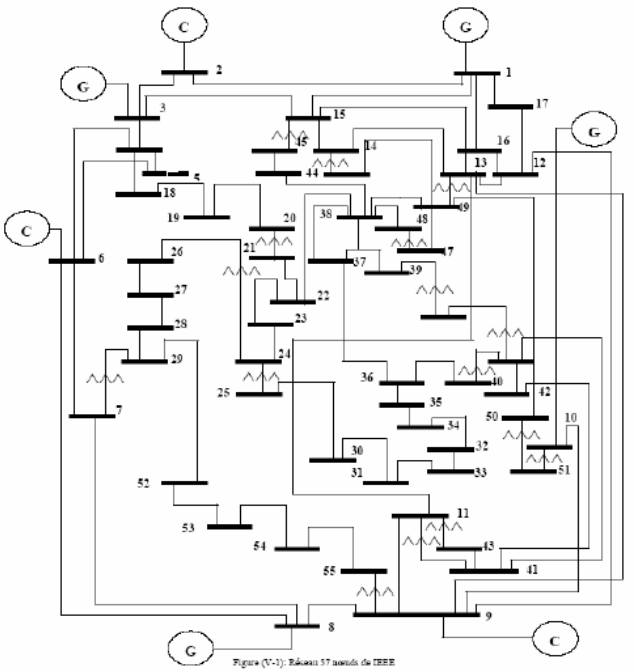

Figure 11. Electrical supply Network with 57 IEEE nodes

5. RESULTS AND DISCUSSIONS

The main objective of this work is to apply the calculation of the power flow by Newton-Raphson method in an electrical supply network model with 57 IEEE nodes, by inserting a TCSC power transit controller [10]. The network represented in Fig. 11 includes:

- 57 nodes including 48 consumption nodes;
- 03 production nodes (generators) and consumption;
- 03 production nodes (compensators) and consumption;

- 78 lines;
- 18 transformers

5.1 Network analysis without FACTS device

The analysis of our network is realized with a program developed under MATLAB™. This program enables us to follow the evolution of each network parameter by the means of the power flow calculation. It includes also the operating and the controlling subroutines of TCSC devices. The power flow calculation is a necessary stage to be able to compare our results. It is carried out initially for the determination of the system initial conditions before the default. Indeed, it allows finding the voltage at different nodes and thereafter the transmitted and injected powers. The results of the power flow calculation are obtained with a program using the Newton-Raphson method. This program converges in 4 iterations with an accuracy of 10^{-4}.

Table 1. Active and reactive losses of the network

	P_L (Mw)	Q_L (Mvar)
Results	28.059	35.395

In the first calculation, we have determined the values of the transmitted powers, the injected powers, the voltage, the angles and the losses, using the traditional calculation of the power flow with the Newton-Raphson method. This program converges in 4 iterations with an accuracy of 10^{-4}. We noticed that the transmitted powers, which are connected directly with the most powerful generator, have more significant values.

5.2 Basic parameters to insert the TCSC

There are several control strategies. In our case, we have chosen the control by the angle transmission of modulation

1) The basic value is: $S_b = 100$ MVA

2) The parameters of the power transit controller TCSC are:

   - The frequency $f = 50$ Hz
   - The inductive reactance: $X_L = 0.3$ p.u
   - The capacitive reactance: $X_C = 0.1$ p.u
   - Gating angle α.

Let us note that the choice of α values and their operating limits was based on research which was already done on the best angle of transits control [15].

The choice of α is as follows:

Capacitive effect: $\alpha = 148^o$, $\alpha_{min} = 142^o$, $\alpha_{max} = 180^o$

Inductive effect: $\alpha = 125^o$, $\alpha_{min} = 90^o$, $\alpha_{max} = 129^o$

5.3 Capacitive effect results

The computation results of the power flow with insertion of the TCSC, power transit controller, are obtained with the same program used previously; using the Newton-Raphson method, for this test we have chosen two different values of α, so that each value belongs to an operating zone out of the resonance zone.

Table 2. Transmitted powers with insertion of the TCSC transit controller (capacitive)

$\alpha_1 = 148^o$		$\alpha_{1min} = 142^o$		$\alpha_{1max} = 180^o$
$\Delta P = 0.0001$		iteration = 4		pr% = 60.7758%
	Before insertion of the TCSC		After insertion of the TCSC	
k-m	P_{km} (p.u)	Q_{km} (p.u)	P_{km} (p.u)	Q_{km} (p.u)
52-53	06.396	04.124	06.40	004.12
53-52	-06.349	-03.524	03.86	- 011.43

Table 3. Comparison of the voltage and angle without and with insertion of the TCSC transit controller (capacitive)

$\alpha_1 = 148^o$		$\alpha_{1min} = 142^o$		$\alpha_{1max} = 180^o$
$\Delta P = 0.0001$		iteration = 4		pr% = 60.7758%
Before insertion of the TCSC		After insertion of the TCSC		
Tension (p.u)	Angle (degree)	Tension (p.u)	Angle (degree)	
0.975	-12.321	1.1112	-12.3213	
0.931	-16.099	1.1112	-16.0991	

Table 4. Active and reactive losses of the network with injection of TCSC (capacitive)

	P_L (Mw)	Q_L (Mvar)
Results	19.13	26.34

According to these results, Tables 1-4 (where pr% is the Percentage%, k-m bus k to bus m, ΔP Precision calculation, P_{km} Active power, and Q_{km} is the Reactive power) we notice that depending on the disposition of the TCSC, the compensated systems may cause more or less losses compared to the case of no compensation. These losses are reduced with an optimal emplacement of the TCSC, which is, according to our results, related to the branches 53-52 and 24-26.

Indeed, for a compensation level of 70%, the losses of the network transmission power obtained after insertion of the transit controller are reduced by 60.8% for line 53-52 and 67.96% for line 24-26. The position of the TCSC in other branches of the network generates more active losses. For this reason, it is preferable to place the TCSC through the branch 53-52 since the losses are minimized with a good percentage and less iterations. After having chosen the optimal TCSC emplacement, the power flow in an electrical supply networks is distributed along the transport network according to the lines characteristics.

Also, according to the obtained results, we notice that the TCSC influences the voltage at nodes 53 and 52. The latter

which were 0.931 p.u without TCSC, was improved to become 1.1112 p.u. with a compensation of 60.8% for node 53 and 0.975 p.u without TCSC, was improved to become 1.1112 p.u with the same compensation (60.8%) for node 52. We also notice that the transmitted powers either active or reactive were increased smoothly but always remaining on the same order of magnitude. The goal of this application is to control the way of the power flow, by increasing its transfer in a network branch (53-52).

5.4 Inductive effect results

In this simulation the TCSC transit controller is inserted with inductive effect on the branch 41-43. This program

converges in 4 iterations with an accuracy of 10-4 and a compensating percentage pr% = 11.5165%. The obtained results are shown in Tables 5-7.

Table 5. Powers transmitted with insertion of the TCSC transit controller (Inductive)

$\alpha_2 = 125^o$		$\alpha_{2min} = 90^o$		$\alpha_{2max} = 129^o$
$\Delta P = 0.0001$		it = 4		pr% = 11.5165%
	Before insertion of the TCSC		After insertion of the TCSC	
k-m	P_{km} (p.u)	Q_{km} (p.u)	P_{km} (p.u)	Q_{km} (p.u)
41-43	-11.527	0.516	-13.275	0.5275
43-41	11.527	0.065	11.53	0.0651

Table 6. Comparison of the voltage and angle without and with insertion of the TCSC transit controller (Inductive)

$\alpha_2 = 125^o$		$\alpha_{2min} = 90^o$		$\alpha_{2max} = 129^o$
$\Delta P = 0.0001$		it = 4		pr% = 60.7758%
	Before insertion of the TCSC		After insertion of the TCSC	
k	Tension (p.u)	Angle (degree)	Tension (p.u)	Angle (degree)
41	0.972	-16.341	1.0556	-16.3405
43	0.971	-13.456	1.0556	-13.4560

Table 7. Active and reactive losses of the network with injection of TCSC (Inductive)

	P_L (Mw)	Q_L (Mvar)
Results	26.431	27.660

In the inductive zone, we have reduced the transmission power losses and the total losses with an adequate place of the TCSC, which are according to our results, related to the branches 3-15, 27-28, 32-34, 38-44, 41-43.

Indeed, for a compensation level of 60%, the network transmission power losses obtained after insertion of the transit controller are reduced by 0.5% for line 3-15, 0.67% for line 27-28, 7.6% for line 32-34, 0.45% for line 38-44 and 3.45% for line 41-43. While, the TCSC disposition in the other network branches, generates more active losses. For this reason, the best place of the TCSC is through the branch 41-43.

6. CONCLUSIONS

The use of series condensers to compensate the inductive reactance through a long distance of the line is the most effective and economic method to improve the transit of the powers. One of the principal reasons to incorporate series condensers in the grid systems is to reduce the losses in the transmission line by optimizing the shared active power between parallel lines. By the adjustment of the line impedance, this type of compensator is able to control the transit of the active powers. Our results check clearly, one of the principal reasons to incorporate series condensers in the transmission systems. The other significant point is the choice of the variation range of the firing angle. The continuous TCSC controller was also checked by our obtained results, when the operating zone is chosen. Finally, we have treated the problem of the power transit control in the transport lines, and we have tried to illustrate the utility, the effectiveness and the speed of control of the power transits between the network lines by inserting the TCSC transit controllers.

REFERENCES

[1] K. Clark et al.," Thyristor controlled series composition Application Study-Control Interaction Consideration", IEEE Transactions on Power Delivery, Vol. 10, No. 2, April 1995, pp. 1031-1037.

[2] X. X. Zhou, J. Liang," Non-Linear Adaptive Control of TCSC to Improve the Performance of Power Systems", IEE Proc. Gener., Transm, Distrib, Vol. 146, No. 3, May 1999, pp. 301-305.

[3] F. Z. I. Gherbi, M. Rahli, S. Hadjeri, "Optimal power flow using PowerWorld", AMSE Journal Modelling, Vol.77, No. 5, 2004, ISSN 0761-2508, pp. 33.

[4] S. A. Zidi, S. Hadjeri, M. K. Fellah, FZI. Gherbi,"The performance of an HVDC line", AMSE Journal Modelling C, 2005, ISSN 0761 -2508.

[5] Thyristor controlled series compositor, ABB Utilities AB, Power Systems, S-712 64 Vasteras, Sweden, 2002.

[6] Masaki Takahashi, Jeau-Pierre Charpentier, Kurt Schenk, "FACTS-For cost effective and reliable transmission of electrical energy ", Of the World Bank, available at: http://www.worldbank.org/html/fpd/em/transmission/facts_siemens.pdf, last date accessed 30/1/2008.

[7] Theodore Wildi et Gilbert Sybille," Electrotechnique", ingenieur, institut de recherche d'Hydro-Quebec, 3eedition, De Book Universite, 2000.

[8] M. Noroozian, G. Adersson," Power Flow Control by use of Controllable Series Components", department of Electric Power Systems et Royal Institute of Technology, S-100 44

Stockholm, Sweden, IEEE Transaction on power Delivery, Vol. 8, No. 3, July 1993, pp. 1420-1429.

[9] R.Grunbaum, Jacques Pernot, "La compensation series controlee par thyristor: une approche nouvelle pour optimiser le transport d'electricite", ABB Power System AB, SE-72164 Vasteras, Sweden, 2001.

[10] Allaoui Tayeb," Reglage robuste de l'UPFC pour optimiser l'ecoulement des puissances dans un reseau electrique", These de magister USTO, Avril 2002.

[11] Z. T. Faur," Effects of FACTS devices on Static Voltage Collapse Phenomena", Thesis requirement for the degree of Master of Applied Science in Electrical Engineering, Waterloo", Ontario, Canada,1996.

[12] T. Orfanogiannia, "A flexible software environment for steady-state power flow optimization with series", for the degree of doctor of technical sciences, Swiss federal institute of technology, Zurich, 2000.

[13] H. Ambriz Perez, E. Acha, C. R. Fuerte-Esquivel,"Advanced SVC Models for Newton-Raphson Load Flow and Newton Optimal Power Flow Studies", IEEE Transactions on Power Systems, 2000.

[14] F. Lakdja, M. Khiat, A.Chaker,"Dispositif TCSC pour le controle avancedes Reseaux d'energie electrique", 1ere Conferences Internationale sur le Transport de l'Electricite en Algerie, ALGER, 2005.

[15] F. Lakdja,"Controle des transits de puissance par dispositifs FACTS: Application à un reseau d'energie electrique", ICEEA'06 International Conference in Eletric Energy and its Applications, Sidi Bel-Abbès, 22 - 23 Mai 2006.

[16] F. Lakdja,"Minimisation des pertes actives et reactive et controle des transits de puissance par dispositifs TCSC (effet inductif)", Seconde Conference Internationale sur le Genie Electrique CIGE'2006, 11-12 Novembre 2006.

[17] F. Lakdja," Control of the power transits with TCSC device: Application to an electrical power network", The International Conference on Modelling and Simulation (MS' 07 Algeria), July 2 - 4, 2007, (A,M,S,E), Algiers, Algeria.

[18] F. Z. I.Gherbi, M. Rahli, S. Hadjeri, S. A. Zidi,"Analysis in Different Operating Scenarios by Optimal Power Flow", ICEEE'2004, International Conference on Electrical and Electronics Engineering. Laghouat, Algerie, 24-26 Avril 2004, ISSN 1112-4652.

[19] F. Z. I. Gherbi, S. A. Zidi, S. Hadjeri, "Using contouring visualisation for analysis and monitoring of electricity markets", ALGER, 2005 (1ere Conferences Internationale sur le Transport de l'Electricite en Algerie).

Biographies

Lakdja Fatiha was born in Oran, Algeria. She received the diploma of Electro technical Engineering degree from the University of Djillali Liabes of Sidi Bel-Abbes, Algeria in 1994, The Master degree, from the University of Oran, Algeria in 2005. She is currently working towards her Ph.D. degree at the University of Djillali Liabes of Sidi Bel-Abbes, Algeria. She is currently interested in power systems and FACTS.

Fatima Zohra Gherbi was born in Oran, Algeria. She received the diploma of Electro technical Engineering degree from the University of Science and Technology of Oran, Algeria. The Master degree, from the University of Djillali Liabes of Sidi Bel-Abbes, Algeria in 1992. The Ph.D. degrees from the University of Sidi Bel-Abbes, Algeria, in 2004. Her research activities are mostly concentrated in the study of stability issues in AC/DC/FACTS power systems.

Table of Contents

Volume 4 / Number 3 / 2008

INSTRUCTIONS FOR AUTHORS (Title is Helvetica size 18)

Author 1[a,*], Author 2[b], Author 3[c] (Helvetica size 12)

[a]Affiliation a (Helvetica size 10)

[b]Affiliation b (Helvetica size 10)

[c]Affiliation c (Helvetica size 10)

ABSTRACT (Times New Roman size 12)

An abstract, not exceeding 200 words, is required for all papers (font is Times New Roman size 9).

Keywords (Times New Roman size 12)

The author should provide a list of key words, up to a maximum of six (font is Times New Roman size 9).

1. INTRODUCTION (Times New Roman size 12)

(Body text is Times New Roman size 9). The introduction of the paper should explain the nature of the problem, previous work, purpose, and the contribution of the paper. It is assigned the number "1" and following sections are assigned numbers as needed. format. The paper must be (Letter) page size with margins of 1.25" for the top of first page, 0.75" for left, right, and bottom, and 0.75" for top, bottom, left, and right of ALL subsequent pages. The paper must be double column format, single line spacing with an extra line added between paragraphs. Please limit the title to a maximum length of 10 words. The author's name(s) follows and is also centered on the page. A blank line is required between the title and the author's name(s). Last names should be spelled out in full and preceded by author's initials. The author's affiliation, complete mailing address, and e-mail address are provided below. Phone and fax numbers do not appear. Do not underline any of the headings, or add dashes, colons, etc. The headings, starting with "1. INTRODUCTION", appear in upper case letters and should be set in bold and aligned flush left. All headings from the Introduction to Conclusions are numbered sequentially using 1, 2, 3, etc. Subheadings are numbered 1.1, 1.2, etc. If a subsection must be further divided, the numbers 1.1.1, 1.1.2, etc. are used and the number and associated title are set in italics instead of bolded. A colon is inserted before an equation is presented, but there is no punctuation following the equation. All equations are numbered and referred to in the text solely by a number enclosed in a round bracket (i.e. (2) reads as "equation 2"). Ensure that any miscellaneous numbering system you use in your paper cannot be confused with a reference [3] or an equation (2) designation.

*Corresponding author: *E-mail:*

For more details, please visit

www.medjmc.com

1.1 Initial Submission

The manuscript must be a single file (including tables, figures, etc.) using either an Adobe-compatible portable document format (*.pdf) or an MS Word (*.doc) or Adobe FrameMaker (*.fm). Submit the manuscript without the authors' names, affiliation, and biographies. Along with it, submit a cover page that includes the manuscript title, authors' names and affiliation, and the corresponding author's name and contact information (full postal and e-mail addresses, phone and fax numbers), and biographies. The corresponding author will be given a reference number assigned to the paper and it is to be used in all future correspondence. Formatting your paper correctly saves a great deal of editing time, which in turn ensures publication of papers in a timely manner. Authors submit electronic versions of their manuscript to:

isubmission@medjmc.com

1.1.1 Figures

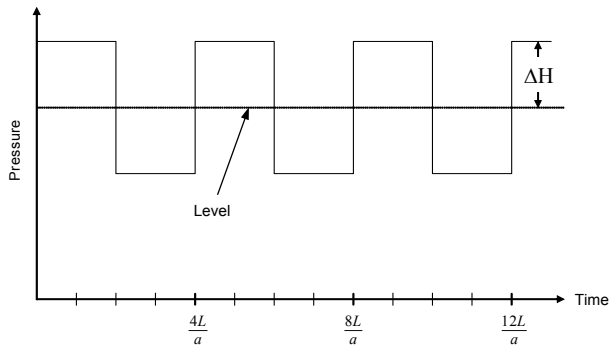

Figure 1. Sample graph

A reference list must be included. Only cited text references are included. Each reference is referred to in the text by a number enclosed in a square bracket (i.e., [3]). References must be numbered and ordered according to where they are first mentioned in the paper, not alphabetically.

REFERENCES

[1] Anderson, B. O. D. and D. J. Clements, "Algebraic Characterization", Vol. 17, 1981, pp. 703-712.

The Mediterranean Journal of Measurement and Control
www.medjmc.com

Published by SoftMotor Ltd. ISSN: 1743-9310

For complete information regarding
subscription and ordering,
please contact

SoftMotor Ltd
Provincial House, Solly Street, Sheffield S1 4BA
United Kingdom

Tel: (+44) 0114 201 4916
Fax: (+44) 0114 201 3524
E-mail: order@medjmc.com
Website: www.medjmc.com
Website: www.softmotor.co.uk

Volume 4 / Number 3 / 2008